

Institute of Agronomy and Plant Breeding I
Department of Plant Breeding
Justus Liebig University Giessen

**Genetic analysis of Fusarium root and crown rot
(FCR) resistance in wheat (*Triticum aestivum*)**

A thesis submitted for the requirement of the doctoral degree in
Agricultural Sciences from the Faculty of Agricultural and
Nutritional Sciences and Environmental Management
Justus Liebig University Giessen, Germany

Submitted by
Beiqi Shao

Examiners
Prof. Dr. Rod Snowdon
Prof. Dr. Karl-Heinz Kogel

Giessen 2021

Table of contents

List of figures.....	IV
List of tables.....	VI
List of abbreviation.....	VII
1 Introduction.....	1
1.1 Origin and genome structures of wheat.....	1
1.2 Diseases of wheat caused by <i>Fusarium</i> species.....	3
1.3 Current status of Fusarium head blight (FHB) research.....	5
1.4 Current status of soil-borne diseases including FCR research.....	11
1.5 Life cycles of <i>Fusarium</i> species causing FHB and FCR diseases.....	15
2 Objectives.....	19
3 Materials and methods.....	20
3.1 Development of mapping population.....	20
3.2 Climate chamber experiments for evaluation of FCR resistance.....	20
3.2.1 Fungal material.....	20
3.2.2 Root-dip inoculation and plant tissue sampling.....	20
3.2.3 Seed-dip inoculation and plant tissue sampling.....	21
3.3 Fusarium root and crown rot (FCR) bioassay.....	22
3.3.1 Root and shoot length, dry weight assessments upon root inoculation.....	22
3.3.2 Root and shoot length, dry weight assessments upon seed inoculation.....	22
3.3.3 Visible symptom assessments.....	23
3.4 Data Analysis.....	23
3.5 Genotyping and genetic linkage map construction.....	24
3.6 QTL mapping.....	25
3.7 <i>In-silico</i> annotation of putative genes linked to FCR resistance.....	25
4 Results.....	27
4.1 <i>F. graminearum</i> root inoculation experiment.....	27
4.1.1 Phenotypic variation between parents of the mapping population.....	27
4.1.2 Phenotypic variation for parents of the mapping population between sub-experiments.....	28
4.1.3 Phenotypic variation of the mapping population.....	31
4.1.4 Trait correlations.....	35
4.2 <i>F. graminearum</i> seed inoculation experiment.....	37
4.2.1 Phenotypic variation between parents of the mapping population.....	37

4.2.2 Phenotypic variation for parents of the mapping population between sub-experiments.....	38
4.2.3 Phenotypic variation of the mapping population.....	42
4.2.4 Trait correlations.....	46
4.3 Correlation of phenotypic data between root and seed inoculations experiment	47
4.4 Genetic map construction.....	49
4.5 QTL identification in the root inoculation experiment	55
4.5.1 Identification of FCR resistance QTL upon <i>F. graminearum</i> root inoculation	55
4.5.2 Identification of morphological traits QTL upon mock root inoculation	58
4.6 QTL identification in the seed inoculation experiment.....	59
4.6.1 Identification of FCR resistance QTL upon <i>F. graminearum</i> seed inoculation	59
4.6.2 Identification of morphological traits QTL upon mock seed inoculation ...	59
4.7 Comparison of FCR resistance QTL between <i>F. graminearum</i> root and seed inoculations	63
4.8 Comparison of FCR resistance QTL in the current study with reported QTL in the literature.....	64
4.9 Identification of putative FCR resistance related genes in the selected QTL	69
5 Discussion	75
5.1 Commonly used disease indices need to be reconsidered to characterize FCR resistance	75
5.2 FCR resistance is quantitatively inherited and plant organ/developmental stage dependent	78
5.3 QTL for FCR resistance and tolerance can be dissected using different disease indices.....	80
5.4 FCR affects root biomass whereas resistance/tolerance is not associated with high root biomass accumulation.....	81
5.5 Some FCR resistance QTL are co-localizing with FCR/FHB resistance QTL reported in the literature	82
5.6 FCR resistance QTL is associated with a semi-dwarfing gene linked to FHB susceptibility.....	84
5.7 Putative resistance genes identified in FCR and FHB overlapped QTL encoding cytochrome P450 and receptor-like kinase	86
6 Summary	91
7 Zusammenfassung.....	92
References.....	94

Appendix.....	124
Declaration.....	127
Acknowledgement	128

List of figures

Figure 1. The evolution of wheat from the prehistoric Stone Age grasses to modern macaroni wheat and bread wheat (Peng, 2011).	2
Figure 2. The life cycle of <i>F. graminearum</i> Schwabe [teleomorph: <i>Gibberella zeae</i> (Schw.) Petch] in wheat.	17
Figure 3. Comparison of relative reduction upon <i>F. graminearum</i> root inoculation between two parental genotypes of the mapping population combining data from nine sub-experiments.	28
Figure 4. Comparison of phenotypic data for different traits of cv. Tobak in nine sub-experiments upon mock and <i>F. graminearum</i> root inoculations.	30
Figure 5. Comparison of mean phenotypic data for 104 DH lines derived from the cross of line 162.11 × cv. Tobak before (raw data) and after (normalized data) normalization in <i>F. graminearum</i> root inoculation experiment.	32
Figure 6. Comparison of relative reduction phenotypic data for 104 DH lines derived from the cross of line 162.11 × cv. Tobak before (raw data) and after (normalized data) normalization in <i>F. graminearum</i> root inoculation experiment.	32
Figure 7. Comparison of phenotype frequency distributions of 104 DH lines derived from the cross of line 162.11 × cv. Tobak before (raw data) and after (normalized data) normalization in <i>F. graminearum</i> root inoculation experiment.	33
Figure 8. Root inoculation experiment: Correlation matrix of normalized phenotypic data upon mock and <i>F. graminearum</i> treatments for different traits of 104 wheat DH lines.	35
Figure 9. Comparison of phenotypic data upon mock and <i>F. graminearum</i> seed inoculations for two parents of the mapping population combining data from eight sub-experiments.	38
Figure 10. Comparison of phenotypic data for different traits of line 162.11 in eight sub-experiments upon mock and <i>F. graminearum</i> seed inoculations.	40
Figure 11. Comparison of phenotypic data for different traits of cv. Tobak in eight sub-experiments upon mock and <i>F. graminearum</i> seed inoculations.	41
Figure 12. Comparison of mean phenotypic data for 103 DH lines derived from the cross of line 162.11 × cv. Tobak before (raw data) and after (normalized data) normalization upon <i>F. graminearum</i> seed inoculation.	43
Figure 13. Comparison of relative reduction phenotypic data for 103 DH lines derived from the cross of line 162.11 × cv. Tobak before (raw data) and after (normalized data) normalization in <i>F. graminearum</i> seed inoculation experiment.	43

Figure 14. Comparison of phenotype frequency distributions of 103 DH lines derived from the cross of line 162.11 × cv. Tobak before (raw data) and after (normalized data) normalization in <i>F. graminearum</i> seed inoculation experiment.....	45
Figure 15. Seed inoculation: Correlation matrix of normalized phenotypic data upon mock and <i>F. graminearum</i> treatments for different traits of 103 DH lines.	46
Figure 16. Correlation matrix of normalized phenotypic data for different traits between root and seed inoculations experiment.	48
Figure 17. Genetic map developed by using a double haploid population from line 162.11 × cv. Tobak.	51
Figure 18. Dot plot depicting the marker order collinearity between line 162.11 × cv. Tobak map (cM) and high-density consensus map (cM) for 21 chromosomes of wheat.	52
Figure 19. Synteny of the mapped SNPs on chromosome 4B from two consensus maps (in red) and the line 162.11 × cv. Tobak map (in blue) based on the homologies between markers on adjacent linkage groups.....	53
Figure 20. Synteny of the mapped SNPs from the consensus map reported by Wang et al. (2014; in red) and the line 162.11 × cv. Tobak map (in blue) based on the homologies between markers on adjacent linkage groups.....	54
Figure 21. SNP-based genetic map and distribution of FCR resistance QTL (solid bars) and morphological traits QTL (hollow bars) for <i>F. graminearum</i> and mock root inoculations in the line 162.11× cv. Tobak DH population.....	57
Figure 22. SNP-based genetic map and distribution of FCR resistance QTL (solid bars) and morphological traits QTL (hollow bars) for <i>F. graminearum</i> and mock seed inoculations in the line 162.11× cv. Tobak DH population (n=103).....	62
Figure 23. Distribution of FCR resistance QTL co-localizing or overlapping upon <i>F. graminearum</i> root and seed inoculations.	64
Figure 24. Comparative map of FCR resistance QTL (in black) detected in the present study and published FCR (in red) and FHB resistance QTL or cloned resistance genes (in green) and other putatively involved genes (in pink).	66
Figure 25. Comparison of proteins encoded by resistance related genes and other genes in 81 differentially expressed genes between resistant and susceptible genotypes after <i>Fusarium</i> inoculation.	74
Figure A 1. Comparison of phenotypic data for different traits for line 162.11 in seven sub-experiments upon mock and <i>F. graminearum</i> root inoculations.	124

List of tables

Table 1. Examples of novel <i>Fusarium</i> resistance QTL for head blight and crown rot identified in previous studies.....	10
Table 2. Normalized phenotypic data in mock and <i>F. graminearum</i> root inoculations experiment.....	34
Table 3. Normalized phenotypic data in mock and <i>F. graminearum</i> seed inoculations experiment.....	45
Table 4. Marker statistics of the linkage map constructed from doubled haploid population derived from the cross of line 162.11 and cv. Tobak.	50
Table 5. FCR resistance QTL for <i>F. graminearum</i> root inoculation in the line 162.11× cv. Tobak DH population.....	56
Table 6. Morphological traits QTL for mock root inoculation in the line 162.11× cv. Tobak DH population.....	56
Table 7. FCR resistance QTL for <i>F. graminearum</i> seed inoculation in the line 162.11× cv. Tobak DH population.....	61
Table 8. Morphological traits QTL for mock seed inoculation in the line 162.11× cv. Tobak DH population.....	62
Table 9. FCR resistance QTL upon <i>F. graminearum</i> root and seed inoculations in the line 162.11× cv. Tobak DH population.....	67
Table 10. Summary of novel FCR and FHB resistance QTL in the literature.....	68
Table 11. Differentially expressed and regulated genes between resistant and susceptible genotypes from QTL identified in this study analyzed via ‘expVIP’ database.....	71
Table 12. Selected <i>F. graminearum</i> resistance genes functional annotation reported in the literature.....	73
Table A 1. Raw phenotypic data in mock and <i>F. graminearum</i> root inoculations experiment.....	125
Table A 2. Raw phenotypic data in mock and <i>F. graminearum</i> seed inoculations experiment.....	126

List of abbreviation

CIM	Composite interval mapping
CoV	Coefficient of Variation (relative standard deviation)
DBD	DNA binding domain
DEG	differentially expressed genes
DES	Discoloration extension scale
DH	Doubled haploid
DL	Length of discoloration section on stem base
DL_SLi	Length of discoloration section on stem base to shoot length ratio of <i>F. graminearum</i> -inoculated plants
DON	Deoxynivalenol
DS	Discoloration scale
FCR	<i>F. graminearum</i> root and crown rot
FHB	Fusarium head blight
LOD	Logarithm of odds
LRR	Leucine-rich repeat
NBS	Nucleotide-binding site
PAMP	Pathogen-associated molecular pattern
PRR	Protein recognition receptor
PTI	PAMP-triggered immunity
QTL	Quantitative trait loci
RDWi	Root dry weight of <i>F. graminearum</i> -inoculated plants
RDWm	Root length of mock-inoculated plants
RDWR	Root dry weight reduction
RLi	Root length of <i>F. graminearum</i> -inoculated plants
RLm	Root length of mock-inoculated plants
RLR	Root length reduction
SbSI	Stem base symptom index
SDWi	Shoot dry weight of <i>F. graminearum</i> -inoculated plants
SDWm	Shoot dry weight of mock-inoculated plants
SDWR	Shoot dry weight reduction
SD	Standard deviation
SLi	Shoot length of <i>F. graminearum</i> -inoculated plants
SLm	Shoot length of mock-inoculated plants
SLR	Shoot length reduction
SNP	Single nucleotide polymorphism
Sr	Survival rate

1 Introduction

1.1 Origin and genome structures of wheat

Bread wheat (*Triticum aestivum*), also known as common wheat, is a cultivated wheat species. About 95% of the wheat produced is bread wheat, which is the most widely grown crops and cereals with the highest monetary yield. Bread wheat is one of the world's three main cereal crops, along with rice and maize. In 2018, 734 million tons of bread wheat were produced in the world, of which 131.4 million tons were produced in China followed by India and the Russian Federation. In Germany the production of wheat was 20.3 million tons (FAO 2019). Wheat was one of the first cereals to be domesticated in the Middle East and subsequently spread over the Old World during the Neolithic revolution (Charmet, 2011). Wheat gradually became the world's foremost crop plant (Gustafson et al., 2009), representing a major renewable resource for food, feed, and industrial raw materials (Charmet, 2011).

Modern wheat cultivars belong to hexaploid bread wheat, *Triticum aestivum* ($2n = 6x = 42$, AABBDD), and tetraploid, hard or durum-type wheat, *T. durum* ($2n = 4x = 28$, AABB) used for macaroni and low-rising bread (Peng et al., 2011). 95% of wheat cultivated is hexaploid with the remaining 5% being durum wheat (*T. turgidum* L.) and few other less important types (Venske et al., 2019). Wheat is cultivated in practically all areas of the world, from the equator to temperate lands and at altitudes as high as 3000 meters above sea level. It is the staple food for 40% of the world's population, mainly in Europe, North America and the western and northern parts of Asia (FAO 2019). A diploid ancestor of the *Triticeae* subtribe with seven chromosomes was produced by the common ancestor of the grass (Poaceae) family with putatively five chromosomes and evolved 50-70 million years ago (Kellogg, 2001; Huang et al., 2002; Charmet, 2011). Wild emmer wheat (*T. dicoccoides*, $2n = 4x = 28$, genome AABB) was produced by wild diploid wheat (*T. urartu*, $2n = 2x = 14$, genome AA) which hybridized with the B genome ancestor that is the closest relative of goat grass (*Aegilops speltoides*, $2n = 2x = 14$, genome BB) 300,000-500,000 years before present (BP; Huang et al., 2002; Dvorak and Akhunov, 2005; Peng et al. 2011). A cultivated emmer (*T. dicoccum*, $2n = 4x = 28$, genome AABB) was gradually created by hunter-gatherers at about 10,000 BP, which was naturally hybridized with another grass (*Ae. tauschii*, $2n = 2x = 14$, genome DD) around 9,000 BP to produce an early spelt (*T. spelta*, $2n = 6x = 42$, genome AABBDD; McFadden and Sears 1946; Dvorak et al.,

1998; Matsuoka and Nasuda, 2004; Charvet, 2011). A more easily threshed type that later evolved into the free-threshing ears of modern types of durum wheat (*T. durum*) and bread wheat (*T. aestivum*) was created from the ears of both emmer and spelt by natural mutation at about 8,500 BP (Figure 1).

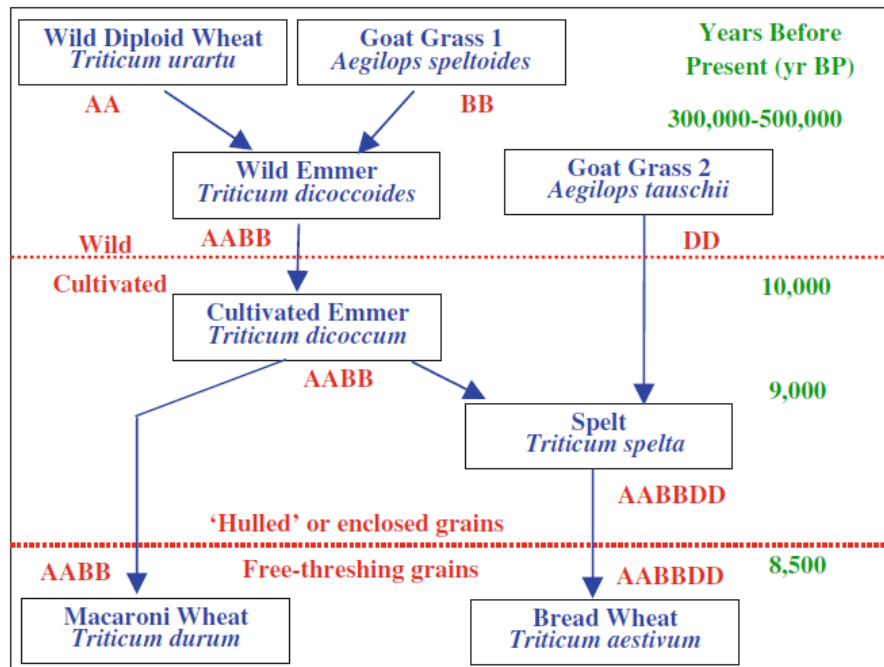


Figure 1. The evolution of wheat from the prehistoric Stone Age grasses to modern macaroni wheat and bread wheat (Peng, 2011).

The bread wheat genome is classified as a hexaploid genome with six copies of its seven chromosomes and the complete set numbering 42 chromosomes. Compared with other major crops such as rice (~ 430 megabases, Mb) the size of the bread wheat genome is very large (~ 17 gigabases, Gb) and approximately 85% of it consists of repetitive sequences (Eckardt, 2000; Shi et al., 2017; Appels, 2018). Due to the large genome size and high amount of repetitive DNA, it is a tremendous challenge to understand the molecular basis of key agronomic traits and diseases resistance which are necessary to improve wheat breeding. To provide a foundation for improvement through molecular breeding, the International Wheat Genome Sequencing Consortium (IWGSC) established a high-quality reference genome sequence of the bread wheat cultivar Chinese Spring (CS). In 2018, an ordered and annotated assembly (IWGSC RefSeq v1.0) of the 21 haploid chromosomes of the bread wheat was generated from Illumina short-read sequences which provides insights into global genome composition and enable the construction of complex gene co-expression networks to identify central regulators in critical pathways. In the resulting 14.5 Gb genome assembly, along the 21

chromosomes 14.1 Gb (97%) sequences assigned and ordered and 13.8 Gb (98%) of the assigned sequence scaffolds were oriented relative to each other. The unassigned chromosome (ChrUn) bins were formed by unanchored scaffolds comprising 2.8% (481 Mb) of the assembly length (Appels, 2018). Each chromosome is represented by 76 superscaffolds and 90% of them are larger than 4.1 Mb. The RefSeq Annotation v1.1 was built by the predicted gene model with two independent pipelines and a set of manually curated gene models on A, B, and D subgenomes. 107,891 high-confidence (HC) protein-coding loci are relatively equally distributed (35,345, 35,643, and 34,212, respectively). 27% (29,737) of bread wheat HC genes are concatenation duplicates and most of them are found in the B subgenome (29%). Although most of the genes are present in homeologous groups, only 18,595 (47%) of the groups contained triads with a single gene copy per subgenome (an A:B:D configuration of 1:1:1). The functional innovation was driven by higher levels of expression divergence with recent homeologs gene and genome duplicates (Soltis et al., 2015; Appels, 2018). With the help of the annotated and ordered reference genome sequence, the necessary changes in the genomes for breeding programs can be precisely defined by accessing sequence-level information, such as the expression of complex traits including yield and diseases resistance controlled by the genome-wide gene networks.

1.2 Diseases of wheat caused by *Fusarium* species

The growth and development of plants are influenced by the constantly changing environments which require adaptation to suboptimal and stressful conditions. These disadvantageous conditions include abiotic stress, such as drought, heat, nutrient deficiency and excess of salt or toxic metals, and biotic stress such as infection by pathogens like viruses, bacteria, fungi and herbivores (Wang, 2015; Zhu, 2016). The small grain cereals including wheat and maize are severely damaged by fungi of the genus *Fusarium*. Major diseases of wheat including Fusarium head blight (FHB), Fusarium root rot (FRR) and crown rot (FCR) are induced by several fungal pathogens of the genus *Fusarium* mostly in co-infection and with different prevalence. *F. graminearum* is the primary pathogen causing Fusarium head blight (FHB). The predominant causal agents of Fusarium crown rot (FCR) are *F. pseudograminearum*, *F. culmorum* and *F. graminearum* (Smiley and Patterson, 1996; Fernandez and Conner, 2011; Wang, 2015; Xu et al., 2018). The term ‘Fusarium root rot’ is also frequently used to describe wheat diseases associated with root and crown rot symptoms caused

by co-infection of *Fusarium* species. Thus, in the following the term Fusarium root and crown rot (FCR) is used. *F. pseudograminearum* has been described to be the dominant *Fusarium* species associated with FCR in arid zones, e.g. in Australia (Poole et al., 2013). In contrast, *F. culmorum* has been described to be the dominant *Fusarium* species in the cooler, higher altitude and high rainfall areas, e.g. the Pacific Northwest of the US (Smiley et al., 2005). *F. graminearum* was reported to be the dominant *Fusarium* species associated with FCR in eastern Australia and southern Europe (Xu et al., 2018; Jevtić et al., 2019). Jevtić et al. (2019) showed that *F. graminearum* predominated as the causal agent of FCR over the other *Fusarium* species with the frequency of 72.6% in Serbia. As a country in the cooler temperate climates of Europe, *F. culmorum* used to be the prevalent species in Germany (Moretti et al., 2019). However, in the last decade *F. graminearum* has become the dominant species because the higher temperature favors its dominance in these regions. In general, the mycotoxigenic *Fusarium* species profile on wheat in Europe is in continuous change in Northern, Central and Southern-Europe with a worrisome growing contamination of *F. graminearum* in the Central and Northern Europe (Miedaner et al., 2008; Parikka et al., 2012).

Because *F. graminearum* is involved in causing both important wheat diseases, FHB and FCR in Europe, this study is focusing on the less studied FCR disease caused by *F. graminearum* and on the genetic comparison of FCR and FHB resistance.

1.3 Current status of Fusarium head blight (FHB) research

Fusarium head blight (FHB) was first recorded in England in 1884 by W.G. Smith. During the early years of the twentieth century, it was considered as a main threat to wheat and barley crops (Goswami and Kistler, 2004; Shah et al., 2018). From then on, FHB occurs worldwide and outbreaks have been reported in most wheat growing regions, such as Europe, Asia, North and South America. It has been considered as a major factor limiting wheat production in many parts of the world by Wheat Improvement Centre (CIMMYT) (Stack, 1999; Goswami and Kistler, 2004; Shah et al., 2018). Wheat production can be decreased by FHB up to 50-60% and such losses are induced by flower abortion, elimination of damaged grains during threshing, decrease in grain size, and reduction in grain weight. A yield loss of 1 Mg ha⁻¹ is predicted to occur at 19% FHB incidence and can occur every 3-5 years (Salgado et al., 2015; Miedaner et al., 2017; Shah et al., 2018). In the United States, FHB reappeared in 1980s as a destructive disease in the cereal crops in north America and in the Northern Great Plains of the US. From 2007 to 2008 FHB occurred in several states causing US \$13.3 and 57 million losses respectively. In 2012, approximately 1.64 million hectares were lost due to FHB which was 68.3% of the wheat acreage in the Huang-Huai Area in China. It was the highest reduction in China's recorded history (Dai, 2012). In Europe the loss due to FHB in wheat harvest is estimated from 10 to 30% (Bottalico et al., 2002).

Nowadays, there are some strategies for management of FHB in wheat and other small grain production. The efficiencies of these methods are based on the environmental conditions like flowering times and plants susceptibility to FHB including: I) cultural practices, II) chemical control, III) biological control, IV) harvesting strategies, V) disease forecasting and, VI) planting resistant or tolerant cultivars.

Crop rotation with non-hosts and burying host plant residue could decrease FHB intensity and accumulation of DON in wheat (Dill-Macky and Jones, 2000). The risk of FHB development and DON accumulation can be dramatically decreased by irrigation management to preclude extreme moisture. Producing lodging resistant cultivar also can decrease DON and FHB in small grain cereal crops like wheat, because lodged plants are easier to be inoculated by pathogen on the soil surface with the higher moisture and humidity (Kubo et al., 2010; Wegulo et al., 2015). The demethylation

inhibitors (DMI) are the most worldwide fungicide used for chemical management of FHB and DON (Mcmullen et al., 2012). However, a DMI fungicide resistant *F. graminearum* isolate was discovered in the New York, U.S. recently, which make it is important to create new fungicide that can reduce FHB and DON but with different action modes (Spolti et al., 2015). Bacterial biological control agents (BCAs) have been found with antagonists against several *Fusarium* species inducing *F. graminearum*. It is most effective to apply BCAs and fungicides simultaneously to prevent *F. graminearum* infection during the pre-harvest period (McMullen et al., 2012; Xue et al., 2014). During the harvest, the lighter *F. graminearum*-damaged kernels (FDK) can be blown away by higher fan speed and a larger shutter opening than standard configurate, which lead to the lower FDK and DON (Salgado et al., 2011, 2015). Disease forecasting systems can help farmers to apply fungicide optimally in growing seasons based on the FHB disease risk outbreaks. In the U.S., the Fusarium head Blight Risk Assessment Tool (<http://www.wheatcab.psu.edu/>) can predict FHB risk at over 75% accuracy and is configured in all wheat and barley growing regions.

The genetic resistance is considered as the most efficient and cost-effective management strategy for FHB and DON, although it is complex and inherited quantitatively (Ruckenbauer et al., 2001; Bai and Shaner, 2004). In Europe, two major breeding projects “FUCOMYR” and “MYCOTOCHAIN” are supported by multiple European Union nations including public and private plant breeding institutes and food processing companies to identify and development FHB and DON resistant genotypes using traditional and molecular techniques (Ruckenbauer et al., 2007).

Based on host response to pathogen infection, five resistance types are described: Type I, resistance against initial penetration (Schroeder and Christensen, 1963); Type II, resistance to spread of FHB symptoms within a spike (Schroeder and Christensen, 1963); Type III, resistance to kernel infection (Mesterhazy, 1996); Type IV, tolerance against FHB (Mesterhazy, 1996); and Type V, resistance to toxins (Miller et al., 1985). Because in wheat type II resistance is the most stable and is easiest to be assessed (Bai and Shaner, 2004). This type resistance can be evaluated by single floret inoculation with injecting fungal suspensions into a central spikelet of a spike in greenhouse or inoculating with hypha infected grain in field. The percent of infected spikelets over all spikelets in the head is used to measure FHB severity on a 0-9 scale (Kubo et al., 2010).

Since 1999 more than 100 QTL for different types of FHB resistance from at least 50 resistance sources have been reported from different studies (Buerstmayr et al., 2009). The FHB resistance QTL were mapped on all 21 wheat chromosomes, of which the QTL on five chromosomes (2D, 3A, 3B, 4B, 5A, 6B) could be detected in more than two populations of different geographic origins (Buerstmayr et al., 2009; Liu et al., 2009; Bai et al., 2018; Venske et al., 2019). Among all FHB resistance QTL, only seven have been formally assigned with a gene name. *Fhb1* was firstly named and identified on chromosome 3BS from Chinese wheat cultivar Sumai 3 (Cuthbert et al., 2006). Another named QTL *Fhb2* was also detected on chromosome 6BS from Sumai 3 (Cuthbert et al., 2007), *Fhb4* and *Fhb5* were mapped on Chromosomes 4B and 5A from another Chinese wheat cultivar Wangshuibai respectively (Xue et al., 2010, 2011). Other three FHB resistance QTL designated as *Fhb3* on chromosome 7AS, *Fhb6* on chromosome 1A and *Fhb7* on chromosome 7D were all transferred into wheat from alien species including *Leymus racemosus* (Qi et al., 2008), *Elymus tsukushiensis* (Cainong et al., 2015) and *Thinopyrum ponticum* (Guo et al., 2015) respectively.

Among the seven named FHB resistance QTL, *Fhb1* explained the highest phenotypic variation up to 60% and showed stable type II resistance in different populations and backgrounds (Buerstmayr et al., 2003; Cuthbert et al., 2006; Malla et al., 2012; Schweiger et al., 2016; Zhang et al., 2016; Bai et al., 2018). *Fhb1* has been widely used and studied in wheat breeding programs globally and majority FHB resistance wheat genotypes produced carry this QTL (Zhang et al., 2018). *Fhb2* was identified on chromosome 6BS and a wide range of the phenotypic variation (4.4-23%) for FHB type II resistance was explained (Waldron et al., 1999; Anderson et al., 2001; Yang Z et al., 2005b; Semagn et al., 2007; Bonin and Kolb, 2009; Li et al., 2011; Bai et al., 2018). *Fhb4* was identified on chromosome 4B from the Chinese wheat cultivar Wangshuibai, which showed FHB type I resistance and explained 4.7%-17.5% of phenotypic variation (Yang J et al., 2005a; Lin et al., 2006). *Fhb5* has been associated with type I and type II resistance in more than 10 populations. It was detected on chromosome 5A and explains up to 30% of the phenotypic variation (Lin et al., 2006; Liu et al., 2009; Buerstmayr et al., 2011, 2012). In addition, a major effect on type II resistance was shown by the QTL on chromosome 2DL with an additive effect with *Fhb1* in different backgrounds (Jiang et al., 2007a; Bai et al., 2018). A QTL on 3AS has been identified in germplasm from several places including Europe, China, USA and Brazil. It

explained up to 17.9% phenotypic variation (Table 1; Zhang et al., 2012; Bai et al., 2018). Jia et al. (2018) conducted fine mapping of *Fhb1*, *Fhb2*, *Fhb4* and *Fhb5* reducing the interval of each to 0.19 cM, 2.2 cM, 0.14 cM and 0.09 cM respectively. As a subsequent step after a QTL mapping project, fine mapping can be used to discover markers closely linked or co-segregating with genes of interest followed by map-based cloning (Zheng et al., 2015). However, fine-mapping and map-based cloning is a resource- and time-consuming process and among the seven named wheat FHB resistance QTL, until now only the gene underlying *Fhb1* and *Fhb7* have been successfully cloned. Recent advances in genomics, proteomics and metabolomics could provide opportunities to speed up the analyses of the complex genetic mechanism and identification of candidate and causative genes.

Su et al. (2019) identified a gene, designated as *TaHRC*, encoding a putative histidine-rich calcium-binding protein via map-based cloning and EcoTILLING, which was shown to be the key determinant of *Fhb1* resistance. A large deletion was found in the open reading frame of this gene in FHB resistant genotypes showing a correlation of low percentage of symptomatic per spike (PSS) with resistance indicating that the loss-of-function of this gene is the determinant of FHB resistance. Using RNA interference (RNAi) and CRISPR-Cas9-mediated gene editing, significantly enhanced FHB resistance after knockdown or knockout of *TaHRC* expression suggested that *TaHRC-S* conditioned FHB susceptibility and that loss of function of *TaHRC-S* confers *Fhb1* resistance.

FHB resistance gene *Fhb7* was cloned by Wang et al. (2020) based on assembling the genome of *Thinopyrum elongatum*, which is used in wheat distant hybridization breeding. *Fhb7* encoded a glutathione S-transferase (GST) and conferred broad resistance to *Fusarium* species with detoxification of trichothecenes. In addition, *Th. elongatum* obtained *Fhb7* from an endophytic *Epichloe* species by horizontal gene transfer (HGT) because *Fhb7* GST homologs are absent in plants. This candidate gene was functional validated by different ways including virus-induced gene silencing (VIGS), EMS-induced mutation, and transgenic approaches.

Moreover, several FHB resistance candidate genes described below have been identified and resistance mechanisms are generally figured out. However, no map-based cloning and functional proof are conducted for those genes. FHB candidate gene

encoding an agmatine coumaroyl transferase, referred to as *TaACT*, was identified in wheat FHB *QTL-2DL*. It involved in cell wall fortification mechanisms against *F. graminearum* (Kage et al., 2017a). A candidate gene for wheat FHB resistance encoding lipid transfer proteins (LTP) was identified in plants carrying the resistant allele of *Qfhs.ifa-5A*, which was constitutively at least 50-fold more abundantly expressed after *F. graminearum* inoculation than mock inoculation. Another *Fhb1*-associated gene, a uridine diphosphate (UDP)-glycosyltransferase gene, designated as *TaUGT12887*, was mapped on the chromosome 5BL, which was able to conjugate DON to the less toxic metabolite D3G and weakly increases FHB resistance (Schweiger et al., 2013; Li, 2017; Zhang et al., 2018). Makandar et al. (2006) generated the *AtNPR1*-expressing transgenic wheat of FHB susceptible genotype and reported that FHB resistance in the *AtNPR1*-expressing wheat plants was associated with the faster and stronger activation of *PR1* (pathogenesis-related gene 1) expression in response to *F. graminearum*, presumably due to the enhanced responsiveness of these transgenic lines to an endogenous activator of plant defense. In wheat genotypes carrying the *Fhb1* QTL, genes encoding pathogenesis-related (PR) proteins such as β -1,3-glucanase (PR2), wheatwaxins (PR4) and thaumatin-like proteins (PR5) showed a significant upregulation, which indicated effective resistance responses to *F. graminearum* infection. In the Chinese FHB resistant landrace Wangshuibai, *Fhb1* mediated FHB resistance associated pathogen-related proteins including *PR14* and ABC transporter were highly expressed in a transcriptome analysis study. A hub gene of the phenylpropanoid pathway, *4CL*, leading to the biosynthesis of lignin and flavonoids has been considered as a potential resistance candidate gene conferring high rachis resistance to FHB. Cell wall appositions or papillae are formed by resistance related metabolites and callose, which might be accumulated by plants to limit fungal spread and reduce FHB severity. A lignin biosynthesis enzyme, Cinnamyl alcohol dehydrogenase (*CAD*), catalyzes the deposition of lignin, which can thicken the cell wall and obstruct the fungus to penetrate into the cell (Golkari et al., 2009; Jia et al., 2009; Xiao et al., 2013 and Dhokane et al., 2016). Although numerous putative FHB resistance related genes have been predicted through the genome-wide association studies, most of them are not in-depth studied and verified so far. Therefore, functions analysis and verification of FHB resistance related genes should be the key to overcome the wheat Fusarium head blight (FHB) disease (Zhang et al., 2018).

Table 1. Examples of novel *Fusarium* resistance QTL for head blight and crown rot identified in previous studies.

QTL names	Disease	Chr.	Resistance types	Flanking markers		QTL CI (cM)	Plant material	Resistance allele source	Phenotyping	References
<i>Fhb1</i>	FHB	3B	II	<i>XSTS3B80</i>	<i>XSTS3B142</i>	1.27	Sumai3*5 x Thatcher	Sumai 3	<i>F. graminearum</i> SFI: 1 greenhouse exp.	Cuthbert et al., 2006
<i>Fhb2</i>	FHB	6B	II	<i>Xgwm133</i>	<i>Xgwm644</i>	6	BW278 x AC Foremost	Sumai 3	<i>F. graminearum</i> SPRAY: 2 field exp.	Cuthbert et al., 2007
<i>Fhb4</i>	FHB	4B	I	<i>Xhbg226</i>	<i>Xgwm149</i>	1.7	Nanda2419 x Wangshuibai	Wangshuibai	<i>F. graminearum</i> SPRAY: 2 field exp.	Xue et al., 2010
<i>Fhb5</i>	FHB	5A	I	<i>Xgwm304</i>	<i>Xgwm415</i>	0.3	Nanda2419 x Wangshuibai	Wangshuibai	<i>F. graminearum</i> SPRAY: 2 field exp.	Xue et al., 2011
<i>Fhb7</i>	FHB	7D	II	<i>XsdauK66</i>	<i>Xcfa2240</i>	1.7	K11463 x K2620	K2620	<i>F. graminearum</i> SFI: 4 greenhouse exp.	Guo et al., 2015
<i>QFhs.nau-2DL</i>	FHB	2D	II	<i>Xgwm157</i>	<i>Xwmc041</i>	6.92	Veery x CJ 9306	CJ9306	<i>F. graminearum</i> SFI: 3 greenhouse exp.	Jiang et al., 2007a
<i>Qfhb.hwwg-3AS</i>	FHB	3A	II	<i>Xgwm5</i>	<i>Xwmc428</i>	17	Trego x Heyne	Heyne	<i>F. graminearum</i> SFI: 3 greenhouse exp. and 2 field exp.	Zhang et al., 2012
<i>Qcrs.cpi-3B</i>	FCR	3B	-	<i>wPt9546</i>	<i>Wpt10505</i>	7	Lang x CSCR6 Janz x CSCR6	CSCR6	<i>F. pseudograminearum</i> / <i>F. graminearum</i> SD: 2 greenhouse exp./ 4 greenhouse exp.	Ma et al., 2010
<i>Qcrs.cpi-5D</i>	FCR	5D	-	<i>barc143</i>	<i>cfid189</i>	-	Wylie x Sumai 3 Wylie x Chile Wylie x NK	Wylie	<i>F. pseudograminearum</i> SD: 3 growth room exp.	Zheng et al., 2014
<i>Qcrs.cpi-2D</i>	FCR	2D	-	<i>DArT</i> <i>Seq1131013</i>	<i>cfid73</i>	-	Wylie x Sumai 3 Wylie x Chile Wylie x NK	Wylie	<i>F. pseudograminearum</i> SD: 3 growth room exp.	Zheng et al., 2014

SPRAY: spray inoculation; SFI: single floret inoculation; SD: seedling dip

1.4 Current status of soil-borne diseases including FCR research

To date, the research of wheat *Fusarium* head blight (FHB) have been conducted at different aspects, including the way of *F. graminearum* penetrating and growing in the spikes and FHB resistance mechanisms for over 40 years. Nowadays, there are four important diseases of wheat roots worldwide, namely *Fusarium* root and crown rot (FCR), common root and foot rot (CRR), sharp eyespot, and take-all disease (Burgess et al., 2005; Fernandez et al., 2009; Xu et al., 2018). However, compared to FHB, *Fusarium* induced soil-borne diseases including the most widespread FCR disease have been much less studied (Backhouse et al., 2004; Burgess et al., 2005; Smiley et al., 2005; Poole et al., 2012; Wang, 2015; Yang et al., 2019). A complex of *Fusarium* species is causing root and crown rot including *F. pseudograminearum*, *F. culmorum* and *F. graminearum* (Leslie and Summerell, 2006; Moya-Elizondo, 2011a). *F. pseudograminearum* is the dominant species in the arid zones of the Pacific Northwest (PNW) and Australia causing FCR (Backhouse et al., 2004; Poole et al., 2013). *F. culmorum* was reported to be the predominant species in eastern Victoria and South Australia causing FCR (Smiley and Patterson, 1996; Backhouse and Burgess, 2002), and *F. graminearum* was reported to be virulent in eastern Australia and southern Europe causing FCR. Recently, *F. pseudograminearum* associated with the FCR complex syndrome in Spain as well as in the rest of Europe has been firstly reported (Agustí-Brisach et al., 2018). In Australia, *F. graminearum* root and crown rot (FCR) can inflict up to 89% yield losses of wheat (Klein et al., 1991) and cost the industry in excess of AU\$79 million per annum (Murray and Brennan, 2009). In the Pacific Northwest of the USA, the yield loss record was up to 35% reduction under normal fungal substance level (Smiley et al., 2005). Since soil-borne diseases cause a mass of losses in grain crops and aggregate to billions of dollars each year, they are considered as an important global problem (Liu and Ogbonnaya, 2015).

After *F. graminearum* inoculation, three infection phases are identified and separate during crown rot development, based on histological qPCR analyses in a time course experiments: (1) surface hyphal mats are formed at the infection spots during the initial spore germination, (2) the adaxial epidermis of outer leaf sheath are colonized and mycelia start to grow from the infection point to the crown, (3) the internal crown tissue is comprehensively colonized by *F. graminearum* (Stephens et al., 2008).

The symptoms of crown rot are necrosis and dry rot of the crown bases with brown color, which can extend up to 2- 4 nodes of the stem, and during humid weather pinkish fungal growth can be observed on the lower nodes (Matny, 2015). In the season with a wet beginning followed by dry conditions, the most severe situation is the formation of white heads. It is the consequence of infected plants suffering water and nutrients deficiency due to the constricted vascular system which causing prematurely ripened spikes during grain development, and very less shriveled or none seeds produced from infected tillers lead to yield loss. In addition, if seeds are infected by pathogens, the pre- or post- emergence seedling blight disease will take place latterly causing serious yield losses (Burgess et al., 2005; Mudge et al., 2006; Fernandez and Conner, 2011; Kazan and Gardiner, 2018; Xu et al., 2018). Poole et al. (2012) conducted an experiment of FCR resistance QTL identification, using seed soaking inoculation and evaluating crown symptoms of wheat. The crown rot also could be induced by *F. graminearum* colonizing wheat roots, because these pathogens are able to grow to the crown from roots. The symptoms of root rot are typically associated with brown and necrotic roots. Functions of roots and crown are impacted and they are losing the ability to stand, absorb water and nutrition are resulting in reduced seedling vigor, yield loss and seeds quality (Beccari et al., 2011; Wang, 2015). Wang (2015) reported that after successful colonization of roots, *F. graminearum* could be transported to the distal parts of wheats through the vascular system but no symptoms were observed in the upper main stem and leaves. The possible reason for such symptomless invasion could be that the life style of *F. graminearum* is shifted from necrotrophic to endophytic phase, and in this phase low concentration DON was released by fungus to disturb programmed cell death. In summary, wheat root rot and crown rot can be induced by the same pathogen for FHB, *F. graminearum*, and can penetrate different tissues (e.g. seeds, roots and stem base). Different organs inoculation experiments including seed, root and stem base infections could be applied to identify *F. graminearum* root and crown rot (FCR) resistance QTL and identify putative candidate genes underlying different resistance mechanisms and acting under different infection scenarios.

Because yield and economic losses caused by soil-borne diseases including Fusarium root and crown rot (FCR) have become more severe globally in recent years, this disease has become more prevalent, partially as a result of the adoption of moisture-preserving cultural practices, such as minimum tillage and stubble retention (Kazan and

Gardiner, 2018). Therefore, diseases management become more necessary and urgent. Different management measures are conducted by farmers, including agronomic practices, biocontrol, fungicides and disease prediction. Stubble burning or incorporation of stubble into the soil could decrease fungal levels. Because the optimal conditions for the initial inoculation of young seedlings are provided by stubble. Crop rotation followed by *Fusarium* non-host crops such as sorghum could have beneficial effects to reduce FCR. In addition, *Fusarium*-induced diseases can be accelerated by the use of high amounts of nitrogen fertilizers. On the contrary, wheat stems colonization can be restricted by zinc. Biocontrol agents including *Trichoderma spp.* and *Bacillus* strains could play roles at irritating and priming of pathogenesis-related (PR) proteins related genes expression by host plants. Meanwhile, applications of both biocontrol agents and fungicides could provide additional FCR protection. For the subsequent year, the levels of FCR inoculum in the soil or stubble can be considered as an indicator of FCR incidence which is significant negatively correlated with grain yield under the years with less rainfall during the grain filling phase. Therefore, it is not sufficient to predict soil borne diseases based on the fungal inoculum levels alone, but also consider environmental factors (Kazan and Gardiner, 2018).

Because incidences of FCR disease have grown in many cereal crops-growing areas globally, agronomic practices might not be the most sustainable methods to control *F. graminearum* soil borne diseases, (Liu and Ogonnaya, 2015). Therefore, creating resistance and tolerant wheat cultivars has been considered to be the most important breeding objective to manage diseases damage (Liu and Ogonnaya, 2015; Kazan and Gardiner, 2018). Several FCR resistance QTL have been identified crossing 14 of 21 wheat chromosomes. Among them, 7, 25 and 11 QTL were located on subgenomes A, B and D, respectively (Wallwork et al., 2004; Collard et al., 2005, 2006; Bovill et al., 2006, 2010; Li et al., 2010; Poole et al., 2012; Zheng et al., 2014; Martin et al., 2015; Liu and Ogonnaya, 2015; Yang et al., 2019; Pariyar et al., 2020). To date, only three QTL showed coincident significant effects in more than two populations (Table 1; Ma et al., 2010; Zheng et al., 2014). The first one with a large-effect FCR resistance QTL was located on the long arm of chromosome 3B, designated as *Qcrs.cpi-3B* and explains up to 48.8% of the phenotypic variance (Ma et al., 2010; Zheng et al., 2017). The second and third QTL, designated as *Qcrs.cpi-5D* and *Qcrs.cpi-2D* were detected on chromosomes 5DS and 2DL explaining up to 31% and 20% of phenotypic variance

respectively (Table 1; Zheng et al., 2014). Furthermore, *Qcrs.cpi-3B* was fine mapped within the interval of 0.7 cM (1.5 Mbp) on chromosome 3B by Zheng et al. (2015). Ma et al. (2010) reported that FCR resistance was not species-specific because overlapping resistance QTL were detected with comparable magnitudes for *F. graminearum* and *F. pseudograminearum* inoculations. Most of QTL analysis were conducted either at seedling stage (Collard et al., 2005, 2006; Bovill et al., 2006, 2010; Li et al., 2010; Zheng et al., 2014; Martin et al., 2015) or at adult stage (Wallwork et al., 2004). Poole et al. (2012) reported that FCR resistance QTL for seedling stage was different to adult stage. QTL contributing to FHB and FCR diseases were also different and not co-localized (Li et al., 2010). However, Pariyar et al. (2020) reported that FCR resistance QTL on chromosomes 3BS, 4BS, 6BS and 6DS were previously identified as FHB resistance QTL for disease incidence, spread and severity. Further comparison of FCR resistance QTL in the current study with FHB resistance QTL should be conducted.

To date, many QTL with different levels of FCR resistance have been detected in wheat (Wallwork et al., 2004; Bovill et al., 2006; Ma et al., 2010; Poole et al., 2012; Martin et al., 2015; Yang et al., 2019; Pariyar et al., 2020; Jin et al., 2020). The effectiveness and durability of FCR resistance could be increased by pyramiding multiple QTL (Bovill et al., 2010; Chen et al., 2015). However, the mechanism of disease resistance provided by FCR resistant QTL are still unknown, because no candidate genes underlying these DNA regions have been cloned. Recently, FHB resistance gene *Fhb7* was cloned and it encoded glutathione S-transferase (GST), which also conferred resistance to Fusarium root and crown rot (FCR). As expect, the large-effect QTL on chromosome 3BL in wheat seems to be the most possible region for the map-based cloning (Liu and Ogbonnaya, 2015). Mining more FCR resistance QTL and putative candidate genes could facility the study of resistance mechanism and provide the perfect markers which can be easily exploited in breeding program.

1.5 Life cycles of *Fusarium* species causing FHB and FCR diseases

Fusarium is a large genus of filamentous fungi widely distributed in plants and soils, which belongs to *Ascomycota* phylum, *Ascomycetes* class, *Hypocreales* order. The teleomorphs of *Fusarium* species are mostly classified in the genus *Gibberella*, only small number of species are classified in *Hemanectria* and *Albonectria* genera (Moretti, 2009). The primary morphological trait for characteristic of *Fusarium* genus is the distinctive septate, curved to crescent or sickle-shaped asexual macroconidia (Bullerman, 2003). Except for macroconidia *Fusarium* species produce other two types of spores: microconidia and chlamydospores. Macroconidia can be produced on monophialides and polyphialides in the aerial mycelium, but also on short monophialides in specialized structures called sporodochia (Moretti, 2009). Microconidia can vary in shape and size, such as pear-shaped, fusiform or ovoid, and straight or curved (Bullerman, 2003). They are produced in the aerial mycelium in clumps or chains, both on monophialides and polyphialides. Chlamydospores are resistance structures with thickened walls and high lipid content, which can form in the middle or termini of the hyphae and can survive in plant debris and the soil (Moretti, 2009). *Fusarium* species produce various pigments, with colors ranging from white, through pink, salmon-pink and carmine red, to purple. Some species also produce yellow and brown pigments. *Fusarium* colony showed velvety to cottony surfaces on potato dextrose agar (PDA). Most *Fusarium* species are common in tropical and subtropical regions with some found in temperate zones (Nucci et al., 2009).

The genus contains more than 20 species, of which 14 are significant to crop producers because they can cause several diseases, including Fusarium head blight (FHB) primarily caused by *F. graminearum*, Fusarium root and crown rot (FCR) caused by complex *Fusarium* species of *F. pseudograminearum*, *F. culmorum* and *F. graminearum* (Leslie and Summerell, 2006; Early, 2009; Moya-Elizondo, 2011a). *F. culmorum* can be distinguished from *F. pseudograminearum* and *F. graminearum* by comparison of the size of the macroconidia under the microscope. The macroconidia of *F. culmorum* are shorter, stout, thick walled and lack a distinctive foot-shaped basal cell which the other two *Fusarium* species show (Leslie and Summerell, 2006). However, it is difficult to separate *F. pseudograminearum* and *F. graminearum* using morphological features. Instead, a species-specific PCR assays can be used to differentiate all three *Fusarium* species (Akinsanmi et al., 2004). Isolates of *F.*

graminearum and *F. pseudograminearum* can cause equally severe CR in bioassays indicating a lack of pathogenic specialization of these two *Fusarium* species (Akinsanmi et al., 2004; Chakraborty et al., 2010). In addition, *F. graminearum* can cause FHB and FCR diseases. *F. graminearum* can invade different plant organs including the root, the stem base and the grain and results in producing deoxynivalenol (DON). FCR severity seems to be increasing in areas where FHB is common, eventually leading to severe yield loss and contamination in wheat production (Dyer et al., 2009). *F. pseudograminearum* also produces DON, but *F. pseudograminearum* in general does not infect wheat heads (Serfling et al., 2017).

Fusarium graminearum Schwabe [teleomorph: *Gibberella zeae* (Schw.) Petch] is a haploid homothallic ascomycete and has sexual and asexual life cycles (Parry et al., 1995; Trail, 2009). Sexual ascospores are produced by *G. zeae*, the sexual stage of *F. graminearum* and are discharged into the air forcibly through flask-shaped perithecia on the crop debris. Ascospores land on flowering spikelets of wheat, germinate and enter the plant through natural openings such as stomates or through degenerating anther tissues (Trail, 2009; wang, 2015; Turkington et al., 2016). The fungus then grows by spreading through the xylem and pith intercellularly and asymptotically (Guenther and Trail, 2005; Jansen et al., 2005, Turkington et al., 2016). In the asexual cycle, macroconidia are produced on the surface of infected plants or on crop overwintering residues then moved to spike via rain-splash dispersal causing head blight (Trail, 2009; Turkington et al., 2016). These macroconidia also can colonize roots, sub-crown internode and leaf sheaths of lower nodes. Symptoms spread to the stems and cause potential formation of whitehead during grain fill (Kazan and Gardiner, 2018; Xu et al., 2018; Jevtić et al., 2019). *F. culmorum* and *F. pseudograminearum* have similar asexual life cycles as described above for *F. graminearum*. However, the former is not known to produce ascospores (teleomorph) and the latter is heterothallic species undergoing a complete sexual cycle to produce ascospores by different mating types in sexual structures called perithecia (Figure 2; Leslie and Summerell, 2006; Kazan and Gardiner, 2018).

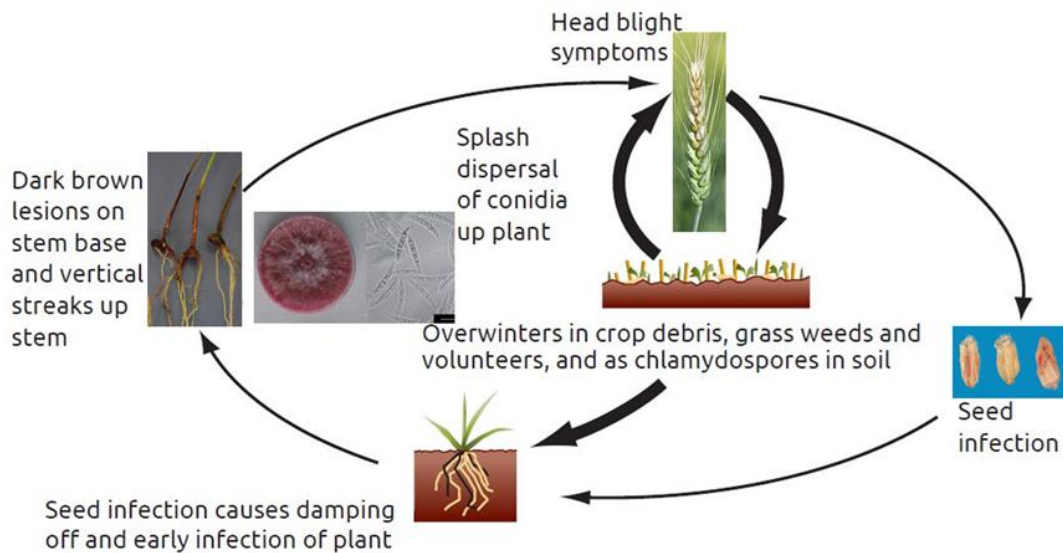


Figure 2. The life cycle of *F. graminearum* Schwabe [teleomorph: *Gibberella zeae* (Schw.) Petch] in wheat.

Based on the lifestyles of plant pathogens, they are generally divided to three groups: biotrophs, necrotrophs and hemi-biotrophs. Biotrophic pathogens take up nutrients from living host tissues, necrotrophic pathogens take up nutrients from dead or dying cells, and hemi-biotrophic pathogens show both modes of nutrition as biotrophs and necrotrophs (Agrios GN, 2004). At the cellular level, the microscope study indicates that during the early floral infection process of *F. graminearum*, the extracellular exudates in the apoplast are initially taken by *F. graminearum* hyphae without specialized feeding structures and no symptoms are observed. After that, *F. graminearum* initiates a stage associated with intracellular colonization, cell death and necrosis. Therefore, *F. graminearum* is a hemi-biotrophic pathogen with a short biotrophic phase followed by necrotrophic phase (Brown et al., 2010; Gunupuru et al., 2017).

Wang (2015) reported that roots of wheat also could be infected by macroconidia of *F. graminearum* causing root and crown rot, which was validated through fluorescence microscopy observation. The invasion of the tissue by the fungus can be separated into three phases including the early infection stage, the main infection stage and the root colonization stage. During the first phase, dense networks of hyphae were formed on the root surface of partially resistant and susceptible cultivars and no symptoms were found. However, infection pegs and penetration hyphopodia were observed at infection sites and an extra- and intracellular hyphal growth occurred at this stage. During the

main infection stage, the first necrotic cells were surrounded by runner hyphae, root structures and infection cushions. Extraordinary symptoms were found on the roots of a susceptible cultivar. At the root colonization stage, the numerous sporangia, macroconidia and chlamydospores were identified in the susceptible cultivar indicating successful systemic root colonization and the beginning of penetration into uninfected regions. On the contrary, partially resistant cultivar showed much healthier and only sporadically necrotic cells were detected. Finally, *F. graminearum* root and seed inoculations were conducted in the present study based on descriptions of Wang (2015) and Poole et al. (2012).

2 Objectives

Although Fusarium root and crown rot (FCR) diseases are causing dramatic losses of yield and billions of dollars each year world-wide, they have been much less studied compared to Fusarium head blight (FHB) disease. Besides *F. pseudograminearum* and *F. culmorum*, *F. graminearum* well known to cause FHB can also cause root and crown rot diseases upon root infection from previous *F. graminearum*-wheat root interactions studies. In addition to seed infection, root infection of *F. graminearum* causing root and crown rot has not been documented yet and will be studied in this thesis. Over decades, comparing to FHB resistance studies much less FCR resistance QTL have been identified in wheat and no resistance candidate genes have been cloned even underlying the QTL with the largest effect although FCR disease has become more severe in the worldwide scale. To accelerate breeding and create FCR resistant and tolerant wheat cultivars, it is necessary to understand the mechanisms of wheat responses against *F. graminearum* at the genetic and molecular level.

Thus, the objectives of the present study were (1) to evaluate and analyze different disease-related traits and trait correlations of a segregating DH population after *F. graminearum* root and/or seed inoculations; (2) to identify broad-range and infection-specific FCR resistance QTL; (3) to compare QTL with previously reported FCR and FHB resistance QTL; and (4) to mine for and predict candidate genes involved in FCR resistance from selected QTL regions.

3 Materials and methods

3.1 Development of mapping population

A doubled haploid (DH) wheat population of 104 lines was developed from a cross between line 162.11 and cv. Tobak. The generation of DH lines was conducted at the breeding company W. von Borries-Eckendorf GmbH and Co. KG. Wheat-maize pollination followed by embryo rescue and colchicine treatment were used to develop the doubled haploid population (Thomas et al. 1997). Line 162.11 was considered to be partially resistant to Fusarium root and crown rot (FCR) after *F. graminearum* root infection whereas cv. Tobak was susceptible, and both showed susceptibilities to Fusarium head blight (FHB). The pedigree of line 162.11 is Tyberius/Opus and cv. Tobak has the pedigree Ellvis/ Drifter// Koch, and two parents of DH lines are winter wheat from Germany (Wang, 2015).

3.2 Climate chamber experiments for evaluation of FCR resistance

3.2.1 Fungal material

F. graminearum isolate 'IFA 65' (IFA, Department for Agrobiotechnology, Tulln, Austria) was grown on synthetic nutrient agar (SNA) medium 'Spezieller Nährstoffarmer Agar' (Leslie and Summerell, 2006) at 20°C under cool-white and near-UV light illumination. After nine days, macroconidia were collected by washing into 0.02% (v/v) Tween-20 solution. After filtration of the spore suspension through four layers gauze, the concentration of macroconidia suspension was determined using a hemocytometer and was adjusted to 5×10^4 macroconidia ml⁻¹ for root-dip inoculation and 2.5×10^5 macroconidia ml⁻¹ for seed-dip inoculation (Wang, 2015; Poole et al., 2012).

3.2.2 Root-dip inoculation and plant tissue sampling

For the seedling root infections, wheat seeds were sterilized in 6% sodium hypochlorite for 40 min on a rotary shaker and then washed 10 times with distilled water. Subsequently, seeds were sown in autoclaved sand in the climate chamber with a 16 h photoperiod of 22°C/18°C day/night and 60% humidity until Zadoks stage (Z) 11 according to Zadoks et al. (1974), when the 1st leaf was unfolded. The seedling roots were inoculated with *F. graminearum* spore suspension as described below.

Prior to inoculation, plants were carefully removed from the sand to avoid root injury and immersed in water to obtain intact roots. To protect them from undesired

inoculations, hypocotyl and stem above the roots of five plants were covered by a wrapped aluminum foil, and were transferred into a small flat tray by submerging their roots in 5 ml (5×10^4 macroconidia ml⁻¹) inoculum. The flat tray with plants were gently shaken for 2 h on a rotary shaker. For control plants, mock inoculations with double-distilled water instead of fungal suspension. After root inoculation, five seedlings were planted in one pot (7.5 × 7.5 × 8.0 cm) with autoclaved sand and three pots per DH lines and parental genotypes. Plants were cultivated in a climate chamber under a 16/8 h day/night rhythm with approximately 60% relative humidity at 20 °C, which was in the temperature range of 15-32°C required for successful *F. graminearum* infection (Sitton and Cook, 1981). Plants were irrigated as needed, and allowed to dry significantly prior to harvest to stimulate the onset of symptoms.

Considering the space of climate chamber and labor force the 104 DH lines were split into nine sub-experiments each including two parental genotypes (references) and eight to 13 wheat DH lines with 15 replicates. Two sub-experiments were conducted per week and the climate chamber was cleaned by surface disinfection with MENNO Florades (Menno Chemie Norderstedt, Germany) prior to each cultivation and inoculation. At 21 days after inoculation (dai), 15 plants were collected per line and reference. The roots of each plant were washed in distilled water, and three pools of each five plants were sampled after root, shoot length measured and disease symptoms scored. Immediately after harvesting, plants were freeze-dried at -60 °C for four days before measurement of root and shoot dry weight of each plants pool.

3.2.3 Seed-dip inoculation and plant tissue sampling

Wheat seeds were sterilized in 6% sodium hypochlorite for 40 min on a rotary shaker and then washed 10 times with distilled water. Seeds of each line and references were placed in 50 ml Falcon tube with 20 ml macroconidia suspension for 3 min and dried approximately two days prior to planting. For control plants, mock inoculations were performed with double-distilled water instead of fungal suspension. After seed inoculation, 48 seeds per treatment were sown in pots (7.5×7.5×8.0 cm) with autoclaved sand. Plants were cultivated in the climate chamber with a 16 h photoperiod of 22°C /18°C day/night and 60% humidity until they were rated at 35 days after inoculation. Plants were irrigated as needed, and allowed to dry significantly prior to harvest to stimulate the onset of symptoms.

Considering the space of climate chamber and labor force 103 DH lines (seeds of DH68 were used up) were split to eight sub-experiments each including two parental genotypes and 12 to 13 wheat DH lines. Two sub-experiments were conducted per week and the climate chamber was cleaned by surface disinfection with MENNO Florades (Menno Chemie Norderstedt, Germany) prior to each cultivation and inoculation. At 35 days after inoculation (dai), 48 plants were collected per line and reference. Three pools of each 16 plants were sampled after shoot length measured and disease symptoms scored. Immediately after harvesting, plants were freeze-dried at -60 °C for four days before measurement of root and shoot dry weight of each plants pool.

3.3 Fusarium root and crown rot (FCR) bioassay

3.3.1 Root and shoot length, dry weight assessments upon root inoculation

Root and shoot length were measured for 15 plants of each DH line and references under *F. graminearum* and water treatments at 21 dai. The dry weight of plants in three pools including a total of 15 plants root and shoot were measured and divided by plant number to obtain the mean single plant dry weight value. To eliminate the putative variation in the root and shoot growth of different lines, relative reductions of root length (RLR), shoot length (SLR), root dry weight (RDWR) and shoot dry weight (SDWR) were calculated as ‘(control-inoculated) / control×100’ (Wang, 2015).

3.3.2 Root and shoot length, dry weight assessments upon seed inoculation

The number of surviving plants under *F. graminearum* and water treatments were counted. Shoot length of 48 infected plants were measured for each DH line and references at 35 dai, and shoot length of dead plants were scored as 0 cm. The dry weight of plants in three pools including a total of 48 plants root and shoot were measured and divided by plant number to obtain the mean single plant dry weight. As described for the *F. graminearum* root inoculation experiment, relative reductions of root dry weight (RDWR) and shoot dry weight (SDWR) were calculated as ‘(control-inoculated) / control×100’ (Wang, 2015). Root and shoot reduction values of dead plants were calculated as the maximum 100%.

3.3.3 Visible symptom assessments

As disease symptoms on roots were not evident, the scoring was only performed for the stem bases of the plants. Symptoms on stem bases were rated by applying discoloration and symptom extension scale (0 to 4) of each seedling between the root-stem-junction and the first leaf node. The discoloration scale (DS) ranged from 0 to 4 (0, symptomless; 1, slightly necrotic; 2, moderately necrotic; 3, severely necrotic; 4, completely necrotic). The discoloration extension (length of discoloration section) scale (DES) ranged from 0 to 4 (0, no lesions; 1, 1-25%; 2, 25-50%; 3, 50-75%; 4, >75% of stem bases; Wang, 2015). Stem base symptom index (SbSI) was calculated using the equation: $SbSI = \frac{\sum B_1 \dots B_n}{n} + \frac{\sum E_1 \dots E_n}{n}$; where B and E each represents the parameter browning and extension index, and n represents the number of assessed individuals (Wang, 2015). In addition, the ratio of stem discoloration (DL_SLi) was calculated from the length of discoloration section (DL) on the stem base and the total shoot length (SLi) according to Mitter et al. (2006). This value was termed crown severity index by Mitter et al. (2006). In this study the stem base was defined as the area extending from the sub crown up to the first stem internode.

3.4 Data Analysis

Relative standard deviation of phenotypic data for each reference were analyzed in every sub-experiment. Combined data from all sub-experiments were firstly compared between *F. graminearum* and mock treatments, and then two references were compared for each trait. Phenotypic data of DH lines in each sub-experiment were normalized by references (internal controls) when significant differences and multiple groups were obtained among sub-experiments in ANOVA and Duncan's multiple range test. The normalized value of each trait was calculated as follows:

$$Traits\ value_{normalized} = \frac{Traits\ value}{(Traits\ value_{line\ 162.11} + Traits\ value_{cv.\ Tobak})/2}$$

(Rygulla et al., 2007)

Correlations between pairs of all traits were measured as Pearson's correlation coefficient (r), all phenotypic data were analyzed using MS-excel 2016, SPSS. 22, SigmaStat 4.0 and R package 'corrplot'.

3.5 Genotyping and genetic linkage map construction

104 DH lines and two parents (line 162.11 and cv. Tobak) were genotyped using a 15k Infinium SNP array, which is an optimized and reduced version of the 90k iSELECT SNP-chip described by Wang et al. (2014). The 15k SNP-chip was developed by TraitGenetics GmbH (Gatersleben, Germany) and genotyping was performed by this company.

Marker alleles were scored as correlating to the respective parents for line 162.11 (A) and cv. Tobak (B). Bad quality SNP markers, with more than 10% of missing data and more than 0.30 segregation distortion were excluded from the 13,006 SNPs. In the end, the linkage map was constructed with 3305 polymorphic SNP markers using the software Joinmap 4.0 (Van Ooijen, 2006). However, many SNPs were mapped at the same loci (recombination frequency was estimated as zero) or within 0.01cM among them. Therefore, a customer Perl script was applied to integrate BIN markers. Markers were assigned to linkage groups applying the independence LOD parameter with LOD threshold values ranging from 2.0 to 20.0 in steps of 2.0. The Kosambi mapping function was used to calculate the genetic distance between the markers (Kosambi, 1944) with the default calculation setting (using linkages with a recombination frequency smaller than 0.40 and LOD higher than 1; goodness-of-fit jump threshold for removal of loci 5 and performing a ripple after adding 1 loci). Within each linkage group, SNP markers clustered together with logarithm of odds (LOD) of 5 or greater were selected for ordering. The short and long arms of chromosomes were confirmed according to the wheat 90K consensus SNP maps (Wang et al., 2014). And the software MapChart 2.32 was used to draw the linkage map (Voorrips, 2002). To confirm the marker order in the present linkage map, marker assignments to linkage group were compared with the corresponding positions in the consensus map constructed by Wang et al. (2014) and Wen et al. (2017).

3.6 QTL mapping

For QTL mapping, trait data, genotype data, and map information were imported and composite interval-regression mapping (CIM) was performed using the computer program QGene v 4.3.1. The scan interval was set at 2 cM and forward cofactor selection was applied. To detect significant and putative QTL, a critical LOD threshold value of 2.5 was used, because DH population size was small (104 DH). The 95% confidence intervals of QTL were estimated using the ‘one-LOD support interval,’ which is determined by reducing 1 LOD score of regions on both sides of a QTL peak (Lander and Botstein, 1989; Visscher et al. 1996; Hackett, 2002; Collard et al., 2005). The proportion of phenotypic variance explained by the QTL was determined by the square of the partial correlation coefficient (R^2). A QTL that explained more than 10% of the phenotypic variance (R^2) is classified as a major QTL and those explaining less than 10% as minor QTL according to Collard et al. (2005). For QTL add effects, positive and negative signs of the estimates indicated the contribution of line 162.11 or cv. Tobak according to traits. Graphical representation of linkage groups was carried out using MapChart 2.32 software (Voorrips, 2002).

3.7 *In-silico* annotation of putative genes linked to FCR resistance

The gene expression database ‘Wheat expression browser’ (expVIP; <http://www.wheat-expression.com/>) was used to perform an *in-silico* analysis of the expression of model genes underlying selected FCR resistance QTL from the IWGSC RefSeq v1.0. The database contains 850 RNA-Seq samples derived from 32 tissues at different growth stages and/or challenged by different stress treatments including *F. graminearum*/*F. pseudograminearum* treatment (Borrill et al., 2016). Generally, a cutoff value of >2 TPM (transcript per million) is considered as a threshold for gene expression (Wagner et al., 2013). For comparing multiple genes expression across several categories, log₂(tpm) is suggested as the expression unit providing better resolution in heatmap. Therefore, the gene expression threshold is 1 calculated as log₂(2) (Borrill et al., 2016). Genes showing at least two times higher expression or specific expression under *F. graminearum*/*F. pseudograminearum* treatment between resistant and susceptible genotypes were selected. Further functional annotation is based on the column ‘Human readable descriptions’ in the file ‘iwgsc_refseqv1.0_FunctionalAnnotation_v1_HCgenes_v1.0.TAB’ downloaded from https://urgi.versailles.inra.fr/download/iwgsc/IWGSC_RefSeq_Annotations/v1.0/, the

transcriptomics database for plant defense responses to pathogens (PlaD, http://systbio.cau.edu.cn/plad/wheat_search.php#result) and based on further literature analyses (Google scholar).

4 Results

4.1 *F. graminearum* root inoculation experiment

4.1.1 Phenotypic variation between parents of the mapping population

Phenotypic data obtained in nine sub-experiments for the two parents of the mapping population were combined to evaluate if the general performances of each parent under control and infection conditions across experiments was statistically different. As expected, significant differences (P -value= 0.001) were found for each of the two genotypes between the two treatments (mock- and *F. graminearum*-inoculated) for root length (RL), shoot length (SL), root dry weight (RDW) and shoot dry weight (SDW) applying ANOVA indicating that infection was affecting these traits in both genotypes. When comparing the traits between two parents for the mock-inoculated data set and for the *F. graminearum*-inoculated data set, root and shoot length under mock and root length under *F. graminearum* inoculations and stem base symptom index (SbSI) showed significant differences indicating that genotype-specific differences exist in healthy as well as in infected parental genotypes. In contrast, significant differences were not found for shoot length (SLi) and for the ratio of the discoloration section length on stem base to shoot length (DL_SLi) under *F. graminearum* treatment as well as dry weight of root and shoot under both treatments for two parents.

However, the morphological traits root and shoot length exhibited significant differences between two parents without *F. graminearum* inoculation indicating that genetic variation for root and shoot growth exists in the non-treated healthy parents. To remove such effects the *F. graminearum*-treated data set was normalized based on the non-inoculated controls and expressed in relative reduction upon *F. graminearum* inoculation. The root dry weight showed the most severe decrease upon *F. graminearum* inoculation and the reduction of shoot length was the lowest for both parental genotypes (Figure 3). Line 162.11 has previously been described to be partially resistant to *F. graminearum* root infection and cv. Tobak has been described to be susceptible (Wang, 2015). Also, in the present study line 162.11 showed less reduction of root and shoot length, root and shoot dry weight compared to cv. Tobak under *F. graminearum* treatment (Figure 3). However, significant differences for the reduction upon *F. graminearum* treatment were not found between two parents in ANOVA.

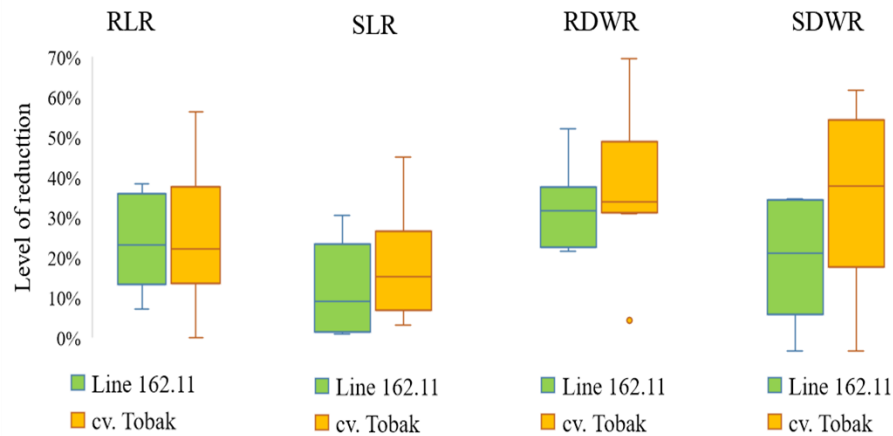


Figure 3. Comparison of relative reduction upon *F. graminearum* root inoculation between two parental genotypes of the mapping population combining data from nine sub-experiments. RL= Root length, SL= Shoot length, RDW= Root dry weight, SDW= Shoot dry weight, R= Relative reduction values calculated as '(mock-infected)/mock×100' (Wang, 2015).

4.1.2 Phenotypic variation for parents of the mapping population between sub-experiments

Because the phenotyping of two parental genotypes were applied in all nine sub-experiments they could be used for evaluation of variation between sub-experiments. The relative standard deviation (coefficient of variation, $SD/mean \times 100$) values of cv. Tobak for root length (RL), root dry weight (RDW), shoot length (SL) and shoot dry weight (SDW) ranged from 8% to 65% in 9 sub-experiments. In contrast to the lower relative SDs observed for length and dry weight parameters, the relative SD values for disease symptom traits ranged from 30% up to 110%. Another parent line 162.11 showed the similar range of relative SD for morphological traits and disease symptom traits as that of cv. Tobak. Such high relative SD value of disease symptom traits might indicate that disease scoring based on visual observation of symptoms, e.g. using discoloration scale, can be expected to be more biased and less precise compared to root and shoot length and weight measurements by ruler and scale.

For cv. Tobak, SD values of shoot length and shoot dry weight were less than that of root length and root dry weight under both treatments (compare A with B and C with D in Figure 4). This indicates that shoot traits are less environmentally dependent compared to root traits. For another parent line 162.11, similar results were found with lower SD values for shoot length and shoot dry weight than that for root length and root dry weight under *F. graminearum* and mock treatments, and high SD values for disease symptom traits (Figure A1).

In each sub-experiment, as expected cv. Tobak showed lower mean values for length and dry weight of root and shoot under *F. graminearum* treatment than that under mock treatment (Figure 4). Most of the minimum values of above traits were found in sub-experiment 4, which might indicate more extreme suboptimal growing conditions or stress in this sub-experiment. The poor performance of plants in sub-experiment 4 is unlikely to be due to high levels of *F. graminearum* infection caused by inaccurate inoculum preparation because disease severity measures did not show the highest values compared to other sub-experiments (Figure 4 E and F).

ANOVA showed significant differences for most of traits between nine sub-experiments for two parents. Also, Duncan's multiple range test classified more than one group (Figure 4). However, for line 162.11 only one group was classified for root and shoot dry weight under both treatments except shoot dry weight under mock treatment, indicating that dry weight of line 162.11 may be a trait which is less environmentally-sensitive (Figure A1). In conclusion, nine sub-experiments should be treated as different environments, although they were conducted in the climate chamber according to the protocol described by Wang (2015). This may be due to effects such as differences in infection levels, light, humidity and evaporation in the growth chamber. Therefore, the phenotypic data of DH lines in each sub-experiment should be normalized using the two parental genotypes as references. This is a common approach used to compensate for a fluctuating infection level (environment variance) between multiple independent trials applying reference genotypes as internal control (Happstadius et al., 2003; Rygulla et al., 2007; Eynck et al., 2009). However, because of some missing phenotypic data for line 162.11 in two sub-experiments, the values from cv. Tobak were applied for normalization of the data for all DH lines in different sub-experiments and all subsequent analyses for *F. graminearum* root inoculation.

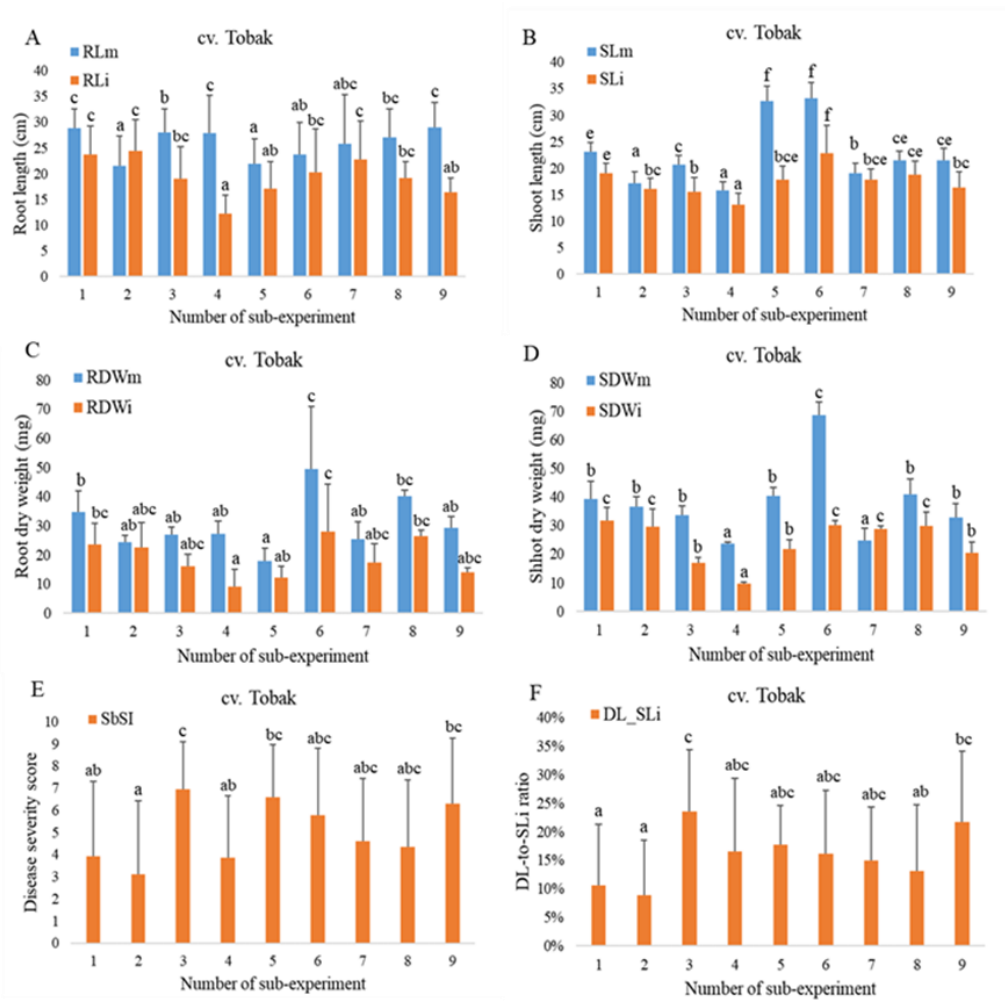


Figure 4. Comparison of phenotypic data for different traits of cv. Tobak in nine sub-experiments upon mock and *F. graminearum* root inoculations. (A) root length, (B) shoot length, (C) root dry weight, (D) shoot dry weight, (E) and (F) disease severity indices. Bars represent standard deviation. RL= Root length, SL= Shoot length, RDW= Root dry weight, SDW= Shoot dry weight, SbSI= Stem base symptom index, DL_SL= Ratio of discoloration section length on stem base to shoot length, i= infected, m= mock, a-f= Groups from a Duncan's multiple range test. Three biological replicates were assessed in each sub-experiment for dry weight, 15 biological replicates for all other traits.

4.1.3 Phenotypic variation of the mapping population

Generally, for the DH population the mock-inoculated data set showed lower relative standard deviations (SD) compared to the *F. graminearum*-inoculated plants at 21 days after inoculation (dai) for length and dry weight of root and shoot. Relative standard deviations (SDs) for shoot length and for shoot dry weight were smaller compared to those for root length and root dry weight under mock and *F. graminearum* treatments. Disease severity values showed the highest relative standard deviations (SD) up to 180% in all traits.

In the ANOVA significant differences were found for root and shoot length, root and shoot dry weight when *F. graminearum* and mock treatments were compared for raw data (Figure 5A-D at top), indicating that *F. graminearum* infection impacts all measured traits as expected. However, for some traits the statistical significance between the mock- and *F. graminearum*-inoculated data sets for 104 lines after normalization was reduced or not reaching the threshold of 0.05. This is visualized in Figures 5. For example, the root length and root dry weight were not statistically significantly different anymore after normalization (Figure 5 A and C at bottom). This suggests that root length and weight traits are strongly influenced to different levels in the mock- and *F. graminearum*- inoculated data sets by the environment and using them in subsequent statistic and QTL analyses without normalization may lead to wrong biological interpretation.

For raw data, infected plants showed more serious reduction of dry weight compared to reduction of length for root and shoot. Among them, the root dry weight under *F. graminearum* treatment exhibited the most severe average reduction value of 45% whereas the shoot length showed the lowest reduction value of 13% (Figure 6). After normalization root dry weight of *F. graminearum*-inoculated plants also showed the most severe reduction comparing to other traits (Figure 6). Raw and normalized data sets both showed significant difference between length and dry weight of root and shoot reductions indicating that reduction values may not be strongly affected by the environment variance.

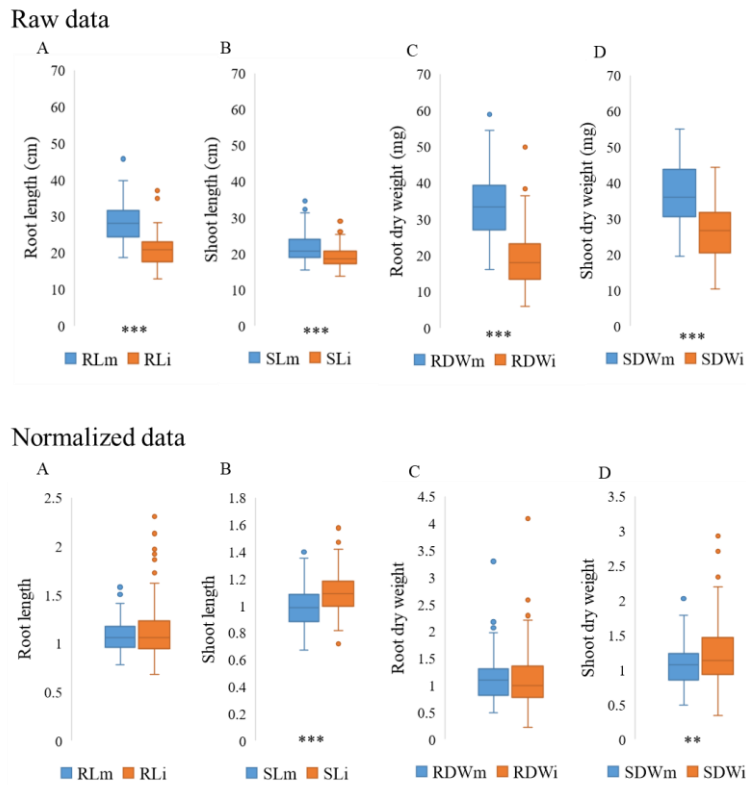


Figure 5. Comparison of mean phenotypic data for 104 DH lines derived from the cross of line 162.11 × cv. Tobak before (raw data) and after (normalized data) normalization in *F. graminearum* root inoculation experiment. (A)-(D) length and dry weight of root and shoot. Stars indicate *P*-values from an ANOVA comparing the phenotypic data of the two groups: * = 0.05, ** = 0.01 and * = 0.001. RL= Root length, SL= Shoot length, RDW= Root dry weight, SDW= Shoot dry weight, i= infected, m= mock.**

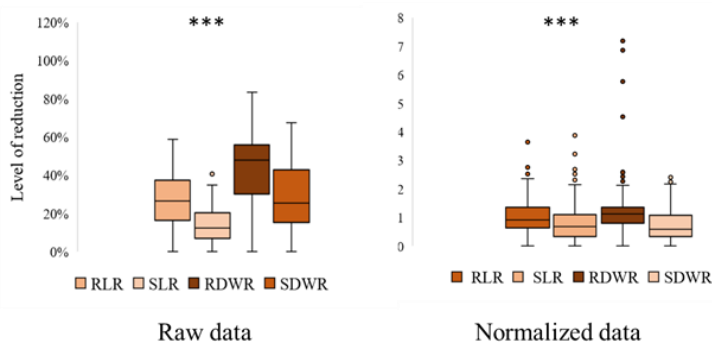


Figure 6. Comparison of relative reduction phenotypic data for 104 DH lines derived from the cross of line 162.11 × cv. Tobak before (raw data) and after (normalized data) normalization in *F. graminearum* root inoculation experiment. Stars indicate *P*-values from an ANOVA comparing the phenotypic data of the two groups: * = 0.05, ** = 0.01 and * = 0.001. RL= Root length, SL= Shoot length, RDW= Root dry weight, SDW= Shoot dry weight, R= Relative reduction.**

Details on raw and normalized phenotypic data sets are reported in Table A1 and Table 2. For raw data, the population means of traits under mock treatment are between the means of parents except for root dry weight (RDWm) which slightly exceeded the parent with the higher value. In contrast, most of populations means for traits under *F. graminearum* treatment and reduction values are higher than means for the parent with the higher values except for three traits (root length, root dry weight and shoot dry weight reduction). This indicates a transgressive segregation can be observed for a number of traits (SLi, RDWi, SDWi, DS, DES, SbSI, DL, RLR, SLR, RDWR), where positive or negative alleles are inherited from both parents (Table A1). This is also visible from Figure 7. After data normalization based on the parent cv. Tobak cross nine sub-experiments, the frequency distributions of the population shifted to left skewed distribution. It suggests that environment variance may have impacts on morphological traits reduction and disease severity of pants after *F. graminearum* root inoculation.

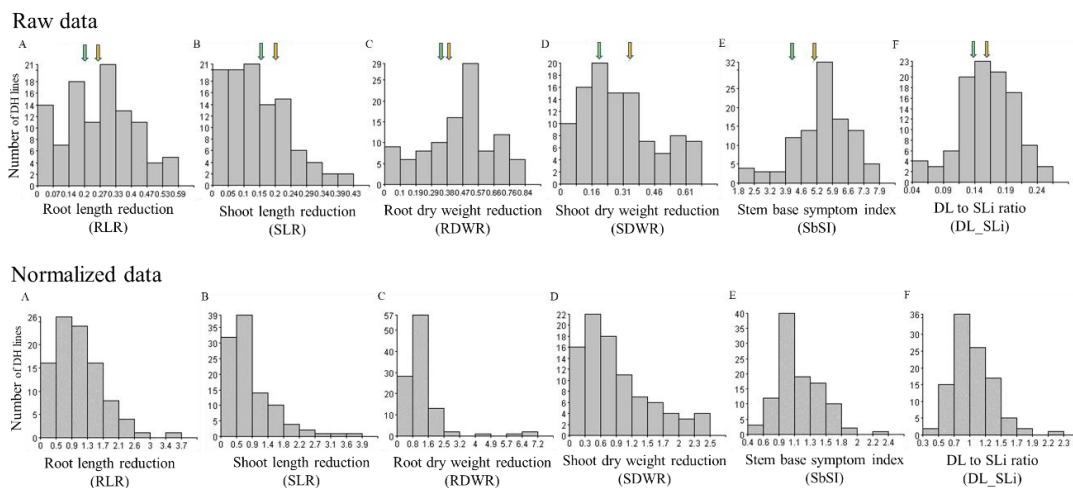


Figure 7. Comparison of phenotype frequency distributions of 104 DH lines derived from the cross of line 162.11 × cv. Tobak before (raw data) and after (normalized data) normalization in *F. graminearum* root inoculation experiment. (A)-(D) reduction of length and dry weight of root and shoot. (E) and (F) disease severity indices. RL= Root length, SL= Shoot length, RDW= Root dry weight, SDW= Shoot dry weight, SbSI= Stem base symptom index, DL_SL= Ratio of discoloration section length on stem base to shoot length, i= infected, R= Relative reduction. Green arrow indicates line 162.11 and yellow arrow indicates cv. Tobak.

Table 2. Normalized phenotypic data in mock and *F. graminearum* root inoculations experiment.

Treatment	Traits	Traits (Abbreviations)	Population statistics				
			Min.	Max.	Mean	Median	CoV (%)
Control	Root length	RLm	0.78	1.58	1.07	1.06	2.28
	Shoot length	SLm	0.67	1.40	0.99	0.98	1.17
	Root dry weight	RDWm	0.49	3.30	1.15	1.10	2.00
	Shoot dry weight	SDWm	0.50	2.03	1.06	1.07	1.24
Infected	Root length	RLi	0.68	2.30	1.13	1.06	2.47
	Shoot length	SLi	0.72	1.58	1.09	1.09	1.49
	Root dry weight	RDWi	0.23	4.08	1.10	0.99	2.61
	Shoot dry weight	SDWi	0.34	2.93	1.21	1.13	1.86
	Discoloration scale	DS	0.45	2.92	1.20	1.08	5.09
	Discoloration extension scale	DES	0.27	2.00	1.05	1.00	5.44
	Stem base symptom index	SbSI	0.36	2.39	1.11	1.03	4.97
	Discoloration section length	DL	0.30	2.88	1.08	1.06	6.05
	DL to SL ratio	DL_SLi	0.23	2.30	0.98	0.94	20.89
Reduction	Root length	RLR	0.00	3.64	1.01	0.92	11.52
	Shoot length	SLR	0.00	3.87	0.80	0.68	12.65
	Root dry weight	RDWR	0.00	7.18	1.26	1.13	5.67
	Shoot dry weight	SDWR	0.00	2.45	0.83	0.67	6.16

4.1.4 Trait correlations

Significant trait correlations for normalized phenotypic data measured as Pearson's correlation coefficient (r) have been calculated and are shown ($P < 0.05$) in the correlation matrix (Figure 8). The correlation of three different disease indices (DS, SbSI and DL_SLi) between each other and between morphological traits of healthy (mock-treated) and infected plants were analyzed (root and shoot length, root and shoot dry weight).

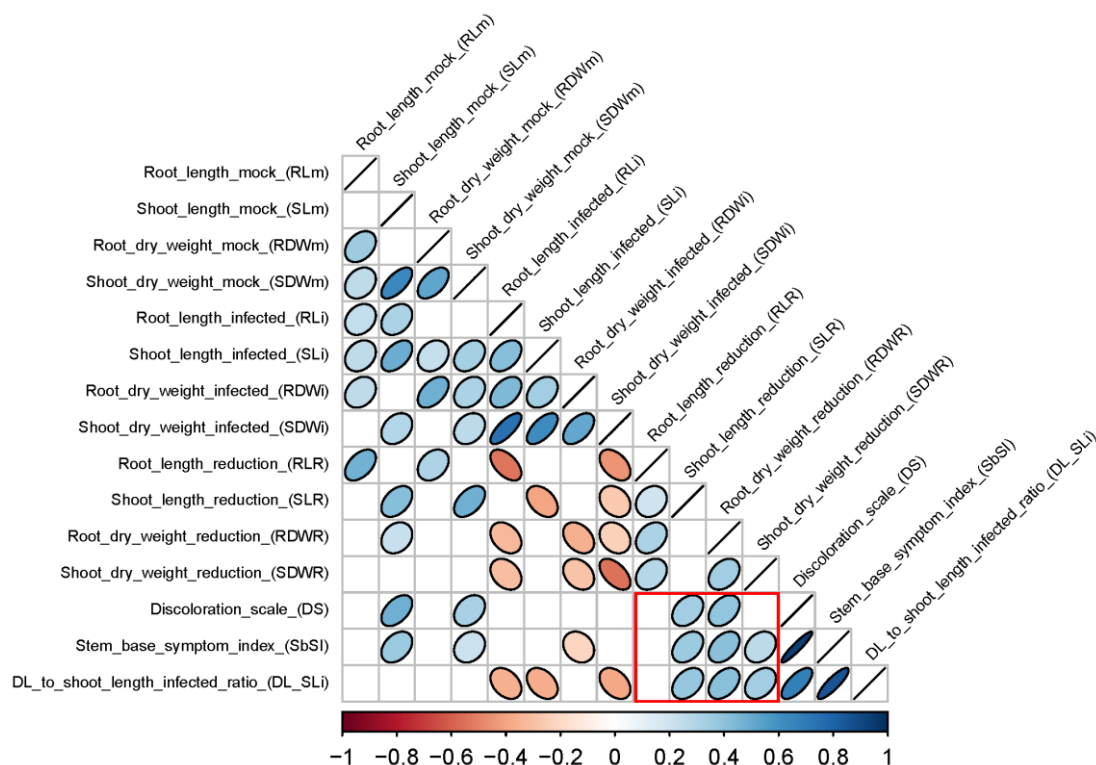


Figure 8. Root inoculation experiment: Correlation matrix of normalized phenotypic data upon mock and *F. graminearum* treatments for different traits of 104 wheat DH lines. Correlations were measured as Pearson's correlation coefficient. Only significant correlations shown ($P < 0.05$). RL= Root length, SL= Shoot length, SDW= Shoot dry weight, RDW= Root dry weight, DS= Discoloration scale, SbSI= Stem base symptom index, DL_SL= Ratio of discoloration section length on stem base to shoot length, i= infected, m= mock, R= Relative reduction. The red box shows correlations between disease severity indices (DS, SbSI and DL_SLi), RLR, SLR, RDWR, SDWR.

In the untreated healthy population, some morphological traits including root length positively correlated with root and shoot dry weight ($r = 0.35$, P -value < 0.001 for RDWm; $r = 0.26$, P -value 0.008 for SDWm). Such positive correlation was also found between shoot length and shoot dry weight in the healthy plant dataset ($r = 0.65$, P -value < 0.001). This indicates that as expected healthy plants having long shoots also have more root and shoot dry weight. However, there was no correlation observed between root and shoot length which indicated that healthy plants with long roots might

have long or short shoots and vice versa. A strong correlation ($r= 0.93$, P -value < 0.001) was found between two different disease rating methods, the SbSI (the stem base symptom index) and the DS (discoloration scale) rating system. The correlation between both of these indices with the third used disease index, the crown rot severity index after Mitter et al. (2006) here called DL_SLi index was less strong ($r= 0.86$, P -value < 0.001 for SbSI and $r= 0.69$, P -value < 0.001 for DS). Correlation of these different disease rating methods with morphological traits in the mock- and in the *F. graminearum*-inoculated data sets revealed differences. Root dry weight of plants under *F. graminearum* treatment (RDWi) negatively correlated with the stem base symptom index (SbSI, with $r= -0.21$, P -value 0.03) but not correlated with DS and DL_SLi. Other morphological traits of infected plants (RLi, SLi and SDWi) were negatively correlated with DL_SLi. In contrast, morphological traits in the healthy plant dataset weakly positively correlated with disease symptoms measured on the stem base (DS, SbSI). As expected, positive correlations were found between relative root length reduction (RLR), root and shoot dry weight reduction ($r= 0.31$, P -value 0.002 for RDWR; $r= 0.28$, P -value 0.005 for SDWR). Root length reduction (RLR) also positively correlated with shoot length reduction (SLR) with $r= 0.2$, P -value 0.05. Such positive correlation was also discovered between root dry weight reduction and shoot dry weight reduction ($r= 0.35$, P -value < 0.001). As shown in the red box in Figure 8, relative reduction values of shoot length, root and shoot dry weight are positively correlated with disease severity measures (DS, SbSI and DL_SLi) with r values ranging from 0.26 to 0.42. No significant correlations are found between root length reduction (RLR) and disease severity measures of the stem.

Finally, for FCR resistance QTL identification after *F. graminearum* root inoculation, positively correlated reduction of root length, shoot length, root and shoot dry weight were selected because relative reduction values of traits could remove genetic variation in the root and shoot growth. In addition, FCR severity rating assessments for SbSI and DL_SLi were also selected since similar methods were used in other FCR resistance QTL studies. Furthermore, morphological traits of root and shoot in the control data set were also applied for QTL mapping to discover putative connections between QTL for FCR resistance and plant morphology.

4.2 *F. graminearum* seed inoculation experiment

4.2.1 Phenotypic variation between parents of the mapping population

Similar to the root inoculation experiment, phenotypic data from eight sub-experiments for the seed inoculation experiment were combined and evaluated for the reaction of parents of the mapping population to mock and *F. graminearum* treatments. Survival rate of plants showed significant differences (P -value= 0.001) under mock and *F. graminearum* treatments for both parents separately. As expected, cv. Tobak showed significant difference between root and shoot dry weight under *F. graminearum* treatment comparing to that of plants under mock treatment, whereas another parent line 162.11 did not show significant difference between *F. graminearum* and mock treatments. Because parental genotypes cv. Tobak and line 162.11 have been previously described to be susceptible and partially resistant to *F. graminearum* root infection respectively (Wang, 2015). Also, in the present study cv. Tobak also showed strong crown rot susceptibility than that of line 162.11.

Between two parents, phenotypic data of survival rate of infected plants (Sri) and disease severity indices (SbSI, DL_SLi) exhibited significant differences under *F. graminearum* treatment (Figure 9C, D and E). Regardless which kind of treatment, two parents did not show significant differences between them for root and shoot dry weight (Figure 9A and B), which was consistent with the *F. graminearum* root infection experiment. For each parent, comparing reduction of shoot dry weight with root dry weight, the latter showed more severe reduction (29% for line 162.11; 47% for cv. Tobak; Figure 9F), which was also found in *F. graminearum* root infection experiments (Figure 3). Line 162.11 described in earlier studies to be partially resistant showed less reduction of root and shoot dry weight compared to cv. Tobak after *F. graminearum* seed inoculation, but the differences were not significant in the ANOVA. The same results were also obtained in the *F. graminearum* root infection experiment.

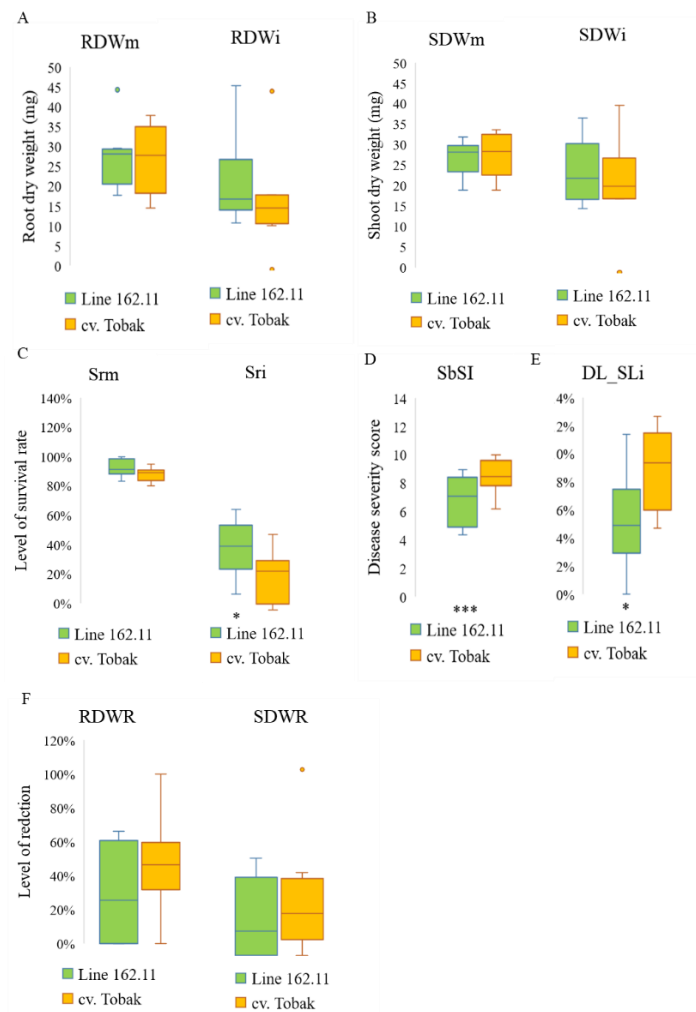


Figure 9. Comparison of phenotypic data upon mock and *F. graminearum* seed inoculations for two parents of the mapping population combining data from eight sub-experiments. (A) root dry weight, (B) shoot dry weight, (C) plant survival rate, (D) and (E) disease severity indices, (F) relative reduction of root and shoot. Stars indicate *P*-values from an ANOVA comparing the phenotypic data of the two groups: * = 0.05, ** = 0.01 and *** = 0.001. RDW= Root dry weight, SDW= Shoot dry weight, Sr= Survival rate, SbSI= Stem base symptom index, DL_SL= Ratio of discoloration section length on stem base to shoot length, i= infected, m= mock, R= Relative reduction.

4.2.2 Phenotypic variation for parents of the mapping population between sub-experiments

Because the phenotyping of two parental genotypes were applied in all eight sub-experiments they could be used for evaluation of variation between sub-experiments. Generally, for line 162.11 root and shoot dry weight under *F. graminearum* treatment showed higher relative standard deviation (SD) than root and shoot dry weight under mock treatment. Similar results were found for root and shoot dry weight between *F. graminearum* and mock treatments of cv. Tobak, which were consistent with the *F. graminearum* root inoculation experiment. High relative SD values were found in survival rate of *F. graminearum*- inoculated plants and were also found in disease

severity measures on the stem base for both parents after *F. graminearum* seed inoculation.

For parental genotypes line 162.11 and cv. Tobak, SD values of shoot dry weight were less than that of root dry weight under both treatments except for cv. Tobak under *F. graminearum* treatment (compare A with B in Figure 10 and 11). This indicates that shoot traits are less environmentally dependent compared to root traits, which were consistent with the results in *F. graminearum* root infected experiments. As described in the *F. graminearum* root infection experiment, disease severity indices (SbSI, DL_SLI) also exhibited high SD values for both parents in the *F. graminearum* seed infection experiment (Figure 10E and F, Figure 11E and F). Shoot length of plants under *F. graminearum* treatment showed extremely high SD for two parents (Figure 10D, 11D). The reason could be that for dead plants a shoot length of zero was introduced which increased the variance in the data. The discoloration section length on the stem base (DL) of dead plants could not be measured and modified, therefore raw data of DL and shoot length under *F. graminearum* treatment (SLi) were used to calculate the ratio between them.

For two parents, as expected in each sub-experiment root and shoot dry weight under *F. graminearum* treatment showed lower mean values than that under mock treatment (Figure 10A and B, Figure 11A and B). The variance of traits between eight sub-experiments were high except for survival rate under mock treatment (Srm) which exhibited over 80% survival rate in each sub-experiment (Figure 10C and Figure 11C). Comparisons of relative SDs and mean values between sub-experiments for two parents indicated that significant differences for most of traits among eight sub-experiments were shown in the ANOVA. Furthermore, more than one group was classified after running Duncan's multiple range test which was consistent with the *F. graminearum* root infection experiments (Figure 10 and 11). Although all eight sub-experiments were conducted in the climate chamber according to the modified protocol from Poole et al. (2012), they should be treated as different environments. Therefore, the phenotypic data of DH lines in each sub-experiment were normalized using the two parents before subsequent analyses.

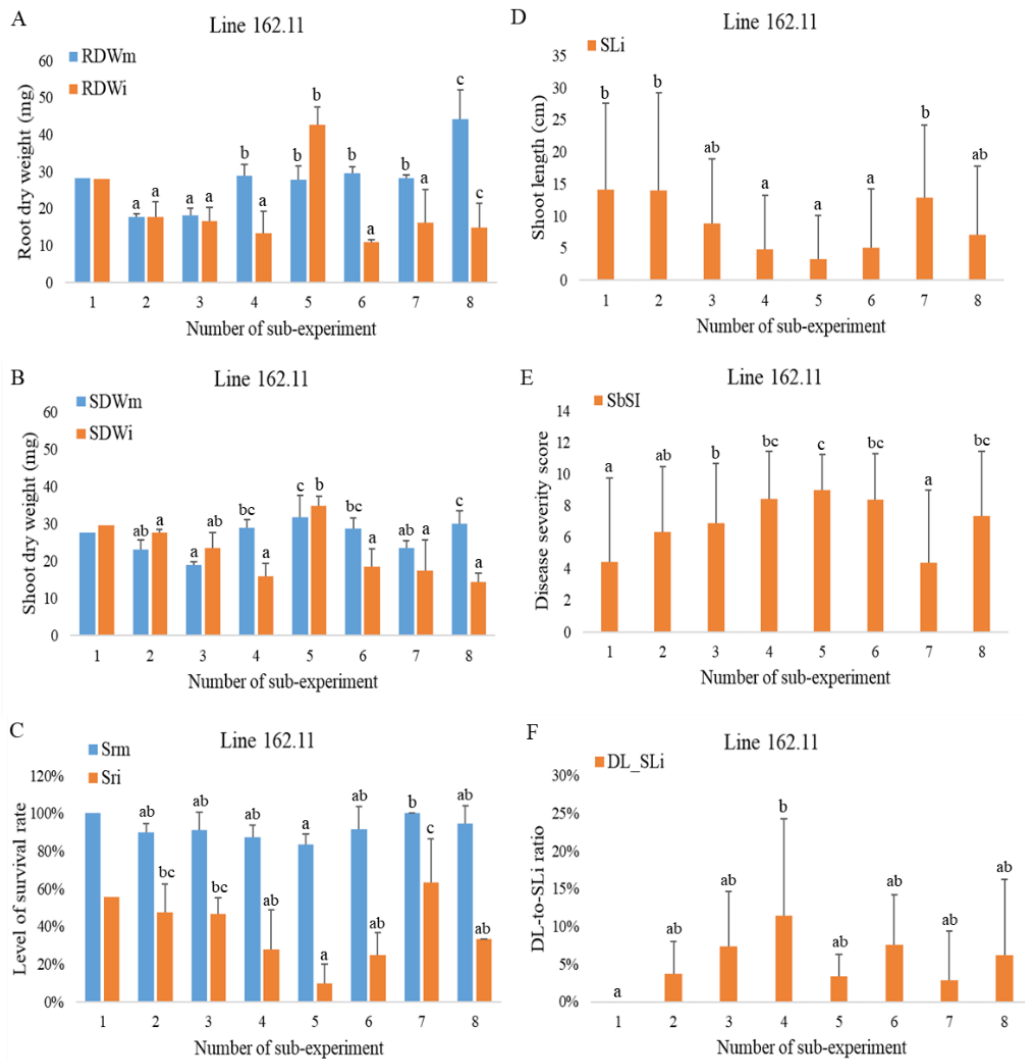


Figure 10. Comparison of phenotypic data for different traits of line 162.11 in eight sub-experiments upon mock and *F. graminearum* seed inoculations. (A) root dry weight, (B) shoot dry weight, (C) plant survival rate, (D) shoot length, (E) and (F) disease severity indices. Bars represent standard deviation. RDW= Root dry weight, SDW= Shoot dry weight, Sr= Survival rate, SL= Shoot length, SbSI= Stem base symptom index, DL_SL= Ratio of discoloration section length on stem base to shoot length, i= infected, m= mock, a-c= Groups from a Duncan's multiple range test. Three biological replicates were assessed in each sub-experiment for dry weight, 48 biological replicates all other traits.

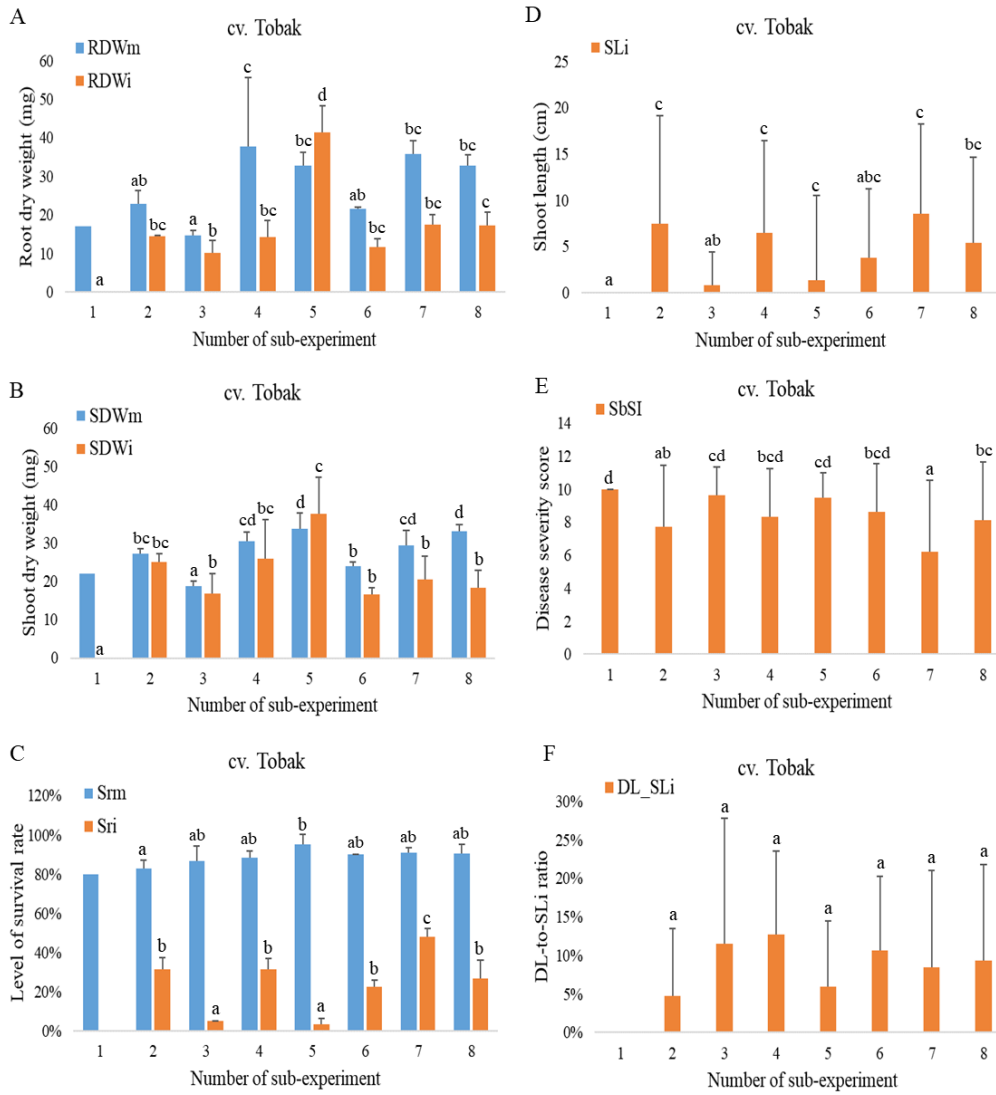


Figure 11. Comparison of phenotypic data for different traits of cv. Tobak in eight sub-experiments upon mock and *F. graminearum* seed inoculations. (A) root dry weight, (B) shoot dry weight, (C) plant survival rate, (D) shoot length, (E) and (F) disease severity indices. Bars represent standard deviation. RDW= Root dry weight, SDW= Shoot dry weight, Sr= Survival rate, SL= Shoot length, SbSI= Stem base symptom index, DL_SL= Ratio of discoloration section length on stem base to shoot length, i= infected, m= mock, a-c= Groups from a Duncan's multiple range test. Three biological replicates were assessed in each sub-experiment for dry weight, 48 biological replicates all other traits.

4.2.3 Phenotypic variation of the mapping population

At 35 days after inoculation all traits for each line of DH population were measured and the relative standard deviation (SD) of mock- and *F. graminearum*- inoculated plants were compared. The former showed lower relative SD of root and shoot dry weight and survival rate. The relative SD values of shoot dry weight were less than that of root dry weight under both treatments. As described in the *F. graminearum* root inoculation experiment, high relative SDs were also found for FCR disease severity indices (SbSI, DL_SLi) in the *F. graminearum* seed inoculation experiment as well as shoot length of plants under *F. graminearum* treatment (SLi).

Similar to the analysis in the root inoculation experiments, the phenotypic data for 103 lines of the mapping population were analyzed in the seed inoculation experiment composed of eight sub-experiments before and after data normalization based on the performance of two parents (Figure 12). For raw data significant differences were found for root and shoot dry weight and survival rate under mock and *F. graminearum* treatments according to the ANOVA (Figure 12A-C at top). However, after normalization root and shoot dry weight were not significantly different between the mock- and *F. graminearum*-inoculated data sets (Figure 12 A and B at bottom). This was similar to the results in the root inoculation experiment including root dry weight, indicating that dry weight of plants is highly influenced by environment variance and normalization should be applied on phenotypic data for subsequent analyses.

For raw data the high reduction of dry weight (41%) was found in root of infected plants and shoot showed about 27% reduction (Figure 13). After normalization root dry weight of infected plants was still higher reduced than shoot dry weight (Figure 13). And for the *F. graminearum* root infection experiment, root dry weight also showed the most severe reduction for two parents and DH population under *F. graminearum* treatment (Figure 6). The raw and normalized data sets both showed significant difference between root and shoot dry weight reductions indicating that reduction values also may not be strongly affected by environment variance in the *F. graminearum* seed inoculation experiment.

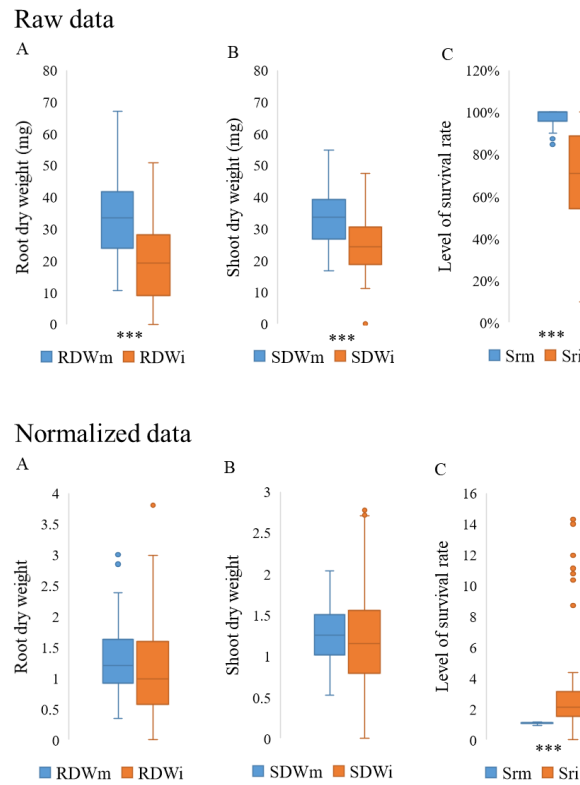


Figure 12. Comparison of mean phenotypic data for 103 DH lines derived from the cross of line 162.11 × cv. Tobak before (raw data) and after (normalized data) normalization upon *F. graminearum* seed inoculation. (A) root dry weight, (B) shoot dry weight, (C) plant survival rate. Stars indicate *P*-values from an ANOVA comparing the phenotypic data of the two groups: * = 0.05, ** = 0.01 and * = 0.001. RDW= Root dry weight, SDW= Shoot dry weight, Sr= Survival rate, i= infected, m= mock.**

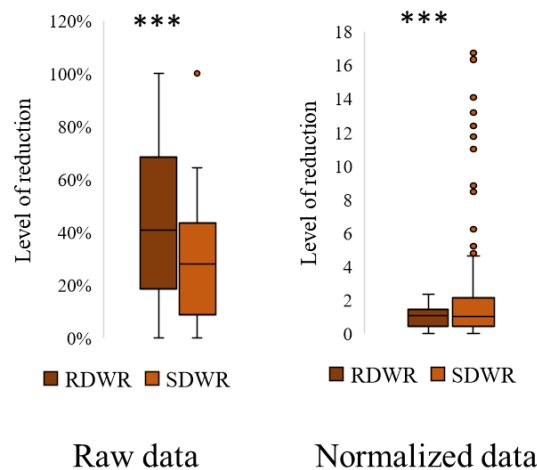


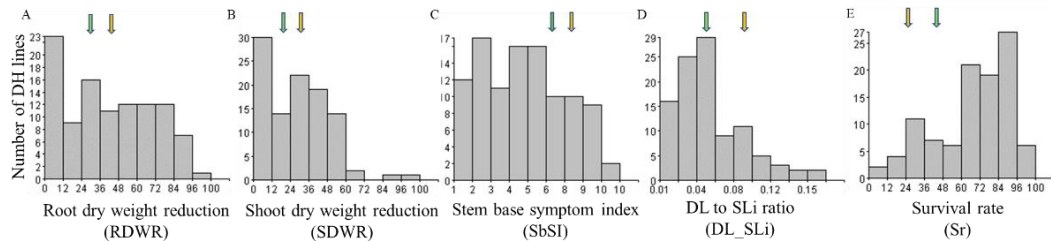
Figure 13. Comparison of relative reduction phenotypic data for 103 DH lines derived from the cross of line 162.11 × cv. Tobak before (raw data) and after (normalized data) normalization in *F. graminearum* seed inoculation experiment. Stars indicate *P*-values from an ANOVA comparing the phenotypic data of the two groups: * = 0.05, ** = 0.01 and * = 0.001. RDW= Root dry weight, SDW= Shoot dry weight, R= Relative reduction.**

Details for the raw and normalized phenotypic data are reported in Table A2 and Table 3. For raw data the population means of traits (RDWm, SDWm, Srm) under mock treatment and SLi, SDWi, Sri under *F. graminearum* treatment exceed the parent with higher values. For discoloration scale (DS), discoloration extension scale (DES) and stem base symptom index (SbSI), the population means are less than that of parent with the lower value. The population means of root and shoot dry weight reduction are within the values of parents. This indicates that a transgressive segregation can be observed where positive alleles are inherited from both parents (Table A2; Figure 14). In addition, disease symptoms are more severe for most DH lines comparing to the susceptible parent cv. Tobak in the root infection experiments whereas in the seed inoculation experiments most DH lines show better performance than line 162.11 after seed inoculation. And mean values of disease symptom measures for DH lines under both infection methods are similar. The reason can be that *F. graminearum* has more impact on two parents after seed inoculation than root infection especially for so called partially resistant line 162.11, which shows high disease severity but still less than susceptible parent cv. Tobak (Table 2 and 3). After normalization of data from all eight sub-experiments based on two parental genotypes the data for the whole population of 103 DH lines show similar distribution for most traits except for survival rate (Figure 14). It suggests that environment variance may have less impacts on reduction and disease severity in *F. graminearum* seed inoculation experiment comparing to root inoculation experiment (Figure 7).

Table 3. Normalized phenotypic data in mock and *F. graminearum* seed inoculations experiment.

Treatment	Traits	Traits (Abbreviations)	Population statistics					
			Min.	Max.	Mean	Median	CoV (%)	
Control	Root dry weight	RDWm	0.35	3.00	1.28	1.21	1.73	
	Shoot dry weight	SDWm	0.52	2.04	1.27	1.26	0.99	
	Survival rate	Srm	0.95	1.16	1.08	1.10	0.38	
Infected	Shoot length	SLi	0.00	11.21	3.19	2.58	6.05	
	Root dry weight	RDWi	0.00	3.81	1.18	0.99	2.22	
	Shoot dry weight	SDWi	0.00	2.83	1.25	1.16	1.21	
	Survival rate	Sri	0.00	14.52	3.20	2.14	2.04	
	Discoloration scale	DS	0.05	1.38	0.60	0.56	7.39	
	Discoloration extension scale	DES	0.07	1.38	0.61	0.59	14.70	
	Stem base symptom index	SbSI	0.06	1.38	0.60	0.59	8.27	
	Discoloration section length	DL	0.10	3.11	0.91	0.76	11.29	
	DL to SL ratio	DL_SLi	0.02	3.43	0.74	0.58	12.46	
	Reduction	Root dry weight	RDWR	0.00	2.31	1.00	1.07	6.11
		Shoot dry weight	SDWR	0.00	16.70	2.69	1.02	5.08

Raw data



Normalized data

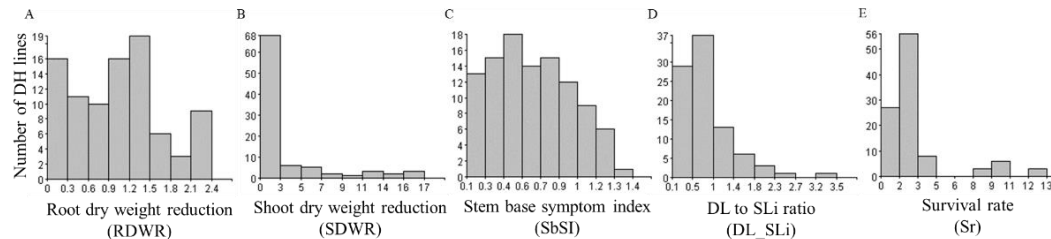


Figure 14. Comparison of phenotype frequency distributions of 103 DH lines derived from the cross of line 162.11 × cv. Tobak before (raw data) and after (normalized data) normalization in *F. graminearum* seed inoculation experiment. (A) root dry weight, (B) shoot dry weight, (C) and (D) disease severity indices, (E) plant survival rate. RDW= Root dry weight, SDW= Shoot dry weight, SbSI= Stem base symptom index, DL_SL= Ratio of discoloration section length on stem base to shoot length, Sr= Survival rate. i= infected, R= Relative reduction. Green arrow indicates line 162.11 and yellow arrow indicates cv. Tobak.

4.2.4 Trait correlations

Trait correlations of normalized phenotypic data measured as Pearson's correlation coefficient (r) and only significant correlations are shown ($P < 0.05$) in the correlation matrix (Figure 15). The correlation of three different disease indices (DS, SbSI and DL_SLi) between each other and between survival rate and morphological traits of healthy (mock-treated) and infected plants were analyzed (shoot length, root and shoot dry weight).

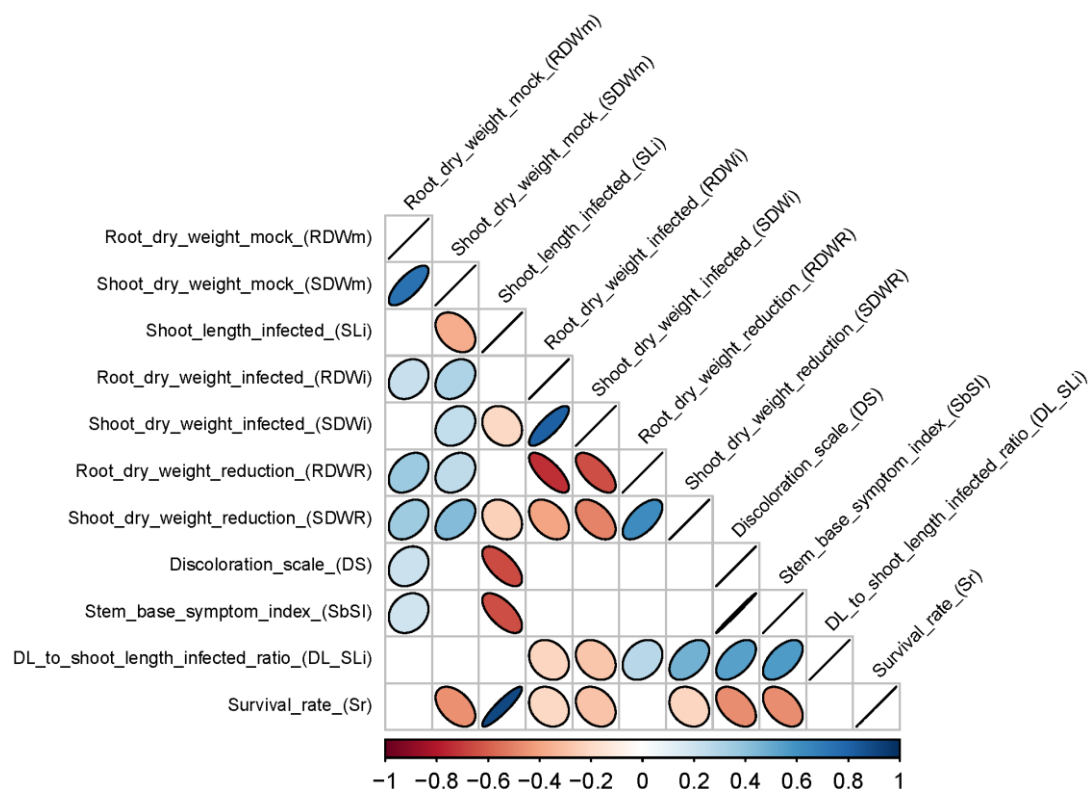


Figure 15. Seed inoculation: Correlation matrix of normalized phenotypic data upon mock and *F. graminearum* treatments for different traits of 103 DH lines. Correlations were measured as Pearson's correlation coefficient. Only significant correlations shown ($P < 0.05$). RL= Root length, SL= Shoot length, SDW= Shoot dry weight, RDW= Root dry weight, DS= Discoloration scale, SbSI= Stem base symptom index, DL_SL= Ratio of discoloration section length on stem base to shoot length, Sr= Survival rate, i= infected, m= mock, R= Relative reduction.

In the seed inoculation experiment root dry weight under mock treatment (RDWm) was strongly correlated with shoot dry weight (SDWm) with $r = 0.75$, P -value < 0.001 . Two disease indices (DS, SbSI) showed strongly positive correlations to each other and showed less strongly positive correlation to DL_SLi. No significant correlations were found between dry weight of root and shoot under mock treatment and DL_SLi, whereas other two disease indices (DS, SbSI) weakly positive correlated with root dry weight of healthy plants. Above similar results were also showed in the root inoculation

experiments. Shoot length of infected plants (SLi) negatively correlated with two disease indices including DS and SbSI, but not correlated with DL_SLi. A fourth disease index, survival rate (Sr), was measured in the seed inoculation experiment. Survival rate (Sr) negatively correlated with stem base symptom index (SbSI) and discoloration scale (DS) with $r = -0.45$, $P\text{-value} < 0.001$; $r = -4.8$, $P\text{-value} < 0.001$ and strongly positive correlated with shoot length of infected plants (SLi) with $r = 0.91$, $P\text{-value} < 0.001$ which as expected means that genotypes which are taller after infection have a better chance to survive. DL_SLi negatively correlated with root and shoot dry weight of infected plants ($r = -0.22$, $P\text{-value} 0.04$ for RDWi; $r = -0.27$, $P\text{-value} 0.009$ for SDWi). Above correlations indicate that resistant plants with pathogen induced resistance show higher survival rate, longer shoot length and higher root and shoot dry weight but less discoloration of the stem base under *F. graminearum* treatment. DL_SLi positively correlated with shoot dry weight reduction (SDWR) ($r = 0.47$, $P\text{-value} < 0.001$) and root dry weight reduction (RDWR) ($r = 0.27$, $P\text{-value} 0.02$). The reduction of root and shoot dry weight exhibited strongly positive correlation with $r = 0.63$, $P\text{-value} < 0.001$ between them.

Finally, for FCR resistance QTL identification, *F. graminearum* seed infection induced relative reduction of root and shoot dry weight were selected, because reduction values of traits could remove genetic variation in the root and shoot growth. Survival rate was also selected and was calculated as 'Sri/Srm' to remove germination rate difference of healthy plants. In addition, FCR severity rating assessments for SbSI and DL_SLi were also selected because the similar methods were generally used in other FCR resistance QTL studies. Furthermore, morphological traits of root and shoot in control were also applied to discovery putative relation between QTL for FCR resistance and morphology.

4.3 Correlation of phenotypic data between root and seed inoculations experiment

Several traits measured in both *F. graminearum* root and seed infection experiments including root and shoot dry weight under mock- and *F. graminearum* inoculations, discoloration scale (DS), stem base symptom index (SbSI), DL_SLi, the reduction of root and shoot dry weight. In the correlation matrix of data sets from two experiments, shoot dry weight reduction induced by *F. graminearum* root infection (SDWR_Rti) weakly negatively correlated with shoot dry weight reduction after seed inoculation (SDWR_Sdi) with $r = -0.24$, $P\text{-value} 0.02$. However, no significant correlations were

found for root dry weight reduction and disease severity measures of stem base between root and seed inoculations (red box in Figure 16). This suggests that the inoculation of different tissues (root and seed) may result in different resistance/tolerance reactions of individual genotypes to *F. graminearum* and different resistance QTL/genes may independently play roles in different organ/ development stage infection by *F. graminearum*. For the morphological traits of the mock inoculated plants data set, a positive correlation was shown between shoot dry weight (SDWm) in two experiments whereas root dry weights were not significantly correlated (red box in Figure 16), indicating that roots may be more sensitive to certain inoculation methods such as root-dip. Because plants have to be taken out of soil/sand before inoculation and then are replanted, which could cause damage to roots healthy leading to reduced root length and dry weight. Therefore, this inoculation method requires much more concentration and labor force.

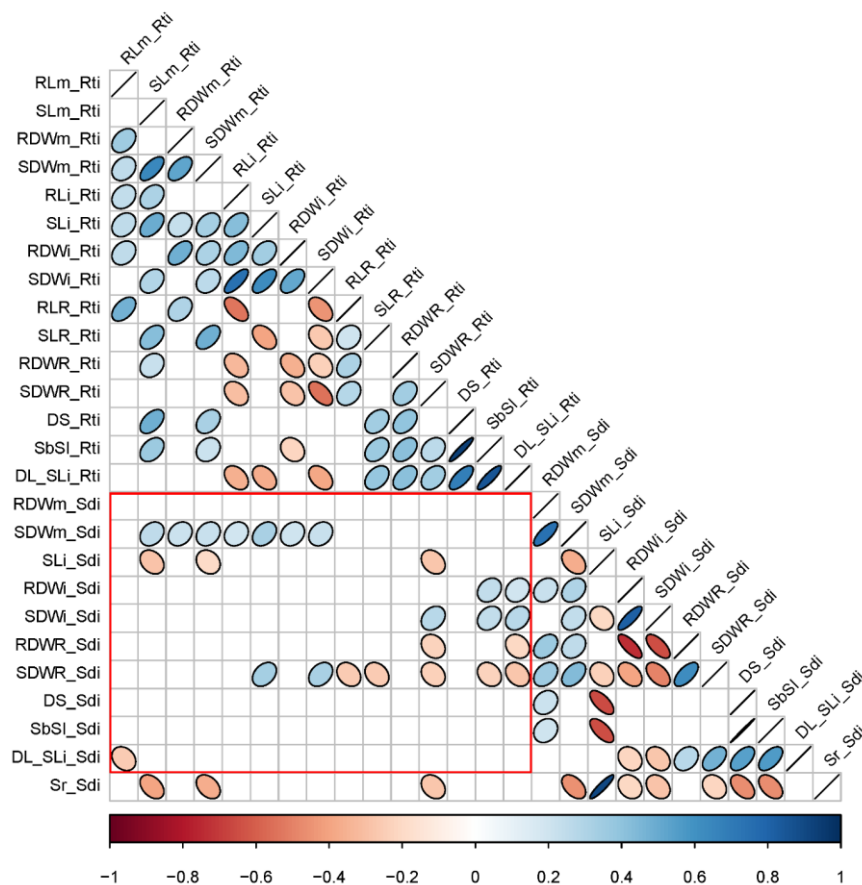


Figure 16. Correlation matrix of normalized phenotypic data for different traits between root and seed inoculations experiment. Correlations were measured as Pearson's correlation coefficient. Only significant correlations shown ($P < 0.05$). RL= Root length, SL= Shoot length, RDW= Root dry weight, SDW= Shoot dry weight, Sr= Survival rate, SbSI= Stem base symptom index, DL_SL= Ratio of discoloration section length on stem base to shoot length, i= infected, m= mock, R= Relative reduction. Rt= Root, Sd= Seed. The red box shows traits correlation between two experiments.

4.4 Genetic map construction

The linkage map comprised 2806 SNP markers (mapped in 1012 polymorphic loci) and spanned a total length of 2161 cM involving all 21 chromosomes represented by 38 linkage groups and ten chromosomes were split into multiple linkage groups (Figure 17). The average length of chromosome was 102.9 cM, ranged from 16.1cM (7D) to 208.5 cM (3A) (Table 4). The A genome included 1228 SNPs covering a length of 1112.9 cM and an average marker density of 1.1/cM; the B genome had 1301 SNPs covering 770.5 cM and an average marker density of 1.69/cM per marker; the D genome included 277 SNPs, a length of 277.7 cM, and an average marker density of 1/cM per marker. The number of SNP markers in each chromosome ranged from 17 (7D) to 368 (5B) and the number of genetic bins (439 bins including 2233 markers) on each chromosome varied from 2 (3D) to 51 (5B), with means of 133.62 and 20.9. The number of loci and intervals of them in each chromosome ranged from 6 (3D), 1.11 cM (4B) to 134 (5B), 4.43 cM (3D), with means of 48.2 and 2.14 cM. The longest chromosome was 3A, and it harbored 57 loci with a genetic length of 208.5 cM, an average loci interval of 3.53 cM and loci density of 0.27/cM. Whereas chromosome 7D showed the shortest genetic length of 16.08 cM, with an average loci interval of 2.06 cM and loci density of 0.48/cM. The highest and lowest loci densities were found in chromosomes 4B (0.9/cM) and 3D (0.23/cM). In the present genetic map, three gaps were larger than 30 cM on chromosomes 1B, 2A and 2D. The average distance of the largest gaps on each genome was 21.65 (A), 20.69 (B) and 18.85 (D) cM. In addition to the gaps, the largest number of markers at one locus (bin) ranged from 5 on chromosomes 4D, 5D and 7D to 66 on chromosome 4A.

Table 4. Marker statistics of the linkage map constructed from doubled haploid population derived from the cross of line 162.11 and cv. Tobak.

Chromosome	# markers	% markers	# loci	% loci	Bins	Total length (cM)	Marker density (marker/cM)	Loci density (loci/cM)	Average loci interval (cM/locus)	Linkage groups	r^*
1A	144	5.13	45	4.45	23	125.87	1.14	0.36	2.80	4	0.89
1B	127	4.53	63	6.23	28	130.96	0.97	0.48	1.84	2	0.94
1D	68	2.42	16	1.58	7	51.83	1.31	0.31	3.24	1	0.47
2A	122	4.35	55	5.43	24	203.78	0.60	0.27	3.58	1	0.97
2B	316	11.26	102	10.08	48	144.07	2.19	0.71	1.33	3	0.81
2D	56	2.00	20	1.98	10	72.77	0.77	0.27	3.64	2	0.96
3A	139	4.95	57	5.63	29	208.52	0.67	0.27	3.53	2	0.94
3B	35	1.25	12	1.19	5	30.24	1.16	0.40	2.33	2	0.61
3D	44	1.57	6	0.59	2	26.56	1.66	0.23	4.43	1	0.86
4A	162	5.77	28	2.77	17	55.73	2.91	0.50	1.92	1	0.90
4B	129	4.60	70	6.92	21	77.75	1.66	0.90	1.11	1	0.68
4D	28	1.00	14	1.38	5	59.39	0.47	0.24	3.96	1	0.70
5A	171	6.09	84	8.30	29	197.86	0.86	0.42	2.06	4	0.51
5B	368	13.11	134	13.24	51	171.78	2.14	0.78	1.24	4	0.90
5D	19	0.68	10	0.99	4	20.63	0.92	0.48	2.06	1	0.79
6A	186	6.63	54	5.34	22	129.00	1.44	0.42	2.26	2	0.64
6B	100	3.56	35	3.46	20	93.71	1.07	0.37	2.68	1	0.99
6D	45	1.60	11	1.09	8	30.44	1.48	0.36	2.17	1	0.80
7A	304	10.83	111	10.97	48	192.13	1.58	0.58	1.73	2	0.79
7B	226	8.05	78	7.71	33	121.95	1.85	0.64	1.35	1	0.97
7D	17	0.61	7	0.69	5	16.08	1.06	0.44	2.01	1	0.82
A genome	1228	43.76	434	42.89	192	1112.88	1.10	0.39	2.56	16	0.81
B genome	1301	46.36	494	48.81	206	770.46	1.69	0.64	1.56	14	0.84
D genome	277	9.88	84	8.30	41	277.70	1.00	0.30	3.31	8	0.77
Total	2806	100	1012		439	2161.04	1.30	0.47	2.14	38	0.81
Min.	17	0.61	6		2	16.08	0.47	0.23	1.11	1	0.47
Max.	368	13.11	134		51	208.52	2.91	0.90	4.43	4	0.99

*Pearson's correlation coefficient of the current map with consensus map reported by Wang et al. (2014)

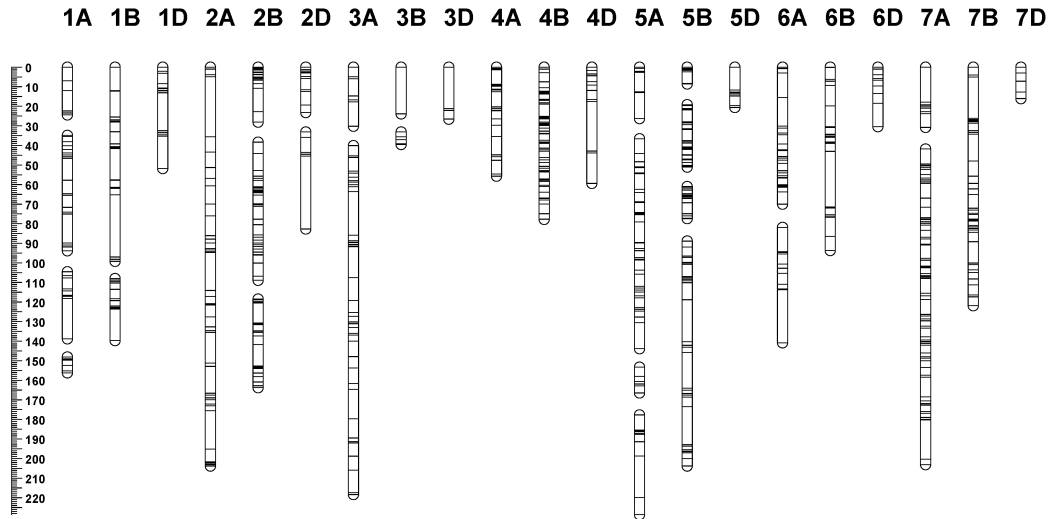


Figure 17. Genetic map developed by using a double haploid population from line 162.11 × cv. Tobak. Chromosomes 1A, 2B, 2D, 3A, 3B, 5A, 5B, 6A and 7A are represented by four, three, two, two, two, four, four, two and two linkage groups, respectively.

After construction of the linkage map, the accuracy and reliability of this map were uncertain and QTL mapping especially requires high quality genetic map. Therefore, the linkage map in the present study was compared with the high-density consensus map based on a 90K SNP assay reported by Wang et al. (2014). A total 2559 SNP markers were shared between two maps and 247 SNP markers were exclusive for the 15K SNP array used in the present study. The orders of the 2559 markers in the present map were mostly consistent with the corresponding positions in the Wang et al. (2014) consensus map with Person correlation coefficients (r) ranged from 0.47 (1D) to 0.99 (6B), and the mean correlation coefficients (r) was 0.81. The A subgenome and B subgenome showed the similar r value of 0.81 and 0.84, the lowest r value was found for subgenome D with r value of 0.77 because of low marker density on D subgenome. Generally, except chromosome 3B and certain chromosomes from D subgenome with low marker density, a strong collinear relationship in marker order on the 21 chromosomes between the current constructed linkage map and the consensus map confirmed the high quality of linkage map built in this study (Table 4; Figure 18). In the constructed genetic map, most of the SNP markers were located on the A (43.8%) and B (46.4%) subgenomes whereas only 9.8% of the polymorphisms were detected on the D subgenome. Comparing the distribution of mapped markers on each subgenome with the study of Wang et al. (2014), the majority of markers were also located in the A (35%) and B (50%) subgenomes, only 15% of markers mapped to the D subgenome.

The low diversity on the D subgenome has been repeatedly reported in the literature and is mainly due to a limited number of ancestral genotypes of the D subgenome donor (*Aegilops tauschii*) that contributed to the origin of hexaploid wheat (Wang et al. 2014; Cui et al., 2014; Jordan et al. 2015; Jin et al., 2016; Hussain et al., 2017; Wen et al., 2017; Apples et al., 2018; Lemes da Silva et al., 2019). This effect was obvious in the current population that only 17 and 19 loci were identified as segregating between line 162.11 and cv. Tobak on chromosomes 7D and 5D respectively (Table 4).

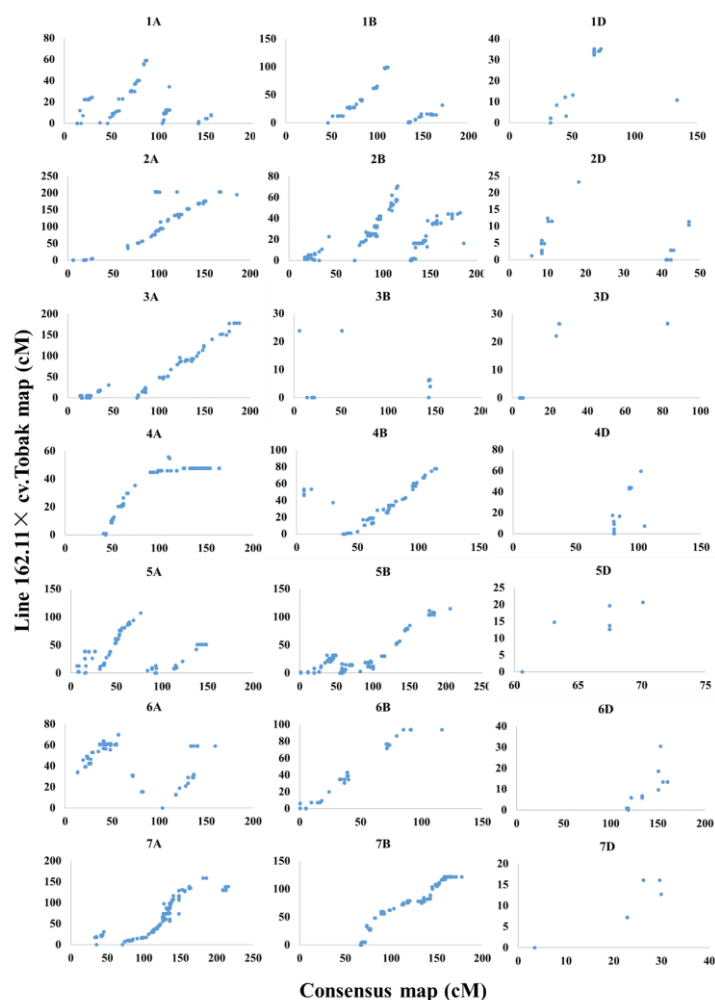


Figure 18. Dot plot depicting the marker order collinearity between line 162.11 \times cv. Tobak map (cM) and high-density consensus map (cM) for 21 chromosomes of wheat. Chromosomes 1A, 1B, 2B, 2D, 3A, 3B, 5A, 5B, 6A and 7A represented by more than one linkage groups.

Furthermore, the synteny of mapped SNPs (90K SNP array vs. 15K SNP array) was analyzed between different mapping populations. The former was based on eight doubled haploid populations and the latter was only developed from one doubled haploid population with 104 lines indicating expected much lower marker density. The two aligned chromosomes illustrated generally consistent marker order based on the

homologies between mapped SNP markers from the consensus map reported by Wang et al. (2014) and the present line 162.11 × cv. Tobak map. A mostly consistent marker order across different mapping populations verifying the accuracy and credibility of the present genetic map (Figure 20). In addition, chromosome 4B might be involved in chromosomal rearrangement and markers translocation because physical position of these markers shifted as a block in the current population in different genetic backgrounds. The algorithm error of software was excluded because linkage map was developed again using different mapping method (MSTmap) and the similar marker positions shift on chromosome 4B were found in both linkage maps. Error of the consensus map was excluded because the present map was aligned with another high-density consensus map reported by Wen et al. (2017) derived from the 90K SNP array across four different DH populations and marker translocations were also discovered on chromosome 4B of the current genetic map (Figure 19, blue segment).

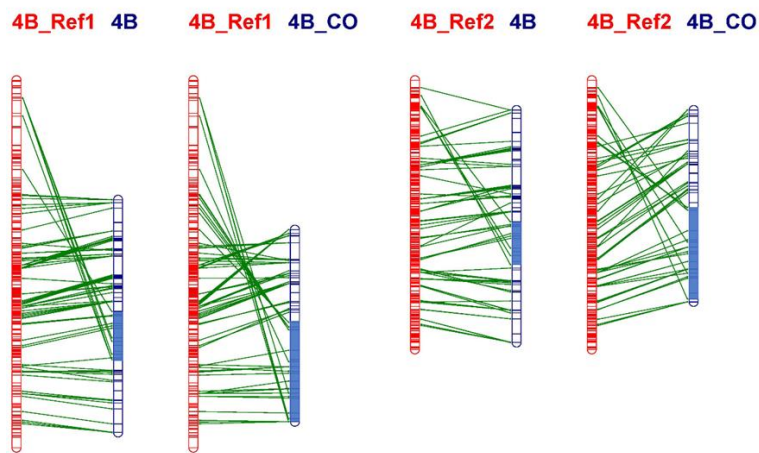


Figure 19. Synteny of the mapped SNPs on chromosome 4B from two consensus maps (in red) and the line 162.11 × cv. Tobak map (in blue) based on the homologies between markers on adjacent linkage groups. Blue segment indicated markers translocation part. Ref1= consensus map reported by Wang et al. (2014), Ref2= consensus map reported by Wen et al. (2017). CO= Line 162.11 × cv. Tobak map created by different method (MSTmap).

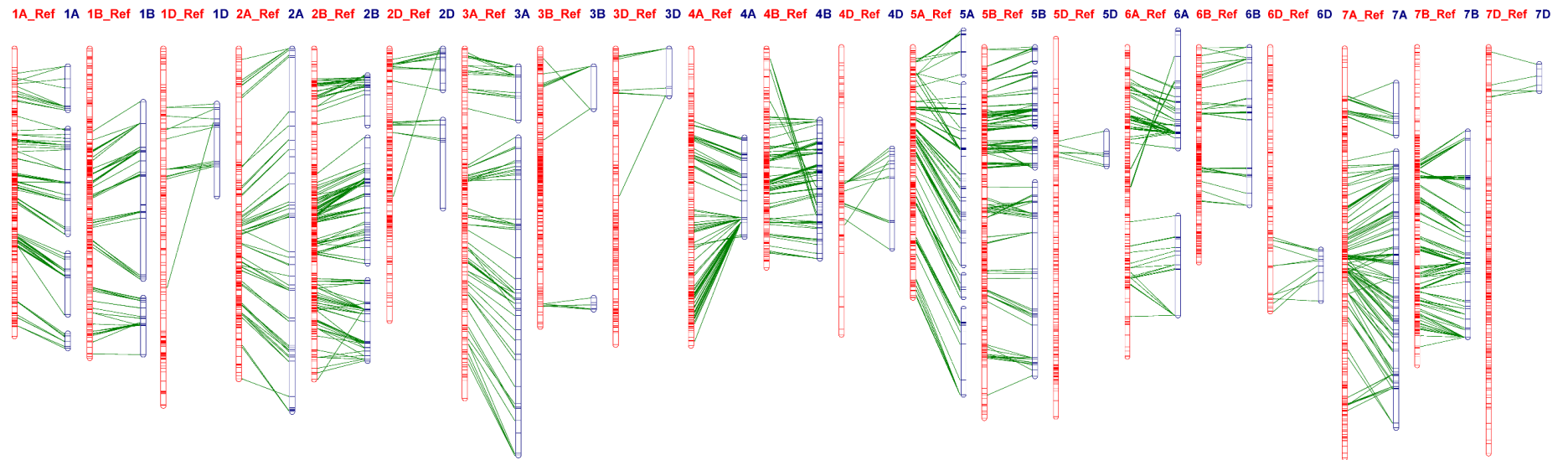


Figure 20. Synteny of the mapped SNPs from the consensus map reported by Wang et al. (2014; in red) and the line 162.11 × cv. Tobak map (in blue) based on the homologies between markers on adjacent linkage groups.

4.5 QTL identification in the root inoculation experiment

4.5.1 Identification of FCR resistance QTL upon *F. graminearum* root inoculation

For the normalized phenotypic data set, nine significant QTL for SbSI, DL_SLi, RLR, and SLR were identified on chromosomes 3A (LG 3A-2), 3B (LG 3B-1), 4B, 5A (LG 5A-2), 5B (LG 5B-2), 6A (LG 6A-1) and 7D with LOD values over 3. The explained phenotypic variance (R^2) by individual QTL ranged from 12.8% to 35.6% with LOD values between 3.08 and 9.94. Alleles increasing FCR resistance were inherited from the partially resistant parent line 162.11 for all above QTL except for two QTL on chromosomes 4B and 5B, where positive alleles were inherited from the susceptible parent cv. Tobak (Table 5).

The most significant FCR resistance QTL, designated as *qSLR-4B.2*, was detected in a 4 cM interval on chromosome 4BL explaining up to 35.6% phenotypic variance with a LOD value of 9.94, where positive allele was derived from line 162.11 (Table 5; Figure 21). Another QTL for SLR was also mapped on chromosome 4B and explained 11.2% phenotypic variance. The distance between them was approximately 14 cM.

The second most significant FCR resistance QTL was mapped in a 4 cM interval on chromosome 7DS, where line 162.11 contributed positive allele. It was designated as *qSbSI-7D* and explained up to 21.9 % phenotypic variance with a LOD value of 5.59.

The highest number of QTL were identified for SbSI including five QTL mapped on chromosomes 3A (LG 3A-2), 3B (LG 3B-1), 4B, 5B (LG 5B-2) and 7D. Besides the QTL on chromosome 7DS explained 21.9% phenotypic variance, the rest of QTL explained less than 20% phenotypic variances.

Table 5. FCR resistance QTL for *F. graminearum* root inoculation in the line 162.11× cv. Tobak DH population.

Trait	Chromosome	Closest marker	Map position (cM)	Confidence interval (cM)	Flanking markers	Add	LOD	R ² (%)	Resistance allele source	
SbSI	3A (LG 3A-2)*	IAAV3851	152	150-160	Ku_c26872_269	IAAV9044	-0.1	3.98	16.1	Line 162.11
	3B (LG 3B-1)*	BS00098868_51	0	0-2	BS00098868_51	Tdurum_contig77551_589	-0.1	4.05	16.4	Line 162.11
	4B	Excalibur_c9901_163	42	38-44	RAC875_c24098_141	BS00039936_51	0.14	3.08	12.8	cv. Tobak
	5B (LG 5B-2)	Excalibur_c58520_78	10	8-14	BS00065135_51	BS00022107_51	0.11	4.87	19.4	cv. Tobak
	7D*	TA016282-1180	2	0-4	TA016282-1180	TA013055-0991	-0.13	5.59	21.9	Line 162.11
DL_SLi	3A (LG 3A-2)*	IAAV3851	154	150-160	Ku_c26872_269	IAAV9044	-0.11	2.73	11.4	Line 162.11
	7D*	TA016282-1180	2	0-4	TA016282-1180	TA013055-0991	-0.12	3.38	13.9	Line 162.11
RLR	5A (LG 5A-2)*	BobWhite_c13238_386	78	76-80	tplb0057m23_716	w SNP_Ku_c14275_22535576	-0.27	4.09	17.8	Line 162.11
SLR	4B.1	Tdurum_contig33737_157	10	8-12	TG0010b	BS00105308_51	-0.44	2.68	11.2	Line 162.11
	4B.2*	BobWhite_c20051_53	28	26-30	RFL_Contig583_419	IACX938	-0.69	9.94	35.6	Line 162.11
	6A (LG 6A-1)	Kukri_c34219_355	52	50-54	RAC875_c22627_315	tplb0024k14_1812	-0.22	3.21	13.3	Line 162.11
RDWR	3A (LG 3A-2)	w SNP_Ex_c28679_37784954	178	176-178	w SNP_Ex_c24085_33332723	w SNP_Ex_c28679_37784954	-0.35	2.34	9.8	Line 162.11
SDWR	7B	Tdurum_contig59755_568	84	84-86	w SNP_Ku_c707_1465395	BS00049730_51	0.21	2.91	13.7	cv. Tobak

*Selected QTL for predicted FCR/FHB resistance related genes identification

Table 6. Morphological traits QTL for mock root inoculation in the line 162.11× cv. Tobak DH population.

Trait	Chromosome	Closest marker	Map position (cM)	Confidence interval (cM)	Flanking markers	Add	LOD	R ² (%)	Allele source	
RLm	3A (LG 3A-2)	Excalibur_c24354_465	106	98-112	w SNP_Ku_c10468_17301042	BS00076772_51	-0.05	2.01	8.5	cv. Tobak
SLm	3A (LG 3A-2)	CAP8_c359_95	18	16-20	w SNP_Ku_c40218_48484410	BS00067216_51	0.06	5.06	20.1	Line 162.11
	3B (LG 3B-1)	BS00098868_51	0	0-2	BS00098868_51	Tdurum_contig77551_589	-0.05	3.37	13.9	cv. Tobak
	4D	w SNP_Ex_c683_1341113	0	0-2	w SNP_Ex_c683_1341113	RAC875_rep_c70284_235	0.05	3.18	13.1	Line 162.11
RDWm	3D	BobWhite_c3902_210	0	0-2	BobWhite_c3902_210	RAC875_c48773_253	0.12	2.21	9.3	Line 162.11
SDWm	3A.1 (3A-2)	CAP8_c359_95	18	16-18	w SNP_Ku_c40218_48484410	CAP8_c359_95	0.23	2.78	11.7	Line 162.11
	3A.2 (3A-2)	Excalibur_rep_c103091_266	22	20-24	BS00067216_51	w SNP_Ex_c1141_2191485	-0.22	2.82	11.9	cv. Tobak
	3D	BobWhite_c3902_210	0	0-2	BobWhite_c3902_210	RAC875_c48773_253	0.09	2.6	11	Line 162.11

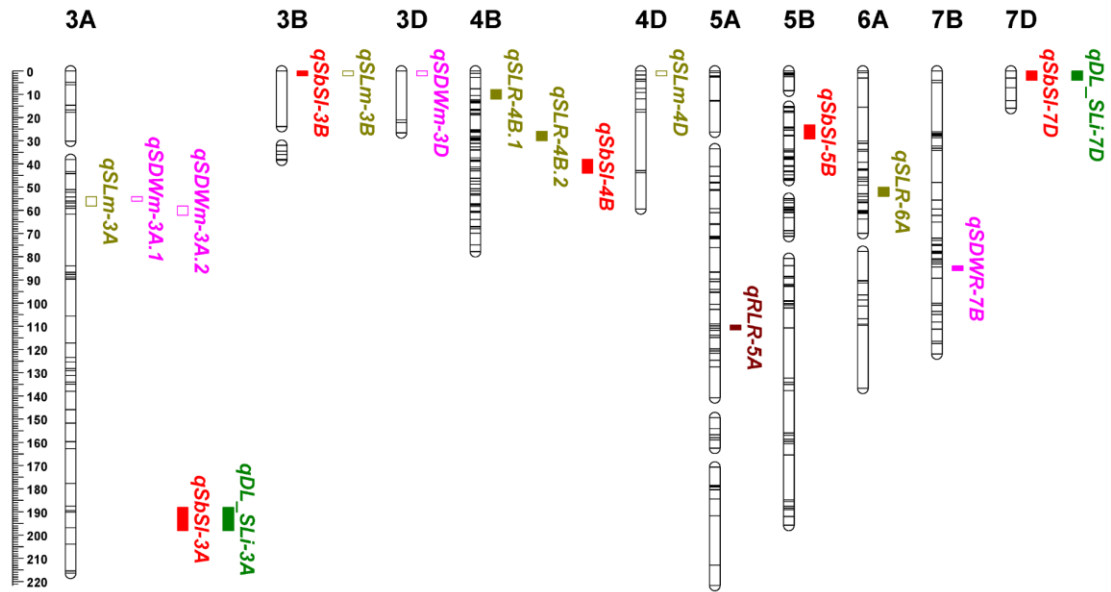


Figure 21. SNP-based genetic map and distribution of FCR resistance QTL (solid bars) and morphological traits QTL (hollow bars) for *F. graminearum* and mock root inoculations in the line 162.11× cv. Tobak DH population. The scale is on the left indicating genetic distance (cM). RL= Root length, SL= Shoot length, RDW= Root dry weight, SDW= Shoot dry weight, SbSI= Stem base symptom index, DL_SL= Ratio of discoloration section length on stem base to shoot length, i= infected, m= mock, R= Relative reduction.

Furthermore, three suggestive QTL for DL_SLI, SLR and SDWR were identified on chromosomes 3A (LG 3A-2), 4B and 7B. Partially resistant parent line 162.11 contributed positive alleles for two QTL on chromosomes 3AL and 4BS, the positive allele for the third QTL on chromosome 7BL was inherited from susceptible parent cv. Tobak. The QTL *qSDWR-7D* explained the highest phenotypic variance of 13.7% with a LOD value of 2.91. In addition, one QTL was detected for RDWR on chromosome 3AL only when LOD threshold was below 2.5 and it might be a ‘ghost’ QTL.

4.5.2 Identification of morphological traits QTL upon mock root inoculation

Three significant QTL were identified on chromosomes 3A (LG 3A-2), 3B (LG 3B-1) and 4D. The most significant QTL was detected in a 4 cM interval on chromosome 3AS. It designated as *qSLm-3A* and explained up to 20.1% phenotypic variance with a LOD value of 5.06, where positive allele was derived from line 162.11 (Table 6; Figure 21). The rest of QTL explained about 13% phenotypic variance, where cv. Tobak and line 162.11 contributed positive alleles respectively. Three suggestive QTL were identified for SDWm on chromosomes 3A (two QTL) and 3D explaining about 11% phenotypic variance. For RLM and RDWm, only when LOD values were below 2.5 QTL could be detected respectively with the risk of mapping 'ghost' QTL.

In summary, multiple QTL for FCR resistance were detected after *F. graminearum* root inoculation for the traits including SbSI, DL_SLi and SLR, whereas only one QTL was identified for RLR, RDWR and SDWR respectively. Positive alleles were contributed by partially resistant parent line 162.11 for 10 QTL and by the susceptible parent cv. Tobak for three QTL. In total 13 QTL (11 QTL considering overlapping QTL as one QTL) were detected and explained over 9% phenotypic variance with LOD values ranging from 2.34 to 9.94. FCR resistance QTL for SbSI and DL_SLi were co-localized on chromosomes 3A and 7D with positive phenotypic correlation respectively (Figure 21). For morphological traits of mock treated plants, three significant and three suggestive QTL were identified for SLM and SDWm respectively. In total eight QTL were identified and explained phenotypic variances ranging from 8.5% to 20.1% with LOD values ranging from 2.01 to 5.06. QTL for SLM and SDWm were co-localized on chromosome 3A with expected strong positive phenotypic correlation.

4.6 QTL identification in the seed inoculation experiment

4.6.1 Identification of FCR resistance QTL upon *F. graminearum* seed inoculation

The most significant FCR resistant QTL, designated as *qDL_SLi-7B*, was located in 4 cM interval on the long arm of chromosome 7B for DL_SLi. It explained up to 29.4% of the phenotypic variation with a LOD value of 6.8, where the positive allele was contributed by line 162.11 (Table 7; Figure 22). The parent cv. Tobak contributed positive alleles for two QTL for DL_SLi identified on the long arm of chromosome 1A (LG 1A-2) and short arm of chromosome 5A (LG 5A-1). The highest number five QTL were identified for SbSI including the second most significant FCR resistance QTL *qSbSI-1A.2*. It was mapped in a 2 cM interval on chromosome 1AS (LG 1A-1) and explained 27% of the phenotypic variance with a LOD value of 7.03, where positive allele was inherited from cv. Tobak. The rest of QTL explained phenotypic variances ranging from 13.2% to 17.7%, where positive alleles were all derived from line 162.11 except for QTL *qSbSI-5B*. Three QTL for survival rate (Sr) and one QTL for each of RDWR and SDWR were detected on chromosomes 2B (LG 2B-2), 3A (LG 3A-2), 4D, 6A (LG 6A-1) and 6D. They explained phenotypic variations ranging from 15.4% to 22.3% and the parent cv. Tobak contributed positive allele for four of them.

Six suggestive QTL for Sr, SbSI, DL_SLi, RDWR and SDWR were identified on chromosomes 1B (LG 1B-1), 2A, 2B (LG 2B-3), 2D (LG 2D-1, two QTL) and 3A (LG 3A-2). The highest phenotypic variance (14.1%) was explained by QTL *qRDWR-2A*, where positive allele was inherited from cv. Tobak (Table 7; Figure 22). This parent cv. Tobak also contributed positive allele for QTL *qSDWR-2B*, whereas positive alleles were derived from line 162.11 for the rest of four QTL.

4.6.2 Identification of morphological traits QTL upon mock seed inoculation

Three significant QTL were identified on chromosomes 3A (LG 3A-2), 4B and 4D for SDWm. The most significant QTL, designated as *qSDWm-4B*, explained 24.2% phenotypic variance with a LOD value of 6.21, where positive allele was contributed by line 162.11 (Table 8; Figure 22). For the rest of QTL positive alleles were inherited from line 162.11 and cv. Tobak, respectively. Only one suggestive QTL *qRDWm-6D* for RDWm was detected on the long arm of chromosome 6D. It explained 11.8% phenotypic variance with LOD value of 2.81, where positive allele was derived from

cv. Tobak. For Srm, two QTL were detectable only with the lower LOD threshold between 2 and 2.5, which might be 'ghost' QTL.

In summary, multiple QTL for FCR resistance were detected for each trait after *F. graminearum* seed inoculation. Six QTL were identified for SbSI, whereas only two QTL were detected for RDWR and SDWR respectively. Positive alleles were derived from partially resistant parent line 162.11 for nine QTL and were derived from the susceptible parent cv. Tobak for 10 QTL. In total 19 QTL (18 QTL when considering overlapping individual QTL as one QTL) were mapped and over 10% phenotypic variance were explained by them with LOD values ranging from 2.59 to 7.03. FCR resistance QTL *qSr-2D* for Sr and QTL *qSbSI-2D* for SbSI were co-localized on chromosome 2D with negative phenotypic correlation. For morphological traits of mock treated plants, three QTL were identified for SDWm and only one was detected for RDWm. In total six QTL were identified and explained phenotypic variance ranging from 9.5% to 24.2% with LOD values between 2.24 and 6.21.

Table 7. FCR resistance QTL for *F. graminearum* seed inoculation in the line 162.11× cv. Tobak DH population.

Trait	Chromosome	Closest marker	Map position (cM)	Confidence interval (cM)	Flanking markers	Add	LOD	R^2 (%)	Resistance allele source	
Sr	1B (LG 1B-1)	TA001473-0980	12	10-24	BS00087784_51	w SNP_Ex_rep_c67036_65492436	0.8	2.83	11.9	Line 162.11
	2B (LG 2B-2)	BobWhite_c41676_137	60	58-62	tplb0048g05_866	TA004957-0405	-0.99	3.74	15.4	cv. Tobak
	2D (LG 2D-1)*	BS00022276_51	22	18-22	GENE-0717_28	BS00022276_51	0.81	2.86	12	Line 162.11
	3A (LG 3A-2)*	CAP8_c359_95	18	16-20	Kukri_rep_c102953_304	Excalibur_rep_c103091_266	-2.03	4.89	19.7	cv. Tobak
	4D	w SNP_Ex_c683_1341113	0	0-2	w SNP_Ex_c683_1341113	TA020319-0161	-1.03	4.83	19.4	cv. Tobak
SbSI	1A.1 (LG 1A-1)	BS00059422_51	6	4-10	RAC875_c95364_259	RFL_Contig3481_1669	-0.13	4	16.4	Line 162.11
	1A.2 (LG 1A-1)*	RAC875_rep_c104335_293	24	22-24	w SNP_Ex_c2868_5293485	RAC875_rep_c104335_293	0.18	7.03	27	cv. Tobak
	2D (LG 2D-1)*	BS00022276_51	22	18-22	GENE-0717_28	BS00022276_51	-0.08	2.92	12.2	Line 162.11
	5A (LG 5A-2)	w SNP_Ex_c49211_53875600	88	86-90	Excalibur_c1208_72	Excalibur_c2598_2052	-0.08	3.17	13.2	Line 162.11
	5B (LG 5B-4)	BS00100707_51	50	46-52	Kukri_c26747_211	w SNP_Ex_c97184_84339976	0.09	3.26	13.6	cv. Tobak
DL_SLi	7B	CAP12_c1587_142	102	100-104	Tdurum_contig97939_64	Kukri_rep_c79716_389	-0.1	4.36	17.7	Line 162.11
	1A (LG 1A-2)	Excalibur_c59894_97	34	30-38	w SNP_Ex_rep_c103087_88124573	Kukri_c3582_87	0.21	4.02	18.6	cv. Tobak
	3A (LG 3A-2)*	IAAV5507	158	150-160	Ku_c26872_269	IAAV9044	-0.17	2.96	14	Line 162.11
	5A (LG 5A-1)	BS00099534_51	0	0-4	Excalibur_c22465_625	tplb0035p20_710	0.18	3.15	14.9	cv. Tobak
	7B*	Tdurum_contig59755_568	84	82-86	IAAV6137	Ku_c9679_441	-0.29	6.8	29.4	Line 162.11
RDWR	2A	w SNP_Ku_c23598_33524490	0	0-2	w SNP_Ku_c23598_33524490	TA002095-0637	0.23	2.96	14.1	cv. Tobak
	6D*	BS00003568_51	18	12-20	Excalibur_c83056_83	IACX5958	-0.26	3.78	17.6	Line 162.11
SDWR	2B (LG 2B-3)	RFL_Contig385_761	12	6-14	BS00026432_51	BobWhite_c12911_788	1.32	2.59	12.4	cv. Tobak
	6A (LG 6A-1)*	Kukri_c89274_86	48	46-50	Tdurum_contig54957_525	Kukri_c34219_355	3.02	4.94	22.3	cv. Tobak

*Selected QTL for predicted FCR/FHB resistance related genes identification

Table 8. Morphological traits QTL for mock seed inoculation in the line 162.11× cv. Tobak DH population.

Trait	Chromosome	Closest marker	Map position (cM)	Confidence interval (cM)	Flanking markers	Add	LOD	R ² (%)	Allele source	
Srm	2D (LG 2D-1)	BS00022276_51	22	18-22	GENE-0717_28	BS00022276_51	0.01	2.24	9.5	Line 162.11
	5B (LG 5B-4)	Ku_c7546_861	114	110-114	RFL_Contig3285_1009	Ku_c7546_861	-0.01	2.29	9.7	cv. Tobak
RDWm	6D	BS00070856_51	26	18-30	IACX5958	BS00070856_51	-0.2	2.81	11.8	cv. Tobak
SDWm	3A (LG 3A-2)	w SNP_Ex_c28679_37784954	178	176-178	w SNP_Ex_c24085_33332723	w SNP_Ex_c28679_37784954	-0.15	5.92	23.2	cv. Tobak
	4B	TG0010b	8	6-12	TG0010a	BS00105308_51	0.16	6.21	24.2	Line 162.11
	4D	BobWhite_c20689_427	58	48-58	IAAV5065	BobWhite_c20689_427	0.13	4.04	16.5	Line 162.11

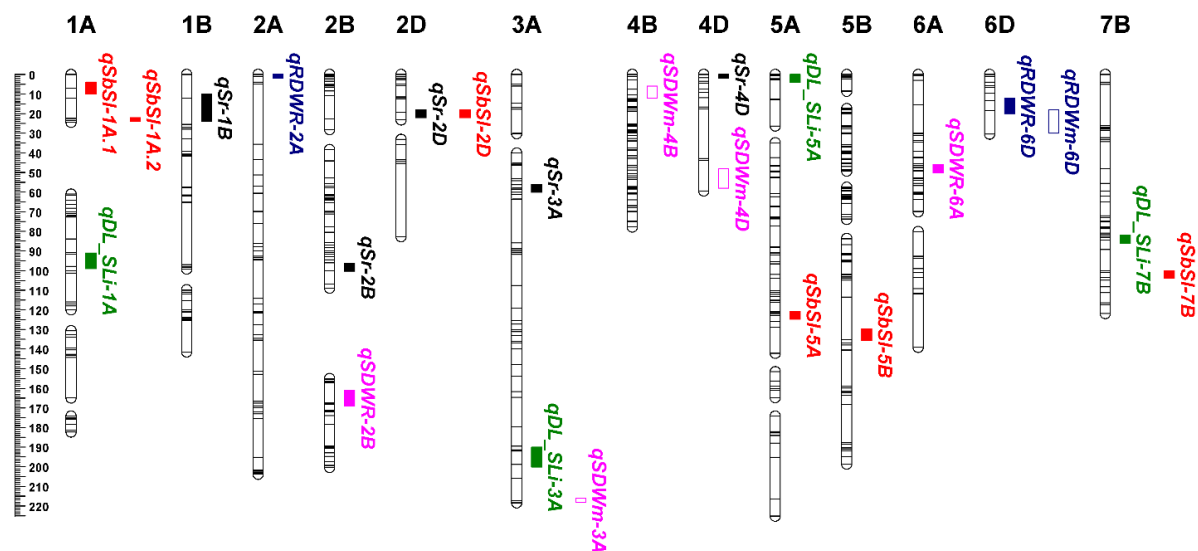


Figure 22. SNP-based genetic map and distribution of FCR resistance QTL (solid bars) and morphological traits QTL (hollow bars) for *F. graminearum* and mock seed inoculations in the line 162.11× cv. Tobak DH population (n=103). The scale on the left is indicating the genetic distance (cM). RDW= Root dry weight, SDW= Shoot dry weight, SbSI= Stem base symptom index, DL_SL= Ratio of discoloration section length on stem base to shoot length, Sr= Survival rate, i= infected, m= mock, R= Relative reduction.

4.7 Comparison of FCR resistance QTL between *F. graminearum* root and seed inoculations

The FCR resistance QTL detected for *F. graminearum* root inoculation were compared with the FCR resistance QTL detected for seed inoculation. In total 11 FCR resistance QTL after root inoculation were detected. On the other hand, 18 FCR resistance QTL were identified after seed inoculation. For DL_SLi, FCR resistance QTL for root and seed inoculations overlapped on the long arm of chromosome 3A (LG 3A-2) and a FCR resistance QTL for SbSI after root inoculation was also mapped at the same region (Figure 23), where positive alleles were contributed by line 162.11, indicating the same QTL might contribute FCR resistance for root and seed inoculations. On chromosome 7BL, QTL for SDWR and DL_SLi were also co-localized but no phenotypic correlation was found. Resistance QTL for SLR and SDWR were adjacently localized on the short arm of chromosome 6A after root and seed inoculations (Figure 23), where positive alleles were inherited from line 162.11 and cv. Tobak respectively. Negative phenotypic correlation was found between them, meaning that resistance QTL for *F. graminearum* root inoculation may reduce plants resistance for seed inoculation and vice versa. In addition, two QTL *qRLR-5A_Rti* and *qSbSI-5A_Sdi* were closely localized on chromosome 5A with 6 cM distance after root and seed inoculations, where positive alleles were contributed by line 162.11. However, no significant phenotypic correlation was found, meaning that these QTL are independent and contributed resistance to FCR for *F. graminearum* root or seed inoculation.

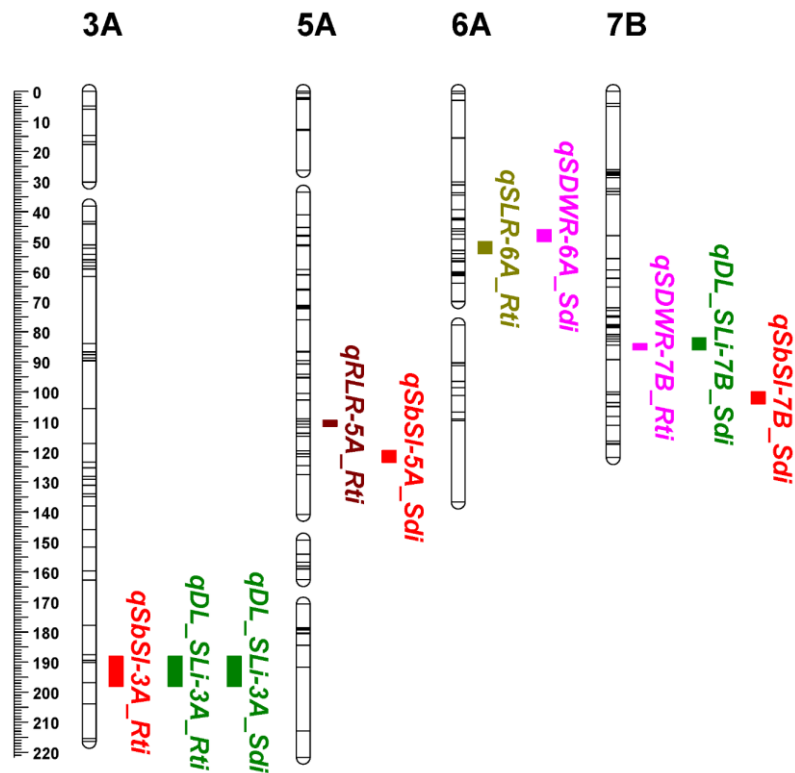


Figure 23. Distribution of FCR resistance QTL co-localizing or overlapping upon *F. graminearum* root and seed inoculations. RL= Root length, SL= Shoot length, RDW= Root dry weight, SDW= Shoot dry weight, SbSI= Stem base symptom index, DL_SL= Ratio of discoloration section length on stem base to shoot length, Sr= Survival rate, i= infected, R= Relative reduction, Rt= Root, Sd= Seed.

4.8 Comparison of FCR resistance QTL in the current study with reported QTL in the literature

In most previous studies, SSR and DArT markers were used for QTL mapping whereas SNP markers were applied in the current study. Therefore, identified QTL positions in the present study could not be directly compared with reported FCR resistance QTL positions. However, it was attempted to anchor the SSR primer or amplicon sequences flanking QTL regions to the physical regions of the wheat reference genome and compare them with the physical positions of the SNP markers flanking the QTL from this study. The physical position of some markers can be obtained from Wheat@URGI portal (<https://wheat-urgi.versailles.inra.fr/>; Alaux et al., 2018). For SbSI, in the current study a QTL *qSbSI-3B* was mapped in a physical region of 2.9–8.1 Mbp on chromosome 3BS after *F. graminearum* root inoculation. Pariyar et al. (2020) reported a FCR resistance QTL identified on chromosome 3B with a moderate effect against *F. culmorum*. These two QTL might be same because the physical distance between them was about 2 Mbp. For SLR, after *F. graminearum* root inoculation a QTL *qSLR-4B.2* was detected on chromosome 4BL in a physical region of 598–611.4 Mbp, which might

be the same QTL as a QTL on 4B reported by Pariyar et al. (2020) with about 6 Mbp distance between physical locations of two QTL (Table 9 and 10; Figure 24). In the *F. graminearum* seed inoculation experiment, a QTL *qSr-1B* for survival rate (Sr) was identified in the physical region of 50.8–445.4 Mbp on chromosome 1B and which overlapped with a FCR resistance QTL reported by Martin et al. (2015), indicating that these two FCR resistance QTL may be same. For SbSI, in the present study a QTL *qSbSI-1A.2* was identified in a physical region of 7.2–9.1 Mbp on chromosome 1AS, which might be the same QTL as a QTL on 1AS reported by Rahman et al. (2020), because these two QTL were overlapped. Two overlapped QTL for Sr and SbSI (*qSr/SbSI-2D*) were detected in the region of 26.8–29.5 Mbp on chromosome 2DS. It might be the same QTL as a QTL on chromosome 2D reported by Erginbasorakci et al. (2018), because the physical distance between them was about 7 Mbp (Table 9 and 10; Figure 24). For the rest of identified FCR resistance QTL, some of them seemed to lie in close proximity with published FCR resistance QTL and mapped on the same chromosomes in Figure 24, but the physical distance between them was more than 10 Mbp (Table 9 and 10). Therefore, these genes were not considered as the putative same FCR resistance QTL as reported.

In summary, if two QTL were mapped at the identical confidence interval and the same parent contributed resistant alleles, they were considered as one FCR resistance QTL. Therefore, 28 FCR resistance QTL were identified after *F. graminearum* root and seed inoculations. Among them five QTL on chromosomes 1A (LG 1A-2), 1B (LG 1B-1), 2D (LG 2D-1), 3B (LG 3B-1) and 4B might be the same FCR resistance QTL as previously reported. In addition, after *F. graminearum* root inoculation a new FCR resistance QTL was identified on chromosomes 7DS for the first time (Liu and Ogbonnaya, 2015; Yang et al., 2019; Pariyar et al., 2020; Jin et al., 2020). Comparison with the FHB resistance QTL *Fhb1* on chromosome 3BS and QTL *Fhb4* on chromosome 4BL revealed that the FCR resistance QTL identified in the present study including *qSbSI-3B_Rti* and *qSLR-4B.2_Rti* might be the same QTL, which might also be the same FCR resistance QTL including *qFCR-3B.1* and *qFCR-4B* as Pariyar et al. (2020) reported (Figure 24).

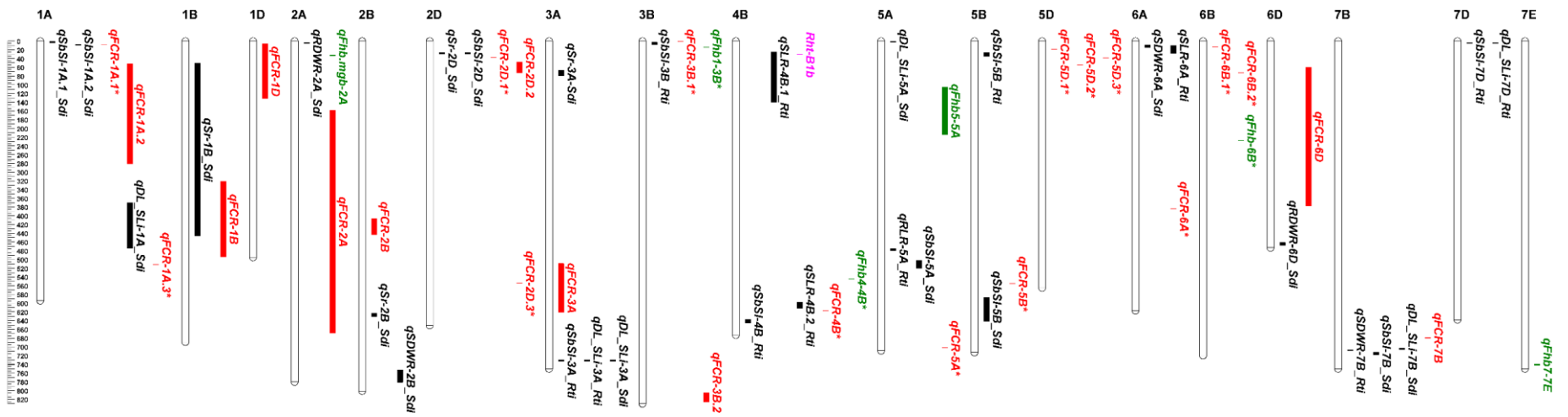


Figure 24. Comparative map of FCR resistance QTL (in black) detected in the present study and published FCR (in red) and FHB resistance QTL or cloned resistance genes (in green) and other putatively involved genes (in pink). The scale is on the left indicating physical distance (Mbp). QTL with the star is indicating that only one side physical position of markers for QTL is available. Chromosome 7E is introduced from *Th. elongatum* (Wang et al., 2020).

Table 9. FCR resistance QTL upon *F. graminearum* root and seed inoculations in the line 162.11× cv. Tobak DH population.

	QTL	Confidence interval (cM)	Physical position (Mbp)	Flanking markers	
Root inoculation	<i>qSbSI-3A</i>	150-160	729.8–732.7	Ku_c26872_269	IAAV9044
	<i>qSbSI-3B</i> ^o	0-2	2.9–8.1	BS00098868_51	Tdurum_contig77551_589
	<i>qSbSI-4B</i>	38-44	637.4–645.3	wsnp_Ku_c12503_20174234	IAAV2725
	<i>qSbSI-5B</i>	8-14	26.4–34.7	BS00065135_51	BS00022107_51
	<i>qSbSI-7D</i>	0-4	4–5.1	TA016282-1180	TA013055-0991
	<i>qDL_SLi-3A</i>	150-160	729.8–732.7	Ku_c26872_269	IAAV9044
	<i>qDL_SLi-7D</i>	0-4	4–5.1	TA016282-1180	TA013055-0991
	<i>qRLR-5A</i>	76-80	475.5–478.8	tplb0057m23_716	wsnp_Ku_c14275_22535576
	<i>qSLR-4B.1</i>	8-12	24.6–139.8	Tdurum_contig41902_1524	BS00105308_51
	<i>qSLR-4B.2</i> ^o	26-30	598–611.4	RFL_Contig583_419	IACX938
	<i>qSLR-6A</i>	50-54	10.7–27.5	RAC875_c22627_315	tplb0024k14_1812
	<i>qRDWR-3A</i>	176-178	743.8–744.4	wsnp_Ex_c24085_33332723	wsnp_Ex_c28679_37784954
	<i>qSDWR-7B</i>	84-86	706.8–708.6	wsnp_Ku_c707_1465395	BS00049730_51
	Seed inoculation	<i>qSr-1B</i> ^A	10-24	50.8–445.4	BS00087784_51
<i>qSr-2B</i>		58-62	622.9–630.8	tplb0048g05_866	TA004957-0405
<i>qSr-2D</i> ^o		18-22	26.8–29.5	GENE-0717_28	BS00022276_51
<i>qSr-3A</i>		16-20	67.3–79.4	Kukri_rep_c102953_304	Excalibur_rep_c103091_266
<i>qSr-4D</i>		0-2	54.4–69.9	wsnp_Ex_c683_1341113	TA020319-0161
<i>qSbSI-1A.1</i>		4-10	1.2–3.3	RAC875_c95364_259	RFL_Contig3481_1669
<i>qSbSI-1A.2</i> ^o		22-24	7.2–9.1	wsnp_Ex_c2868_5293485	RAC875_rep_c104335_293
<i>qSbSI-2D</i> ^o		18-22	26.8–29.5	GENE-0717_28	BS00022276_51
<i>qSbSI-5A</i>		86-90	502.2–520	Excalibur_c1208_72	Excalibur_c2598_2052
<i>qSbSI-5B</i>		46-52	587.1–641.4	Kukri_c26747_211	wsnp_Ex_c97184_84339976
<i>qSbSI-7B</i>		100-104	712.6–718.5	Tdurum_contig97939_64	Kukri_rep_c79716_389
<i>qDL_SLi-1A</i>		30-38	369.7–474.6	wsnp_Ex_rep_c103087_88124573	Kukri_c3582_87
<i>qDL_SLi-3A</i>		150-160	729.8–732.7	Ku_c26872_269	IAAV5507
<i>qDL_SLi-5A</i>		0-4	0.3–2.6	tplb0035p20_710	Excalibur_c22465_625
<i>qDL_SLi-7B</i>		82-86	703.2–705.7	IAAV6137	Tdurum_contig49912_578
<i>qRDWR-2A</i>		0-2	3.4–5.5	wsnp_Ku_c23598_33524490	TA002095-0637
<i>qRDWR-6D</i>		12-20	461.3–466.9	Excalibur_c83056_83	BS00003568_51
<i>qSDWR-2B</i>		6-14	752.5–780.6	BS00026432_51	BobWhite_c12911_788
<i>qSDWR-6A</i>	46-50	9.1–14.4	Tdurum_contig54957_525	Kukri_c34219_355	

Putatively same FCR resistance QTL as reported by ^AMartin et al. (2015), ^oPariyar et al. (2020), ^oErginbasorakci et al. (2018) and ^oRahman et al. (2020)

Table 10. Summary of novel FCR and FHB resistance QTL in the literature.

	QTL	Physical region (Mbp)	Markers		Literature
FCR QTL	<i>qFCR-1A.1</i>	8.3	wsnp_Ku_c183_358844	-	Rahman et al. (2020)
	<i>qFCR-1A.2</i>	52.2–280.6	barc148	gwm164	Martin et al. (2015)
	<i>qFCR-1A.3</i>	511.5	-	wmc312	Collard et al, 2005
	<i>qFCR-1B</i>	321.1–493.6	cf65	gwm11	Martin et al. (2015)
	<i>qFCR-1D</i>	6.3–131.3	Affx-92108178	Affx-109205872	Jin et al. (2020)
	<i>qFCR-2A</i>	158.8–668	gwm95	cfa2043	Martin et al. (2015)
	<i>qFCR-2B</i>	406.5–442.8	cfa2278	gwm630	Martin et al. (2015)
	<i>qFCR-2D.1</i>	37.1	wPt-669517	-	Erginbasorakci et al. (2018)
	<i>qFCR-2D.2</i>	48.2–72.4	gwm484	gwm102	Martin et al. (2015)
	<i>qFCR-2D.3*</i>	553.7	-	cf673	Zheng et al. (2014)
	<i>qFCR-3A</i>	509.5–620.5	cfa2134	cfa2262	Martin et al. (2015)
	<i>qFCR-3B.1</i>	1	CAP12_rep_c3868_270	-	Pariyar et al. (2010)
	<i>qFCR-3B.2*</i>	804.8–826.2	Xgwm299	Xgwm247	Poole et al. (2012)
	<i>qFCR-4B</i>	617	RAC875_rep_c72961_977	-	Pariyar et al. (2020)
	<i>qFCR-4D</i>	-	-	-	Poole et al. (2012)
	<i>qFCR-5A</i>	702	Affx-109253960	-	Jin et al. (2020)
	<i>qFCR-5B</i>	554.8	Excalibur_c23304_353	-	Pariyar et al. (2020)
	<i>qFCR-5D.1</i>	18.3	RAC875_rep_c111521_246	-	Pariyar et al. (2020)
	<i>qFCR-5D.2</i>	54.7	Excalibur_c2795_1518	-	Pariyar et al. (2020)
	<i>qFCR-5D.3*</i>	39	-	cf6189	Zheng et al. (2014)
	<i>qFCR-6A</i>	383.9	wmc754-6A	barc1055	Yang et al. (2019)
	<i>qFCR-6B.1</i>	13.2	RAC875_c17297_341	-	Pariyar et al. (2020)
	<i>qFCR-6B.2</i>	72.8	BobWhite_c19298_97	-	Pariyar et al. (2020)
	<i>qFCR-6D</i>	59.7–377	barc196	barc273	Martin et al. (2015)
<i>qFCR-7B</i>	678.5–679.8	Affx-109846651	Affx-109540847	Jin et al. (2020)	
FHB QTL	<i>Fhb1 (qFhb1-3B)</i>	13.6	Fhb1-TaHRC-S	-	Su et al. (2019)
	<i>Fhb2 (qFhb2-6B)</i>	227.3	Xgwm133	-	Cuthbert et al. (2007)
	<i>Fhb3 (qFhb3-7Lr#1S)</i>	-	BE585744-STs, BE404728-STs, BE586111-STs	-	Qi et al. (2008)
	<i>Fhb4 (qFhb4-4B)</i>	544.7	Xhbg226	Xgwm149	Xue et al. (2010)
	<i>Fhb5 (qFhb5-5A)</i>	105.4–214.2	Xgwm304	Xgwm415	Xue et al. (2011)
	<i>Fhb6 (qFhb6-1Ets#1S)</i>	-	wg1S_snp1	-	Cainong et al. (2015)
	<i>Fhb7 (qFhb7-7E)</i>	739.7–741.5	XSdauK79	XSdauK80	Wang et al. (2020)
	<i>qFhb.mgb-2A</i>	31.7–33	IWB5988	IWA5087	Gadaleta et al. (2019)

*FCR resistance QTL consistently detected in different genetic backgrounds

4.9 Identification of putative FCR resistance related genes in the selected QTL

After identification and comparison of FCR resistance QTL for different traits in *F. graminearum* root and seed inoculation experiments, 11 QTL were selected for further putative FCR/FHB resistance related gene mining for different reasons. One QTL for SbSI identified on chromosomes 3BS was selected because it might be the same FHB resistance QTL *Fhb1*. One QTL for SbSI/DL_SLi was selected because it was repeatedly detected on chromosome 3AL in both experiments. Two overlapping QTL for SbSI and DL_SLi at the same position on chromosome 7DS after *F. graminearum* root inoculation were considered as one FCR resistance QTL. The other two overlapping QTL for Sr and SbSI in *F. graminearum* seed inoculation experiment on chromosome 2DS were also considered as one FCR resistance QTL. Two QTL on chromosomes 4BL and 7BL explained the highest phenotypic variances for SLR (35.6%) and DL_SLi (29.4%) in each experiment. In addition, the former might be the same FHB resistance QTL *Fhb4*. The other five selected QTL also explained the highest phenotypic variances for each trait in both experiments (Table 5 and 7). Finally, 1017 model genes were obtained from the set of high confidence genes of the IWGSC RefSeq v1.0 genome underlying the physical position of selected QTL using Wheat@URGI portal (<https://wheat-urgi.versailles.inra.fr/>; Alaux et al., 2018). And model genes in the physical interval of all 11 selected QTL were analyzed through a web-based gene ontology annotation program WEGO 2.0 (<http://wego.genomics.org.cn/>; Ye et al., 2018). However, from the 1017 genes only six genes in the IWGSC RefSeq annotation v1.0 were associated with the term ‘defense’ with the GO term ‘GO:006952 BP: defense response’ and one with the term ‘GO:0050832: defense response to fungus’ although many more genes contained in the human-readable description annotations were clearly related to ‘defense’. In addition, most of 1017 genes were only annotated with just one GO term or none GO term (59.3%). This indicates that the IWGSC RefSeq annotation v1.0 is not suitable for candidate gene identification based on GO terms and further improvement or other resources are required for functional annotation of wheat genes. Thus, a Blast2GO

analysis was performed for the 1017 genes from the selected QTL regions which improved completeness of functional GO annotations for some genes, but not for all.

Following *F. g/F. p*-inoculation, the number of up-regulated genes in the resistant genotype was 71 and for the susceptible genotype it was 59 up-regulated genes compared to gene expression in mock-treated plant. The numbers of down-regulated genes detected following *F. g/F. p*-inoculation was 52 for the resistant genotype and 70 for the susceptible genotype. In total, 210 induced genes (102 up- and 108 down-regulated) were detected in two genotypes following *F. g/F. p*-inoculation. Of them, 28 were up-regulated and 14 down-regulated in both resistant and susceptible genotypes. Furthermore, differentially expressed genes between resistant and susceptible genotypes were identified to indicate wheat molecular mechanisms might be associated with *Fusarium* resistance. The number of up-regulated and down-regulated genes was 66 and 64 after *F. g/F. p*-inoculation comparing the resistant genotype with the susceptible genotype. Following mock-inoculation 54 and 72 up-regulated and down-regulated genes were detected between two genotypes. Of them, 43 up-regulated and 44 down-regulated genes were identified only after *F. g/F. p*-inoculation excluding identical genes differentially expressed under mock treatment. Finally, differentially expressed genes between resistant and susceptible genotypes following *F. g/F. p*-inoculation were compared with the *F. g/F. p*-induced genes detected above. 81 differentially expressed genes between resistant and susceptible genotypes were selected for further functional annotation and 22 of them are putatively involved in wheat resistance to *F. graminearum* underlying FCR resistance QTL (Table 11, marked with asterisk). These 22 genes encoding *F. graminearum* defense related proteins are widely reported in the literature, including F-box proteins, cytochrome P450s, receptor-like kinases, glycosyltransferases, pathogenesis-related proteins PR4, disease resistance proteins, glutathione S-transferases, bZIP (basic leucine zipper) transcription factors, zinc finger proteins and peroxidases (Table 12).

Table 11. Differentially expressed and regulated genes between resistant and susceptible genotypes from QTL identified in this study analyzed via ‘expVIP’ database.

QTL	Up-and down-regulated genes	Human readable description	
<i>qSbSI-1A_Sdi</i>	TraesCS1A01G015200.2	Tubulin-specific chaperone cofactor E-like protein	
	TraesCS1A01G016200.1*	Disease resistance protein	
	TraesCS2D01G063300.1	E3 ubiquitin-protein ligase	
<i>qSr/SbSI-2D_Sdi</i>	TraesCS2D01G065000.1	Expansin	
	TraesCS2D01G066600.1	Carboxypeptidase	
	TraesCS2D01G067800.1*	Receptor-kinase, putative	
	TraesCS3A01G104800.3*	Receptor-like kinase	
	TraesCS3A01G105000.3	Transcription factor, putative	
<i>qSr-3A_Sdi</i>	TraesCS3A01G105700.1	EEIG1/EHBP1 N-terminal domain-containing protein	
	TraesCS3A01G109600.1*	zinc finger WD40 repeat protein 1	
	TraesCS3A01G111100.3	Protein TWIN LOV 1	
	TraesCS3A01G111700.1*	bZIP transcription factor, putative (DUF1664)	
<i>qSbSI/DL_SLi-3A_Rti/Sdi</i>	TraesCS3A01G513000.1	Mitochondrial carrier protein-like	
	TraesCS3B01G006600.1*	Cytochrome P450 family protein, expressed	
	TraesCS3B01G006900.1	WAT1-related protein	
<i>qSbSI-3B_Rti</i>	TraesCS3B01G009600.1	arabinogalactan protein 18	
	TraesCS3B01G011800.1	O-acyltransferase WSD1	
	TraesCS3B01G014000.1	cyclic nucleotide-gated channel 12	
	TraesCS4B01G313300.1	Cortical cell-delineating protein	
<i>qSLR-4B.2_Rti</i>	TraesCS4B01G314800.1	kinase with tetratricopeptide repeat domain-containing protein	
	TraesCS5A01G263700.2	Serine carboxypeptidase family protein, expressed	
<i>qRLR-5A_Rti</i>	TraesCS5A01G265500.3	2-oxoglutarate (2OG) and Fe (II)-dependent oxygenase superfamily protein	
	TraesCS5A01G266700.1	CCAAT/enhancer-binding protein delta	
<i>qSDWR-6A_Sdi</i>	TraesCS6A01G020300.1	Mitochondrial transcription termination factor-like	
	TraesCS6A01G024300.1	Kinase family protein	
	TraesCS6A01G024500.1	Cytosolic 5'-nucleotidase 3A	
	TraesCS6D01G379900.2	2-phosphoglycerate kinase-related family protein	
	TraesCS6D01G380100.1	OTU domain-containing protein	
	TraesCS6D01G381400.1*	F-box/RNI-like/FBD-like domains-containing protein	
	TraesCS6D01G381500.2*	Leucine-rich repeat protein kinase family protein	
	TraesCS6D01G382300.1	Protein KINESIN LIGHT CHAIN-RELATED 3	
	TraesCS6D01G382800.1*	Cytochrome P450, putative	
	TraesCS6D01G386800.1*	Pathogenesis-related protein PR-4	
<i>qRDWR-6D_Sdi</i>	TraesCS6D01G387100.1	Mitochondrial import inner membrane translocase subunit tim50	
	TraesCS6D01G387300.1	Divinyl reductase	
	TraesCS6D01G388400.1	Smad/FHA domain protein	
	TraesCS6D01G389100.1	RING/U-box superfamily protein	
	TraesCS6D01G389800.1	Acyl-CoA-binding domain-containing protein 4	
	TraesCS7D01G008800.2	Beta-fructofuranosidase 1	
	<i>qSbSI-1A_Sdi</i>	TraesCS1A01G016800.1*	Glutathione S-transferase
		TraesCS1A01G013800.3	Methionine S-methyltransferase
		TraesCS1A01G016900.1	Phosphatidate cytidyltransferase
TraesCS1A01G016000.1		Serine/threonine-protein kinase	
TraesCS2D01G068600.1*		F-box protein	
<i>qSr/SbSI-2D_Sdi</i>	TraesCS2D01G069000.1*	Glycosyltransferase	
	TraesCS2D01G069100.1*	Glycosyltransferase	
	TraesCS2D01G063200.1	mRNA-capping enzyme	
	TraesCS2D01G065100.1	Ribulose biphosphate carboxylase small chain	
<i>qSr-3A_Sdi</i>	TraesCS3A01G109200.4	2-oxoglutarate (2OG) and Fe (II)-dependent oxygenase superfamily protein	
	TraesCS3A01G109100.1*	F-box domain containing protein	
	TraesCS3A01G109900.2	Glycine-rich protein	
	TraesCS3A01G510700.1	Abscisic stress ripening	

<i>qSbSI/DL_SLi-3A_Rti/Sdi</i>	TraesCS3A01G511000.1*	F-box domain containing protein
	TraesCS3A01G510900.1*	Peroxidase
<i>qSbSI-3B_Rti</i>	TraesCS3A01G513500.2	Uridylate kinase
	TraesCS3B01G013500.1	30S ribosomal protein S7, chloroplastic
	TraesCS3B01G014600.1	Murein hydrolase activator NlpD
	TraesCS3B01G012700.1*	Receptor-like protein kinase
	TraesCS4B01G318000.1	Beta-carotene hydroxylase
	TraesCS4B01G319100.1	Chaperone protein dnaJ
	TraesCS4B01G312300.1*	Cytochrome P450, putative
<i>qSLR-4B.2_Rti</i>	TraesCS4B01G317500.1	dipeptide transport ATP-binding protein
	TraesCS4B01G312900.1	Indole-3-glycerol phosphate synthase
	TraesCS4B01G315100.1	Phosphate import ATP-binding protein PstB
	TraesCS4B01G316500.1	Protein KINESIN LIGHT CHAIN-RELATED 3
	TraesCS4B01G313900.2*	receptor kinase 1
	TraesCS5A01G265800.1	Beta-glucosidase, putative
	TraesCS5A01G262100.1	Calcium-binding EF-hand family protein-like
<i>qRLR-5A_Rti</i>	TraesCS5A01G266600.1	DNA-binding bromodomain-containing protein
	TraesCS5A01G266500.2	Peroxisomal (S)-2-hydroxy-acid oxidase
	TraesCS5A01G266800.1	Protein NUCLEAR FUSION DEFECTIVE 5, mitochondrial
	TraesCS5A01G263100.1	Tonoplast dicarboxylate transporter
	TraesCS6A01G026500.2	Lysine-specific demethylase 3B
<i>qSDWR-6A_Sdi</i>	TraesCS6A01G024900.1	U5 small nuclear ribonucleoprotein helicase
	TraesCS6D01G383100.1*	F-box family protein
<i>qRDWR-6D_Sdi</i>	TraesCS6D01G391800.1*	F-box/RNI-like/FBD-like domains-containing protein
	TraesCS6D01G380200.1	Protein kinase
	TraesCS7D01G008400.1	NADH dehydrogenase (Ubiquinone) complex I, assembly factor 6
<i>qDL_SLi-7B_Sdi</i>	TraesCS7D01G011000.1	Protein yippee-like
	TraesCS7B01G438800.1	Ubiquitin system component Cue protein
<i>qSbSI/DL_SLi-7D_Rti</i>	TraesCS7D01G011100.2	Transposon protein, putative, CACTA, En/Spm sub-class

*Genes encoding widely reported *F. graminearum* defense related proteins in wheat

Table 12. Selected *F. graminearum* resistance genes functional annotation reported in the literature.

Human readable description	FCR/FHB resistance QTL	Literature
F-box protein	QTL2, QTL3, QTL4, QTL9	63, 60, 78, 83, 87
Cytochrome P450	QTL5, QTL6, QTL9	9, 20, 25, 31, 33, 41, 42, 46, 47, 48, 57, 69, 75, 80, 82
Disease resistance protein	QTL1	10, 13, 16, 19, 47, 58, 83
Receptor-like kinase	QTL2, QTL4, QTL5	7, 10, 19, 43, 54, 61, 70, 73, 78, 84
bZIP transcription factor	QTL4	18, 27, 78
Zinc finger protein	QTL4	36, 40, 42, 63, 67, 78, 80, 82
Peroxidase	QTL3	2, 3, 4, 5, 8, 11, 14, 18, 24, 33, 42, 45, 51, 52, 56, 57, 58, 72, 77, 78, 86
Glutathione S-transferase	QTL1	4, 11, 31, 33, 41, 42, 43, 49, 56, 57, 58, 61, 73, 78, 88
Glycosyltransferase	QTL2	18, 29, 47, 49, 53, 59, 57, 58, 68, 70, 71, 73, 76, 74, 79, 81
Pathogenesis-related protein PR4	QTL9	2, 3, 15, 19, 26, 39, 43, 51, 56, 78

QTL1: *qSbSI-1A_Sdi*; QTL2: *qSr/SbSI-2D_Sdi*; QTL3: *qSbSI/DL_SLi-3A_Rti/Sdi*; QTL4: *qSr-3A_Sdi*; QTL5: *qSbSI-3B_Rti*; QTL6: *qSLR-4B.2_Rti*; QTL7: *qRLR-5A_Rti*; QTL8: *qSDWR-6A_Sdi*; QTL9: *qRDWR-6D_Sdi*; QTL10: *qDL_SLi-7B_Sdi*; QTL11: *qSbSI/DL_SLi-7D_Rti*

Literature: 1, Chen et al. (1999); 2, Pritsch et al. (2000); 3, Pritsch et al. (2001); 4, Kruger et al. (2002); 5, Mohammadi et al. (2002); 6, Anand et al. (2003); 7, Liu et al. (2003); 8, Bai et al. (2004); 9, Kong et al. (2005); 10, Wang et al. (2005); 11, Zhou et al. (2005); 12, Goswami et al. (2006); 13, Guo et al. (2006); 14, Khan et al. (2006); 15, Klahr et al. (2006); 16, Shen et al. (2006); 17, Zhou et al. (2006); 18, Ansari et al. (2007); 19, Golkari et al. (2007); 20, Kong et al. (2007); 21, Ramamoorthy et al. (2007); 22, Zhang et al. (2007); 23, Desmond et al. (2008a); 24, Desmond et al. (2008b); 25, Handa et al. (2008); 26, Paranidharan et al. (2008); 27, Walter et al. (2008); 28, Xing et al. (2008); 29, Lulin et al. (2009); 30, Jia et al. (2009); 31, Steiner et al. (2009); 32, Walter et al. (2009); 33, Li et al. (2010); 34, Kovalchuk et al. (2010); 35, Van der Weerden et al. (2010); 36, Bahrini et al. (2011); 37, Li et al. (2011); 38, Kaur et al. (2011); 39, Miller et al. (2011); 40, Son et al. (2011); 41, Walter et al. (2011); 42, Cho et al. (2012); 43, Foroud et al. (2012); 44, Gottwald et al. (2012); 45, Gunnaiah et al. (2012); 46, Muhovski et al. (2012); 47, Kugler et al. (2013); 48, Moya et al. (2013); 49, Schweiger et al. (2013); 50, Xiao et al. (2013); 51, Zhang et al. (2013); 52, Al-Taweel et al. (2014); 53, Gunnaiah et al. (2014); 54, Ravensdale et al. (2014); 55, Wu et al. (2014); 56, Erayman et al. (2015); 57, Kosaka et al. (2015a); 58, Kosaka et al. (2015b); 59, Ma et al. (2015); 60, Choura et al. (2016); 61, Dhokane et al. (2016); 62, Hofstad et al. (2016); 63, Schweiger et al. (2016); 64, Sun et al. (2016); 65, Wang et al. (2016); 66, Al-Twaeel et al. (2017); 67, Kage et al. (2017b); 68, Li et al. (2017); 69, Mona et al. (2017); 70, Samad-Zamini et al. (2017); 71, Sorahinobar et al. (2017); 72, Spanic et al. (2017); 73, Biselli et al. (2018); 74, Gatti et al. (2018); 75, Gunupuru et al. (2018); 76, He et al. (2018); 77, Lee et al. (2018); 78, Pan et al. (2018); 79, Sharma et al. (2018); 80, Wang et al. (2018); 81, Xing et al. (2018); 82, Brauer et al. (2019); Fauteux et al. (2019); 84, Hu et al. (2019); 85, Sorahinobar et al. (2019); 86, Yan et al. (2019); 87, Hao et al. (2020); 88, Wang et al. (2020); 89, Yang et al. (2020); 90, Zhu et al. (2020)

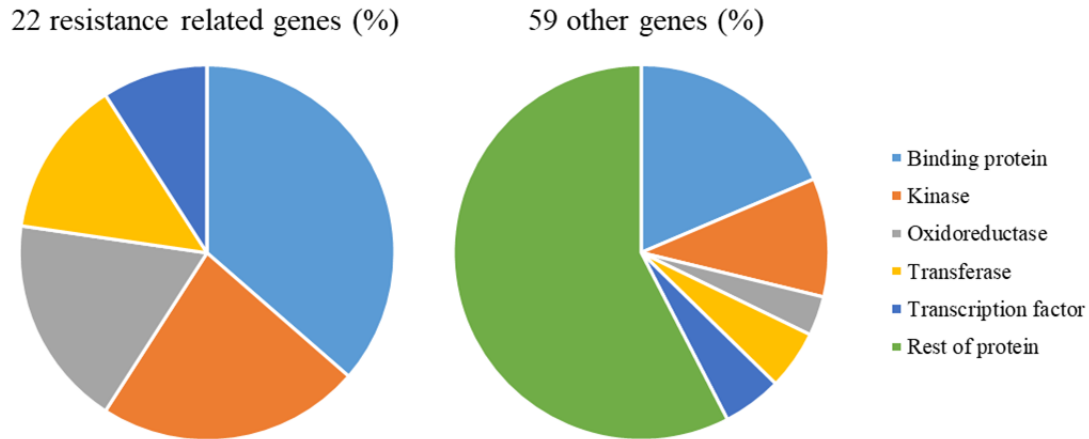


Figure 25. Comparison of proteins encoded by resistance related genes and other genes in 81 differentially expressed genes between resistant and susceptible genotypes after *Fusarium* inoculation.

The human readable functional annotation description of proteins encoded by *F. graminearum*-induced resistance genes were classified as several categories showing in Figure 25. For example, 36.4% well described resistance related proteins could be summarized to binding proteins whereas 18.6% proteins encoded by other genes also could be grouped to the same category. In the category ‘kinase’ 22.7% resistance related proteins and 10.2% other proteins could be found, respectively. It indicates that more other genes maybe involve in *Fusarium* resistance than the well described ones. Furthermore, the QTL had such large intervals (over 1.1Mbp) containing many linked genes encoding proteins might be without any relevance for *Fusarium* resistance. Therefore, it is insufficient to precisely identify promising *Fusarium* resistance candidate genes via QTL analysis alone.

5 Discussion

Fusarium root and crown root (FCR) disease causes severe wheat yield and economic loss worldwide. Along with climate change and adoption of minimum tillage, stubble retention practices in farming systems, the disease has become more prevalent in many countries. Breeding FCR resistance cultivars is considered as the most efficient way against this disease. However, so far information on FCR resistance QTL and useful molecular markers for marker-assisted breeding is limited. In a number of studies mainly different QTL for FCR resistance and only a low number of overlapping QTL have been identified. This may be due to the use of different phenotyping approaches and disease rating systems in the existing studies. Thus, initially a number of the most widely used approaches were compared in the current study.

5.1 Commonly used disease indices need to be reconsidered to characterize FCR resistance

The doubled haploid (DH) population used in this study for genetic mapping of FCR resistance was developed from a cross between line 162.11 and cv. Tobak, which were classified as contrasting resistant/susceptible genotypes based on a disease index incorporating six different parameters including i) relative fungal biomass, percentage average change of mock vs. inoculated plants in ii) root biomass, iii) root length, iv) shoot length, v) root symptom rating and vi) stem base symptom rating (Wang, 2015). However, no statistical evidence was reported in this study for differences in the six single parameters between these two selected parental genotypes. In the present study the phenotypic data for morphological traits including root and shoot length reduction, root and shoot dry weight reduction were frequently not significantly different in ANOVA between the two selected parental genotypes of the mapping population in multiple repeated experiments. In contrast, two disease severity measures (SbSI, DL_SLi) showed significant differences ($P < 0.05$) between the two parental genotypes except DL_SLi in *F. graminearum* root inoculation experiment. This indicates that line 162.11 may not be partially more resistant against FCR than the 'susceptible' cultivar Tobak statistically. The possibly false classification as partial resistant and susceptible to FCR by Wang (2015) might have been due to the limited number of wheat genotypes and replicates in the study. In addition, in the present study and in the study of Voss-Fels et al. (2018), disease indices based on discoloration symptoms on roots were found to be a poor resistance indicator suggesting that 1/6 of the input data for the FDI index

in Wang (2015) might be based on very unreliable measures. Therefore, the ranking scheme of Wang (2015) combining different resistance-related parameters might inadequately reflect the FCR resistance reaction and should be modified and/or other indices need to be considered. Some phenotype measures showed stronger variation compared to others such as the traits involving disease scoring and discoloration rating (DS, SbSI). The reason could be that the measurement cannot be done so accurately based on visual scoring following the standard rating system (0 to 5 levels). This is consistent with results of the study conducted by Voss-Fels et al. (2018) where weakly positive correlations were also found between discoloration rating and dry weight of mock treated plants, suggesting that growth related discoloration on stem base of health plants could influence the accuracy for disease severity evaluation.

A large number of different field and greenhouse inoculation and screening methods have been used in the past to assess crown rot resistance in wheat (Mitter et al., 2006; Liu and Ogbannaya, 2015). Here two different commonly used inoculation methods have been applied in the greenhouse and compared in QTL analysis, root-dip inoculation of young seedlings and seed-dip inoculation using defined *F. graminearum* spore concentrations. Also, many different rating schemes exist for CR resistance evaluation (Dodman et al., 1985; Klein et al., 1985; Liddell et al., 1986; Dodman and Wildermuth, 1987; Wildermuth and McNamara, 1994; Wallwork et al., 2004, Mitter et al., 2006; Li et al., 2008; Poole et al., 2012; Wang et al., 2015; Liu and Ogbannaya, 2015; Voss-Fels et al., 2018). In this study the methods of Mitter et al. (2006), Wang et al. (2015) and Voss-Fels et al. (2018) were compared because they provided differently commonly used rating systems. Voss-Fels et al. (2018) used a stem base discoloration score (in this study called DS). Wang et al. (2015) used the stem base symptom index (in this study called SbSI) which adds to the final disease index calculation a score for the length of the discolored stem base section. Mitter et al. (2006) did not use a discoloration score, but used the length of the discolored stem base section and did set this in relation to the total shoot length (in this study called DL_SLi). Thus, the disease index of Voss-Fels et al. (2018) and Wang et al. (2015) will measure resistance to primary infection at the stem base (and its extension at the stem base) whereas the disease index of Mitter et al. (2006) will also measure tolerance to infection manifested in a reduced disease score for genotypes which are reacting with less stunting of the shoots relative to the discoloration extension at the stem base compared to other

genotypes reacting with strong stunting after infection of the stem base. The comparison of these disease scoring matrices and correlations with morphological traits was applied in this study to try to draw new conclusions on the mechanism of resistance/tolerance inherited in the mapping population mediated by different individual QTL regions.

The strongest correlation was found between two different disease rating systems in root and seed inoculation experiments, the SbSI (stem base symptom index) and the DS (discoloration scale) rating system. This was expected as the SbSI index represents a modified discoloration scale index where also the extension of the discoloration at the stem base is incorporated in the calculation. However, only the SbSI index, but not the DS index showed a correlation with the root dry weight under infection in the root inoculation experiment, suggesting that it is critical to include a measurement of the discoloration along the stem base into the disease index calculation to capture the damaging effect of the disease on the plants whereas measuring the discoloration at the stem base (DS) is not sufficient to judge FCR resistance. The correlation between both indices with the third used disease index, the crown rot severity index after Mitter et al. (2006) here called DL_SLi index was less strong. The DL_SLi index also showed a very different pattern of correlations with morphological traits compared to the DS and SbSI indices in root and seed inoculation experiments. DS and SbSI disease indices were showing correlations mainly with morphological traits in the mock treated data sets, whereas the DL_SLi disease index only showed correlations with morphological traits in the *F. graminearum* treated data sets in root and seed inoculation experiments. This might also suggest that visual stem discoloration scores (DS and SbSI) may be biased by growth related discoloration of the stem base as reported by Voss-Fels et al. (2018). The use of these disease indices (DS, SbSI) to judge resistance should thus be avoided and instead the use of the DL_SLi index corrected by shoot length under infection is recommended. This also indicates that developmental shoot differences interact with the reaction of the population to infection and these interactions should be taken into account when trying to identify QTL regions that are broadly active and independent of developmental and environmental influences.

Root dry weight of plants under *F. graminearum* treatment (RDWi) negatively correlated with the stem base symptom index (SbSI), but not with the Mitter et al. (2006) disease index (DL_SLi). Instead, the DL_SLi was correlated with the root length (RLi), the shoot length (SLi) and the shoot dry weight (SDWi) under *F. graminearum*

treatment. This indicates that a correlation with a disease index can only be detected for the root dry weight if the disease index is not corrected for the shoot length after infection (SbSI). On the other hand, a correlation with a disease index can only be detected for the shoot and root length and for the shoot dry weight if the disease index is corrected for shoot length after infection (DL_SLi). In other words, the disease effects on the root dry weight are masked using the Mitter et al. (2006) index (DL_SLi) and the disease effects on the shoots are masked using the SbSI index. This problem can be avoided by using relative reduction values calculated from the differences of the mock and inoculated data set (SLR, RDWR, SDWR) instead of absolute values (RLi, SLi, RDWi, SDWi) for QTL mapping to only cover the disease impact and resistance/tolerance reactions and remove genetic variation originating from differences of the root and shoot growth development.

5.2 FCR resistance is quantitatively inherited and plant organ/developmental stage dependent

Although the phenotypic data for the relative reductions of morphological traits between the two parents of the mapping population after inoculation were frequently not significantly different from each other in *F. graminearum* root and seed inoculation experiments, the phenotypic data for the DH population showed transgressive segregation for length and dry weight reduction and for disease severity measures (SbSI, DL_SLi). Transgressive segregation is the formation of extreme phenotypes observed in the population compared to phenotypes observed in the parental lines, which has played an important role in improving Fusarium head blight (FHB) resistance. For example, one of the most FHB highly resistant cultivar Sumai 3 was derived from a cross of two moderately susceptible lines (Liu and Wang, 1990). The recently registered FHB resistant wheat variety Emerson and several released durum wheat cultivars were also obtained from populations showing transgressive segregation (Graf et al., 2013; Zhang et al., 2014; Zhang et al., 2018). Transgressive segregation was observed in the population indicating that the susceptible parent as well as the partially resistant parent can contribute positive alleles for different resistance QTL. Significant resistance alleles inherited from the susceptible parent were also reported by researchers for quantitative disease resistances in other crops (Collard et al. 2005; Bovill et al. 2006; Ma et al. 2010; Poole et al., 2012). This indicates that pyramiding of alleles from diverse resources is required for effective enhancement of FCR resistance in breeding (Bovill

et al., 2010; Zheng et al. 2017; Crespo-Herrera et al., 2017).

A number of morphological traits showed correlation with FCR disease traits. These correlations were different in the root and seed inoculation experiments which might reflect the activation of different resistance/tolerance mechanisms when different organs or developmental stages were inoculated. In the seed inoculation experiment, resistant genotypes were less affected in their root dry weight and in their shoot dry weight by *F. graminearum* treatment than susceptible genotypes which could be seen by the negative correlations between the disease index DL_SLi and root and shoot dry weight (RDWi, SDWi) and the positive correlation between DL_SLi and root and shoot dry weight reduction (RDWR, SDWR). This is different from the correlations in the root inoculation experiment. Here root dry weight under *F. graminearum* treatment was not correlated with DL_SLi, but the other three morphological traits (RLi, SLi and SDWi) did. The survival rate (Sr) did correlate with the disease indices DS and SbSI, but not with the disease index DL_SLi in the seed inoculation experiment indicating that the extend of browning at the stem base is associated with the plant survival, but not the extent of browning at the stem base relative to the plant height and it is masked using the Mitter et al. (2006) index (DL_SLi) after seed inoculation. The Sr was excluded in root inoculation experiment because the roots were already well established when seedlings were inoculated and the first leaf unfolds resulting in a high survival rate of infected plants and low variation in the DH population. In the seed inoculation experiment seeds were treated with the spore suspension and the emerging shoot and first fine roots were exposed from the very beginning to infection by the fungus and only plant with strong resistance to *F. graminearum* could survive. Eventually, most of FCR resistance QTL identified after *F. graminearum* root and seed inoculations were not same, which also indicates that FCR resistance is mainly plant organ/developmental stages dependent.

It was realized in this comparative correlation analyses that it is critical for uncovering biological meaningful interactions between morphological root and shoot traits in the *F. graminearum*-treated data set with disease resistance to study and include different disease rating systems. To get QTL relevant for breeding FCR resistant genotypes, researchers are recommended to use different disease rating systems for QTL mapping and use different inoculation procedures (root and seed inoculations).

5.3 QTL for FCR resistance and tolerance can be dissected using different disease indices

Within recent QTL studies for FCR resistance all identified QTL were mainly based on measurements of leaf sheath or stem discoloration of seedlings or adult plants (Liu and Ogbannaya, 2015). In the present study, two rating methods (SbSI = Wang et al., 2015 method, DL_SLi = Mitter et al., 2006 method) were applied for identifying FCR resistance/tolerance QTL of seedlings. In the *F. graminearum* root inoculation experiment, five QTL were identified using the first rating method (SbSI) whereas only two QTL were detected applying the second rating method (DL_SLi). In the *F. graminearum* seed inoculation experiment, six and four QTL were detected using two rating methods, respectively. In the root inoculation experiment, two identical FCR resistance QTL were detected on the chromosome 3AL using Wang et al. (2015) and Mitter et al. (2006) methods. The former explained 16.1% phenotypic variation whereas the latter explained less phenotypic variation (11.4%). Other two identical FCR resistance QTL were identified on chromosome 7DS using both rating methods. 21.9% and 13.9% phenotypic variations were explained by SbSI and DL_SLi respectively. In the seed inoculation experiment, however, different FCR resistance QTL were identified using two methods. These differences might be due to the characteristics of the disease indices used. The Wang et al. (2015) method is an exclusive stem base symptom index (in this study called SbSI) which is only able to map the primary infection resistance, whereas the Mitter et al. (2006) index (in this study called DL_SLi) can in addition map morphological or developmental tolerance QTL. In the root inoculation experiment the QTL exclusively based on resistance to initial discoloration of the stem (SbSI) predominated whereas in the seed inoculation experiment the QTL also associated with plant growth (DL_SLi). It suggests that not only resistance, but also tolerance to FCR may play an important role in wheat and that these QTL are differently expressed in plant developmental stages and organs (roots and seeds) which reinforces the conclusions discussed above for the morphological and disease trait correlations recorded in different experiments. In addition, few QTL mapped by these two different disease indices also overlapped in the root and seed inoculation experiments indicating the broad-spectrum resistance to FCR in different developmental stages and organs of plants.

5.4 FCR affects root biomass whereas resistance/tolerance is not associated with high root biomass accumulation

Plants showed severe relative reduction of root dry weight under *F. graminearum* treatment for both parents (line 162.11, cv. Tobak) and for the DH population compared to reduction of other morphological traits. These outcomes were found not only in the *F. graminearum* root inoculation experiment but also in the *F. graminearum* seed inoculation experiment. Wang et al. (2015) reported a similar result after conducting *F. graminearum* root inoculation on the same parental genotypes, line 162.11 and cv. Tobak. Although the reduction of root dry weight was serious, root length was less impacted by *F. graminearum* and exhibited no significant correlations with symptom-based disease severity measures (SbSI, DL_SLi). This is suggesting that infection-induced structural changes within the roots and/or decreased branching root might only affect the root dry weight, but not the length of the root which should be excluded in the future from calculating a disease index for ranking resistance reactions as done by Wang et al. (2015). Also, reduction of root branching resulting in decreased total root biomass might be triggered by the impaired carbohydrate energy supply for the plant root growth due to successful fungal infection. Plant roots are known to show high plasticity and can sense and respond with developmental and physiological adaptations to changes of soil environment as well as to plant-microbe interactions (Shen et al., 2013; Wang et al. 2015). However, in the present experiments FCR resistance/tolerance was not associated with morphological traits including root biomass. Root dry weight of healthy plants was not significant correlated with measured discoloration section length on stem base to the shoot length (DL_SLi) in root and seed inoculation experiments. This is in contrast to reports of Voss-Fels et al. (2018) in wheat and Alahmad et al. (2020) in durum wheat. Voss-Fels et al. (2018) reported that in a wheat diversity set genotypes with a higher total root biomass were more resistant to *F. graminearum* infection via roots, because negative correlations were found between roots biomass of healthy plants with fungal DNA concentrations in roots after infection. In a recent study of durum wheat yield in drought and crown rot environments, Alahmad et al. (2020) reported a link between root biomass and crown root tolerance based on the proximity of QTL for root biomass and crown rot resistance. However, in the study of Voss-Fels et al. (2018) the correlation was quite low and in the study of Alahmad et al. (2020) no trait correlations were evaluated. Thus, the lack of correlation in the present study might be due to a different inheritance in the biparental population

compared to a wheat diversity set used by Voss-Fels et al. (2018) and/or the effect of root biomass on CR resistance might be weaker than postulated in these studies. Voss-Fels et al. (2018) and Alahmad et al. (2020) both also conjectured that increased total root biomass might be due to a higher number of fine roots and/or a higher number of roots with a different morphological composition on the cellular level in partially resistant genotypes, e.g. with higher fiber/lignin content of root tissues resulting in a physical barrier for fungal growth and consequently leading to reduced susceptibility to *F. graminearum* infection. Another putative explanation has been discussed by Voss-Fels et al. (2018) stating that increased root growth might not represent a partial resistance, but a ‘tolerance reaction’ or ‘escape reaction’ in which fungal infection is counteracted by an increased root biomass growth. Therefore, further studies should be conducted to validate the association between morphological traits including root biomass of healthy plants and FCR resistance/tolerance.

5.5 Some FCR resistance QTL are co-localizing with FCR/FHB resistance QTL reported in the literature

To date, FCR resistance QTL have been reported to reside on 17 of 21 wheat chromosomes, but only three QTL on chromosomes 2DL, 3BL and 5DS could be consistently detected in different genetic backgrounds. FCR resistance QTL have not been identified on chromosomes 3D, 4A, 7A and 7D (Collard et al., 2005; Ma et al., 2010; Poole et al., 2012; Zheng et al., 2014; Liu and Ogonnaya, 2015; Martin et al., 2015; Erginbasorakci et al., 2018; Yang et al., 2019; Jin et al., 2020; Pariyar et al., 2020). In the current study, 28 FCR resistance QTL were identified which reside on 14 of the 21 wheat chromosomes. Also, a QTL was identified on chromosome 7D where no QTL has been reported in the literature before. Five of the 28 identified QTL (18%) are co-localizing with QTL reported in the literature showing medium to high effects (*qSr-1B_Sdi* with 11.9% R^2 , *qSr/SbSI-2D_Sdi* with 12.1% R^2 , *qSbSI-3B_Rti* with 16.4% R^2 , *qSbSI-1A.2_Sdi* with 27% R^2 and *qSLR-4B.2_Rti* with 35.6% R^2). Thus, most detected QTL were found at new genomic regions. This is not unusual and confirms the quantitatively inherited nature and high dependency of FCR resistance/tolerance on the environment and genetic material used. However, although three FCR resistance QTL are known which have been consistently detected in different genetic backgrounds on chromosomes 2DL, 3BL and 5DS in different studies conducting similar seedling inoculation experiments, none of them was detected in this study. This might be due to

the characteristics of the used biparental mapping populations, where spring type genotypes of the taxon *T. aestivum* subspecies *spelta*, CSCR6, and of the Australia wheat cultivar EGA Wylie were used as partially resistant parents in these studies (Ma et al., 2010; Zheng et al., 2014) whereas in the present study a cross between German winter type cultivars were analyzed (line 162.11 is derived from the cultivars Tyberius/Opus, cv. Tobak has the pedigree Elvis/ Drifter// Koch).

It has been reported for spring type crosses before that resistance QTL against FCR are not always *Fusarium* species specific, e.g. some major FCR QTL against *F. graminearum* and against *F. pseudograminearum* mapped to the same chromosomal region and providing the same magnitude of partial resistance against both fungal species (Ma et al. 2010). In addition, it has been reported that QTL against FCR sometimes overlap with QTL against FHB disease which makes identification of these particular QTL an ideal target for effective wheat breeding. Pariyar et al. (2020) reported that three FCR resistance QTL on chromosomes 3BS, 4BL and 6BS were previously identified as FHB resistance QTL. The QTL on chromosome 3BS has shown the strongest effect against *F. graminearum*-induced head blight whereas only a moderate effect to *F. culmorum*-induced crown rot was shown. This QTL, a well-recognized major FHB QTL called *Fhb1*, on chromosome 3BS was also identified in the present study. QTL *Fhb1* on chromosomes 3BS was about 5 Mbp away from QTL *qSbSI-3B_Rti* identified in the current study to provide moderate effects for *F. graminearum*-induced FCR resistance. Another FCR resistance QTL *qSLR-4B.2_Rti* showing high effects against *F. graminearum* identified in the present study might be identical to the FHB resistance QTL *Fhb4* on chromosome 4BL with about 6 Mbp physical distance. This indicates that some QTL against FHB caused by *F. graminearum* are also major components of FCR resistance caused by *F. graminearum* and *F. culmorum*. This would imply that German winter type wheat genotypes might show broad-spectrum resistance to both diseases because of the same QTL contributing resistance. On the contrary, Li et al. (2010) reported that no significant correlation between plant reactions to FHB and FCR was found in diverse accessions from China, the US and Australia. Resistance QTL against the two diseases were mapped on different chromosomes, suggesting that also different host genes were involved in the resistance against FHB and FCR in some wheat accessions. In addition, as a major FHB resistance source the genotype Sumai 3 showed FCR susceptibility in a FCR resistance

study and none of the identified FHB resistance QTL from Sumai 3 were detected to overlap with FCR resistance QTL (Zheng et al., 2014). This suggests that QTL with broad-spectrum resistance against FCR and FHB and disease-specific QTL co-exist in bread wheat genotypes. Therefore, the identification of QTL effective across *Fusarium*-induced diseases is inevitable. Recently, the causal gene from the FHB resistance QTL *Fhb1* had been cloned by Su et al. (2019). The causal gene from the FHB resistance QTL *Fhb7* has been introduced into bread wheat from *Thinopyrum elongatum*. Cloning revealed that the *Fhb7* causal gene for resistance encodes a glutathione S-transferase (GST) that can detoxify trichothecene toxins. *Fhb7* has been transferred from an endophytic *Epichloë* species to *Th. elongatum* through horizontal gene transfer (HGT). Moreover, *Fhb7* has been shown to confer resistance to both *F. graminearum* causing diseases of head blight and crown rot without yield penalty, which showed the potential utility for *Fusarium* resistance breeding (Wang et al., 2020). Thus, some QTL regions identified in the current study (e.g. QTL *qSbSI-3B* and *qSLR-4B.2*) and other studies might confer broad-spectrum resistance to both FHB and FCR diseases caused by *F. graminearum*/*F. culmorum*, whereas other regions might only confer resistance to either FHB or FCR (e.g. QTL *qFhb-6B* from previous study and QTL *qDL_SLi-7D* from this study). Therefore, FCR resistance is not just controlled by pathogen species and disease-overlapping resistance (*Fhb1/qSbSI-3B* + *Fhb4/qSLR-4B.2*, FCR+FHB), but also by disease (FCR/FHB-specific) and *F. graminearum*-specific QTL.

5.6 FCR resistance QTL is associated with a semi-dwarfing gene linked to FHB susceptibility

One particularly interesting and striking result is that QTL *qSLR-4B.1_Rti* with an effect of 11.2% R^2 for shoot length reduction under infection detected on the chromosome 4BS is overlapping with the semi-dwarfing gene *Rht-B1*. Wallwork et al. (2004) also described that plant height seems to influence FCR resistance in Australian wheat and that a QTL conferring increased resistance is linked to the *Rht1* gene, causing reduced height in wheat. In the current study not only a QTL for a disease index was overlapping with the *Rht1* gene locus, but also a QTL *qSDWm-4B* for shoot dry weight of healthy plants. Because shoot length (plant height) positively correlated with shoot dry weight, the active semi-dwarfing gene also negatively mediates the shoot dry weight. A significant but low positive correlation between plant height (shoot length) of healthy plants and stem base symptom index (SbSI) was found in this study, indicating that

expression of *Rht-B1* in shorter plants may increase FCR resistance. Liu et al. (2010) reported consistent results showing that the dwarf isolines of wheat all gave better FCR resistance when compared with their respective tall counterparts, which could be due to that dwarf isolines have shorter cell length with higher cell density and prevent pathogen infection and spread in the plant on a physical level if spread occurs mainly from cell to cell like in a root infection scenario.

For FHB disease resistance, however, the QTL alleles associated with reduced height from this study shows resistance to FCR whereas the QTL alleles associated with reduced height show susceptibility to FHB disease reported in the literature. This is in agreement with the observations of Wang et al. (2018) who found that contrasting resistance reactions were often observed for particular accession of wheat to FHB and FCR disease. The putative reason might lie in the mode of infection for FCR and FHB through the roots or through the heads of the plants. Yan et al. (2011) reported that tall isolines all gave better type I resistance to initial infection than their respective dwarf counterparts. These results showed that less favorable microclimate for disease development in taller plants may have contributed to their greater type I resistance. As spores in infected debris on the ground are a major source of infection under field conditions, tall plants were farther from soil surface where the inoculum was present and ventilation was reduced that lead to high humidity favorable to FHB development. Type II (resistance to spread within infected tissue) infection was induced by injecting inoculum into spikelets and its development was not as affected by microclimate as type I infection. However, it is not clear what other effects *Rht* genes might have on morphological and physiological structures of spikes and whether the higher cell density and smaller cell sizes of stem would have any effect on type II resistance in the spikes. (Yan et al., 2011; He et al., 2016). Comparing to FCR resistance, FHB resistance where infection occurs through inoculation of the spikes by single floret inoculation with *F. graminearum* in the greenhouse, a very different infection scenario where also an effect on anther extrusion mediated by semi-dwarfing gene is involved (He et al. 2016). Major FHB resistant wheat cultivars Sumai 3 and Ning 7840 exhibiting type I resistance to penetration and/or initial infection of the heads were not able to protect against root and stem rot after seedling stage inoculation.

5.7 Putative resistance genes identified in FCR and FHB overlapped QTL encoding cytochrome P450 and receptor-like kinase

As reported in previous FCR/FHB resistance studies, putative resistance candidate genes underlying QTL regions in this study were also identified via looking through human readable annotations, functions description of genes and *in-silico* analysis of the defense related genes expression between resistant and susceptible genotypes. Finally, 22 resistance related genes were identified from 81 differentially expressed genes between resistant and susceptible genotypes. Among them, several genes might arouse more interests including that were detected underlying FCR and FHB overlapped resistance QTL.

Cytochrome P450 was encoded by gene ‘TraesCS3B01G006600.1’ and gene ‘TraesCS4B01G312300.1’ underlying FCR/FHB resistance QTL *qSbSI-3B_Rti (Fhb1)* on the chromosome 3BS and QTL *qSLR-4B.2_Rti (Fhb4)* on the chromosome 4BL, respectively. During infection, *Fusarium* species produce mycotoxins such as the trichothecene deoxynivalenol (DON). It is a protein synthesis inhibitor that inhibits peptidyl transferase activity by binding to a specific site on the 60S ribosomal subunit, which play important roles as a major component of virulence for the pathogens. It has been shown that DON could promote the FCR progression through the stem (Mudge et al., 2006; Powell et al., 2017; Zhao et al., 2018; Jin et al., 2020). Cytochrome P450s involved in detoxification of DON leading to the FCR resistance. Furthermore, cytochrome P450s take part in the biosynthesis of cell wall components. The cell wall is considered as the physical barrier to protect plants from a variety of abiotic and biotic stresses. In a recent study by Gunupuru et al. (2018) it was reported that wheat *TaCYP72A* from the CYP72A subfamily of cytochrome P450s is devoted to DON resistance, because it was only induced by the wild type of *F. graminearum* and not by the DON-minus mutant indicating that *TaCYP72A* is involved in the response to toxin production rather than in a general defense against *F. graminearum*. *TaCYP72A* plays a part in either mitigating DON-induced stress or detoxicating DON as a component of the xenobiotic detoxification pathway (Sobrova et al., 2010). Wang et al. (2018) reported that the gene *CYP709C1* encoding cytochrome P450s was rapidly and highly up-regulated in the resistant wheat cultivar at 1 dai after root inoculated with *F. graminearum* at seedling stage comparing to the susceptible wheat cultivar.

Receptor-like kinase (RLK) was encoded by gene ‘TraesCS3B01G012700.1’

underlying FCR/FHB resistance QTL *qSbSI-3B_Rti (Fhb1)* on the chromosome 3BS. They play pivotal role in plant development, growth, and immunity. A great amount of RLKs as pattern recognition receptors (PRRs) were deployed at the cell surface by plants, which can be the first layer of induced defense to detect pathogen-associated molecular patterns (PAMPs), initiate a set of defense responses termed PAMP-triggered immunity (PTI) after binding their cognate elicitors. According to the N-terminal extracellular domain with ligand specificity, most studied subfamilies with three domains including leucine-rich repeat (LRR) domains, LysM domains (LYM), and the *Catharanthus roseus* RLK1-like (CrRLK1L) domain. In the recently gene expression study, a homologous gene encodes the characteristic domains of surface-localized Leucine rich repeat receptor like kinase (LRR-RLK). This gene is highly expressed in the spikes of FHB resistant cultivar CM82036 as an early response induced by *F. graminearum* and the mycotoxic virulence factor deoxynivalenol (DON; Thapa et al., 2018). Pan et al. (2018) reported that in a transcriptome study, receptor-like kinases were much higher expressed in FHB resistant cultivar than that in FHB susceptible cultivar following *F. graminearum* inoculation.

One of the basic strategies against plant pathogens is the remodeling of the cell wall, or more precisely distribution and accumulation of cell wall-associated proteins. A gene ‘TraesCS3B01G009600.1’ encoding arabinogalactan protein (AGP) was also detected in the QTL *qSbSI-3B_Rti (Fhb1)* on the chromosome 3BS. Arabinogalactan proteins are highly glycosylated members of the hydroxyproline-rich glycoproteins (HRGPs) superfamily of plant cell wall proteins. HRGPs are involved in cross-linking and strengthening of the cell wall which protect against spatial ramification of the pathogen. AGPs are also synthesized by root cap cells and root cap-derived border cells (BCs) and border-like cells (BLCs) and highly expressed at the cell surface of BCs and BLCs to protection against root infection by immobilizing zoospores of soil-borne pathogens at the periphery of the tip or in the surrounding environment (Nguema-Ona et al., 2013; Prieto et al., 2017; Leszczuk et al., 2019). In addition, one gene ‘TraesCS2D01G065000.1’ encoding expansin was identified on the chromosome 2D underlying QTL *qSr/SbSI-2D_Sdi*. Expansins comprise a plant-specific superfamily of proteins that characteristically loosen the plant cell wall by weakening the non-covalent bonding of polysaccharides to one another. Expansins play important roles in diverse processes, including developmental programs, defense and resistance mechanisms (Li

et al., 2016). Jia et al. (2009) found that expansins were increased expression in the resistant wheat genotype compared with susceptible ones during *F. graminearum* infection. Above expressed genes indicate that cell-wall functions could play important roles in protecting the plants against pathogen infection.

Underlying other specific QTL for the FCR resistance several genes were also noteworthy. Genes encoding pathogenesis-related proteins PR4 and disease resistance proteins were identified with the GO terms of ‘defense response to fungus’ and ‘defense response’. They were detected underlying QTL *qRDWR-6D_Sdi* and QTL *qSbSI-1A_Sdi*, respectively. Pathogenesis-related proteins (PR proteins) are defined as proteins encoded by the host plant but induced under pathological or related situations, abiotic stress and toxin related chlorosis as critical mechanism for plant defense (Sudisha et al., 2012; Menezes et al., 2014). PR4 family, chitin binding proteins (CBPs), involves in plant defense responses regulated by several signal molecules including salicylic acid (SA), abscissic acid (ABA), jasmonate (JA) and ethylene (ET). It can diffuse toward and affect (break down) the chitin-supported structure of the cell walls of fungi (Agrios, 2004). Zhang et al. (2013) reported that comparing the two-dimensional protein profiles, PR4 proteins presented only in wheat *Fhb1*⁺NIL spikes after *F. graminearum* inoculation not in mock treated spikes at 72 h, indicating that pathogenesis-related proteins PR4 are *Fusarium*-induced and play important role in pathogen defense in wheat.

Most of the disease resistance genes (R genes) in plants encode nucleotide-binding site leucine-rich repeat (NBS-LRR) disease resistance proteins characterized by nucleotide-binding site (NBS), C-terminal leucine-rich repeat (LRR) domains (McHale et al., 2006). LRRs are highly adaptable structural domains that are dedicated to protein-protein interactions as well as binding effectors secreted by pathogens, indicating that this domain plays a crucial role in pathogen recognition and following activate downstream signaling pathways (Tan and Wu, 2012). A previous study of *F. graminearum* and wheat interaction demonstrated that NBS-LRR gene family exhibited a high number of differentially expressed genes (DEG) and were activated early in the FHB resistant cultivar CM82036. Compared to a susceptible genotype, such higher transcript level and faster induction of putative resistant genes seem to be a determinative element for the successful defense response to the pathogen (Kugler et al., 2013). In a recent FCR resistance study, Jin et al. (2020) reported that a gene

encoding NBS-LRR disease resistance protein was significantly induced by *F. graminearum* infection in the resistant wheat cultivar whereas the gene expression in the susceptible cultivar was not significant.

Furthermore, a gene 'TraesCS3A01G510900.1' encoding peroxidase was identified in the overlapping QTL regions on chromosome 3AL after *F. graminearum* root (*qSbSI/DL_SLi-3A_Rti*) and seed (*qDL_SLi-3A_Sdi*) inoculations. Wang et al. (2015) revealed that a partially resistant genotype against root infection exhibited resistance to cortical root cells infection with a delayed and decreased invasion into stem base and resistance to infection of vascular bundle in stem. On the other hand, seed infection inducing responses against *F. graminearum* might involve preventing seed epidermis invasion and after seed germination, partially resistant genotype might employ defense against *F. graminearum* infection via radicle and coleoptile. Peroxidases can restrict the spread of infection via producing huge amounts of reactive oxygen species (ROS) and reactive nitrogen species (RNS) which are toxic to pathogens. Physical barriers are also formatted by peroxidase to prevent pathogen invasion of host cells and catalyze cross-linking of cell wall components, lignification and suberization participating the formation of a three-dimensional phenolic matrix within the carbohydrate matrix of the primary cell wall (Almagro et al., 2009). Zhang et al. (2013) reported that in the FCR resistance study, the activity of the peroxidase in inoculated seedlings was always higher than control, and it plays an important role in ameliorating damage to plant caused by *F. graminearum* in the partially resistant variety. In a recent genome-wide transcriptome study, wheat class III peroxidase genes showed gradual upregulation from 1 to 4 days after *F. graminearum* inoculation in the *F. graminearum* resistant cultivar Sumai 3, but not in the susceptible cultivar, suggesting that this gene is involved in the defense pathway against *F. graminearum* (Yan et al., 2019).

In addition, as typically dominant resistance genes that are deployed by plants to confer resistance against pathogens. Because resistance is based on recognition of a single pathogen-derived molecular pattern, these narrow-spectrum genes are usually readily overcome leading to diseases with a compatible interaction between plant and pathogen. Therefore, a more broad-spectrum durable resistance can be obtained by altering a plant gene critically facilitating compatibility. These plant genes that facilitate infection and support compatibility can be considered susceptibility (S) genes. Based on the 'expVIP' database, in the current study several genes e.g. 'TraesCS1A01G016000.1' and

‘TraesCS6D01G380200.1’ encoding serine/threonine-protein kinase and protein kinase showed higher expression in the susceptible genotype comparing to that in the resistant genotype, which might relate to the FCR susceptibility. Pan et al. (2018) also reported that genes encoding same proteins in wheat were potentially associated with FHB susceptibility following *F. graminearum* inoculation. Mutation or loss of an S gene can limit the ability of the pathogen causing disease. The potential robustness of an S gene is exemplified by the *Mlo* gene, of which a recessive mutant was shown to confer powdery mildew (PM) resistance in barley and wheat (Jorgensen et al., 1992; van Schie et al., 2014; Wang et al., 2014). In a recent FHB resistance study, a deletion mutation in a S gene *TaHRC* confers *Fhb1* resistance to Fusarium head blight in wheat (Su et al., 2019). Yang et al. (2021) reported that improving FCR resistance caused by loss of function of the *TaDIR-B1* gene (S gene) was attributed to accumulation of lignin in wheat. However, S genes may do not merely exist for the convenience of pathogen but have an evolutionarily conserved function in plant processes. It is necessary to predict S genes functions of pleiotropic effects at certain stage of pathogen infection.

Although resistance/susceptibility related genes located in FCR/FHB resistance QTL intervals are identified in this study via such strategy also applied by other researchers, it is not sufficient to obtain promising candidate genes for a quantitatively inherited trait like *Fusarium* resistance. QTL analysis alone can be used to get linked markers for plant breeding, but it is not possible to detect resistance candidate genes and provide diagnostic markers. In the future, the major FCR/FHB resistance QTL should be validated through fine mapping, marker development and analysis in different genetic backgrounds, and map-based cloning to identify promising FCR/FHB resistance candidate genes, create diagnostic markers for the marker-assisted selection (MAS) and eventually accelerate breeding of FCR/FHB resistance wheat cultivars.

6 Summary

Fusarium graminearum is a predominant pathogen causing Fusarium head blight (FHB) in wheat in most wheat growing regions including Europe. In addition, *F. graminearum* is involved in causing Fusarium root and crown rot (FCR), a soil-borne disease which causes severe yield loss in grain crops including wheat. The predominant causal agents of FCR are *F. pseudograminearum*, *F. culmorum* and *F. graminearum*. In Germany *F. graminearum* has become the dominant species in the last decade along with climate change under higher temperatures. Compared to FHB the FCR disease has been much less studied. Therefore, the present study focused on the genetic analysis of FCR resistance induced by *F. graminearum*. In this study root and seed inoculation experiments were conducted in growth chambers using a wheat DH population produced from German winter type cultivars (line 162.11 and cv. Tobak).

In contrast to other reports in the literature FCR resistance/tolerance was not found to be associated with high root biomass accumulation in this studied biparental population. Some major FCR resistance QTL *qSbSI-3B* and *qSLR-4B.2* were found to overlap with the well-recognized FHB QTL *Fhb1* and *Fhb4*, other QTL were found to be specific for FCR resistance expression. A FCR resistance QTL was found to be linked to the semi-dwarfing gene *Rht1* which has been documented in the literature before to be linked to FCR and FHB resistance. FCR resistance mediated by this QTL was linked to short plants whereas FHB resistance mediated QTL reported in the literature was linked to tall plants. This suggests that pleiotropic effects of the *Rht1* gene exist which might be linked to the mode of *Fusarium* infection for FCR and FHB disease. Furthermore, within the underlying overlapping FCR and FHB resistance QTL putative *F. graminearum* defense related genes were identified and that involved in cell wall strengthening, pathogen-associated molecular pattern (PAMP) detection, immobilization of zoospores of soil-borne pathogens and DON detoxification. The nature of these genes suggests that broad-spectrum resistance to different *Fusarium*-induced diseases is an important part of the resistance reaction in the studied cultivars. Effective wheat breeding for FCR and FHB resistance should target on QTL/genes and alleles involved in resistance against both diseases, but with effects aligned to the same direction without yield penalty.

7 Zusammenfassung

Fusarium graminearum ist ein weit-verbreiteter Schaderreger, der in den meisten Weizenanbaugebieten einschließlich Europas Ährenfusariosen bei Weizen verursacht (Weißährigkeit, Fusarium head blight, FHB). Darüber hinaus ist *F. graminearum* an der Entstehung von Fusariumwurzel- und Kronenfäule beteiligt (Fusarium crown rot, FCR), einer durch den Boden übertragenen Krankheit, die bei Getreidekulturen schwere Ertragsverluste verursacht. Die vorherrschenden Erreger der FCR sind *F. pseudograminearum*, *F. culmorum* und *F. graminearum*. In Deutschland hat sich *F. graminearum* im letzten Jahrzehnt zusammen mit dem Klimawandel bei höheren Temperaturen zur dominierenden Art entwickelt. Im Vergleich zu FHB wurde die FCR-Krankheit viel weniger untersucht. Daher konzentrierte sich die vorliegende Studie auf die genetische Analyse der durch *F. graminearum* induzierten FCR-Resistenz. In dieser Studie wurden Wurzel- und Samen-Inokulationsexperimente in Wachstumskammern unter Verwendung einer Weizen-DH-Population durchgeführt, die aus deutschen Wintersorten hergestellt wurde (Linie 162.11 und cv. Tobak).

Im Gegensatz zu anderen Berichten in der Literatur wurde kein Zusammenhang zwischen FCR-Resistenz und -Toleranz mit einer hohen Akkumulation von Wurzelbiomasse in der untersuchten biparentalen Population festgestellt. Es wurde jedoch festgestellt, dass einige Haupt-FCR-Resistenz-QTL, qSbSI-3B und qSLR-4B.2, mit den bekannten FHB QTL Fhb1 und Fhb4 überlappen, andere QTL waren spezifisch für die FCR-Resistenz-Expression. Es wurde beobachtet, dass eine FCR-Resistenz-QTL mit dem semi dwarf gene *Rht1* überlappt für das in der Literatur eine Korrelation mit FCR- und FHB-Resistenz bereits beschrieben ist. Die durch dieses QTL vermittelte FCR-Resistenz prägte sich jedoch bei niedrig-wachsenden Pflanzen aus, während für das in der Literatur beschriebene FHB-Resistenz des entsprechenden QTL bei hoch-wachsenden Pflanzen auftrat. Dies deutet darauf hin, dass pleiotrophe Effekte des *Rht1*-Gens existieren, die möglicherweise mit der Art der Fusarium-Infektion bei FCR- und FHB-Erkrankungen zusammenhängen. Darüber hinaus wurden innerhalb der zugrunde liegenden überlappenden FCR- und FHB-Resistenz QTL-mutmaßliche *F. graminearum*-Abwehrgene identifiziert, die an der Zellwandstärkung, der Pathogen-assoziierten Molekularen Muster-Erkennung der Immobilisierung von Zoosporen bodengebundener Pathogene und der DON-Entgiftung beteiligt sind. Die Natur dieser Gene legt nahe, dass eine breit wirksame Resistenz gegen verschiedene Fusarium-

Arten-induzierte Krankheiten ein wichtiger Teil der Resistenzreaktion in den untersuchten Sorten ist. Eine wirksame Weizenzüchtung für FCR- und FHB-Resistenz sollte auf QTL / Gene und Allele abzielen, die an der Resistenz gegen beide Krankheiten beteiligt sind, jedoch mit Effekten, die ohne Ertragseinbußen gleichgerichtet wirken.

References

- Agrios GN. 2004. Plant Pathology-5th ed. *Elsevier Press* 984.
- Agustí-Brisach C, Raya-Ortega MC, Trapero C, et al. 2018. First report of *Fusarium pseudograminearum* causing crown rot of wheat in Europe. *Plant Dis.* 102: 1670.
- Akinsanmi OA, Mitter V, Simpfendorfer S, et al. 2004. Identity and pathogenicity of *Fusarium* spp. isolated from wheat fields in Queensland and northern New South Wales. *Australian J. Agr. R.* 55: 97–107.
- Alahmad S, Kang Y, Dinglasan E, et al. 2020. Adaptive traits to improve durum wheat yield in drought and crown rot environments. *Int. J. Mol. Sci.* 21: 5260.
- Alaux M, Rogers J, Letellier T, et al. 2018. Linking the international wheat genome sequencing consortium bread wheat reference genome sequence to wheat genetic and phenomic data. *Genome Biol.* 19: 111.
- Almagro L, Gómez Ros LV, Belchi-Navarro S, et al. 2009. Class III peroxidases in plant defence reactions. *J. Exp. Bot.* 60: 377–390.
- Al-Taweel K, Fernando WG, Brûlé-Babel AL. 2014. Transcriptome profiling of wheat differentially expressed genes exposed to different chemotypes of *Fusarium graminearum*. *Theor. Appl. Genet.* 127: 1703–1718.
- Anderson JA, Stack RW, Liu S, et al. 2001. DNA markers for *Fusarium* head blight resistance QTLs in two wheat populations. *Theor. Appl. Genet.* 102: 1164–1168.
- Ansari KI, Walter S, Brennan JM, et al. 2007. Retrotransposon and gene activation in wheat in response to mycotoxigenic and non-mycotoxigenic-associated *Fusarium* stress. *Theor. Appl. Genet.* 114: 927–937.
- Appels R, Eversole K, Feuillet C, et al. 2018. Shifting the limits in wheat research and breeding using a fully annotated reference genome. *Science* 361: eaar7191.

- Backhouse D, Abubakar AA, Burgess LW, et al. 2004. Survey of *Fusarium* species associated with crown rot of wheat and barley in eastern Australia. *Aus. Plant Pathol.* 33: 255–261.
- Backhouse D, Burgess LW. 2002. Climatic analysis of the distribution of *Fusarium graminearum*, *F. pseudograminearum* and *F. culmorum* on cereals in Australia. *Aus. Plant Pathol.* 31: 321–327.
- Bahrini I, Sugisawa M, Kikuchi R, et al. 2011. Characterization of a wheat transcription factor, TaWRKY45, and its effect on *Fusarium* head blight resistance in transgenic wheat plants. *Breeding Sci.* 61: 121–129.
- Bai GH, Shaner G. 2004. Management and resistance in wheat and barley to *Fusarium* head blight. *Annu. Rev. Phytopathol.* 42: 135–61.
- Bai GH, Su ZQ, Cai J. 2018. Wheat resistance to *Fusarium* head blight. *Can. J. Plant Pathol.* 40: 336–346.
- Beccari G, Covarelli L, Nicholson P. 2011. Infection processes and soft wheat response to root rot and crown rot caused by *Fusarium culmorum*. *Plant Pathol.* 60: 671–684.
- Biselli C, Bagnaresi P, Faccioli P, et al. 2018. Comparative transcriptome profiles of near-isogenic hexaploid wheat lines differing for effective alleles at the 2DL FHB resistance QTL. *Front. Plant Sci.* 9:37.
- Bonin CM, Kolb FL. 2009. Resistance to *Fusarium* head blight and kernel damage in a winter wheat recombinant inbred line population. *Crop Sci.* 49: 1304–1312.
- Borrill P, Ricardo RG, Cristobal U. 2016. expVIP: a customisable RNA-seq data analysis and visualisation platform. *Plant Physiology* 170: 2172–2186.
- Bottalico A, Perrone G. 2002. Toxigenic *Fusarium* species and mycotoxins associated with Head Blight in small-grain cereals in Europe. *Eur. J. Plant Pathol.* 108:611–624.

- Bovill WD, Horne M, Herde D, et al. 2010. Pyramiding QTL increases seedling resistance to crown rot (*Fusarium pseudograminearum*) of wheat (*Triticum aestivum*). *Theor. Appl. Genet.* 121: 127–136.
- Bovill WD, Ma W, Ritter K, et al. 2006. Identification of novel QTL for resistance to crown rot in the doubled haploid wheat population ‘W21MMT70’ × ‘Mendos’. *Plant Breeding* 125: 538–543.
- Brauer EK, Balcerzak M, Rocheleau H, et al. 2019. Genome editing of a DON-induced transcription factor confers resistance to *Fusarium graminearum* in wheat. *Mol. Plant Microbe Interact.* 33: 553–560.
- Brown NA, Urban M, van de Meene AM, et al. 2010. The infection biology of *Fusarium graminearum*: defining the pathways of spikelet to spikelet colonisation in wheat ears. *Fungal Biol.* 114: 555–571.
- Buerstmayr H, Ban T, Anderson JA. 2009. QTL mapping and marker assisted selection for Fusarium head blight resistance in wheat: a review. *Plant Breeding* 128: 1–26.
- Buerstmayr H, Steiner B, et al. 2003. Molecular mapping of QTLs for Fusarium head blight resistance in spring wheat. II. Resistance to fungal penetration and spread. *Theor. Appl. Genet.* 107: 503–508.
- Buerstmayr M, Huber K, Heckmann J, et al. 2012. Mapping of QTL for Fusarium head blight resistance and morphological and developmental traits in three backcross populations derived from *Triticum dicoccum* × *Triticum durum*. *Theor. Appl. Genet.* 125: 1751–1765.
- Buerstmayr M, Lemmens M, Steiner B, et al. 2011. Advanced backcross QTL mapping of resistance to Fusarium head blight and plant morphological traits in a *Triticum macha* × *T. aestivum* population. *Theor. Appl. Genet.* 123: 293–306.
- Bullerman LB. 2003. MYCOTOXINS. Classifications. *Encyclopedia of Food Sciences and Nutrition* 4080–4089.

- Burgess LW. 2005. Intermediate hosts and the management of crown rot and head blight. In: Annual Report of GRDC strategic initiative on crown rot, common root rot and Fusarium head blight. Grains Research and Development Corporation, Kingston, Australia 34–36.
- Cainong JC, Bockus WW, Feng Y, et al. 2015. Chromosome engineering, mapping, and transferring of resistance to Fusarium head blight disease from *Elymus tsukushiensis* into wheat. *Theor. Appl. Genet.* 128: 1019–1027.
- Chakraborty S, Obanor F, Westecott R, et al. 2010. Wheat crown rot pathogens *Fusarium graminearum* and *F. pseudograminearum* lack specialization. *Phytopathology.* 100: 1057–1065.
- Charmet G. 2011. Wheat domestication: Lessons for the future. *C. R. Biologies* 334: 212–220.
- Chen GD, Habib A, Wei Y, et al. 2015. Enhancing Fusarium crown rot resistance by pyramiding large-effect QTL in barley. *Mol. Breeding* 35: 26.
- Chen WP, Chen PD, Liu DJ, et al. 1999. Development of wheat scab symptoms is delayed in transgenic wheat plants that constitutively express a rice thaumatin-like protein gene. *TAG Theor. Appl. Genetics* 99: 755–760.
- Cho S, Lee J, Jung K, et al. 2012. Genome-wide analysis of genes induced by *Fusarium graminearum* infection in resistant and susceptible wheat cultivars. *J. Plant Biol.* 55: 64–72.
- Choura M, Hanin M, Rebaï A, et al. 2016. From *FHB* Resistance QTLs to Candidate Genes Identification in *Triticum aestivum* L.. *Interdiscip. Sci. Comput. Life Sci.* 8: 352–356.
- Collard BCY, Grams RA, Bovill CD, et al. 2005. Development of molecular markers for crown rot resistance in wheat: mapping of QTL for seedling resistance in a ‘2–49’ × ‘Janz’ population. *Plant Breeding* 124: 532–537.

- Collard BCY, Jolley R, Bovill WD, et al. 2006. Confirmation of QTL mapping and marker validation for partial seedling resistance to crown rot in wheat line '2-49'. *Aus. J. Agr. Res.* 57: 967–973.
- Crespo-Herrera LA, Govindan V, Stangoulis J, et al. 2017. QTL Mapping of Grain Zn and Fe Concentrations in Two Hexaploid Wheat RIL Populations with Ample Transgressive Segregation. *Front. Plant Sci.* 8: 1800.
- Cui F, Fan X, Zhao C, et al. 2014. A novel genetic map of wheat: utility for mapping QTL for yield under different nitrogen treatments. *BMC genetics* 15: 57.
- Cuthbert PA, Somers DJ, Thomas J, et al. 2006. Fine mapping *Fhb1*, a major gene controlling Fusarium head blight resistance in bread wheat *Triticum aestivum* L.. *Theor. Appl. Genet.* 112: 1465–1472.
- Cuthbert PA, Somers DJ, Brulé-Babel A. 2007. Mapping of *Fhb2* on chromosome 6BS: a gene controlling Fusarium head blight field resistance in bread wheat *Triticum aestivum*. *Theor. Appl. Genet.* 114: 429–437.
- Dai SJ. 2012. Cause analysis and countermeasures for FHB epidemic of wheat in Huaibei Area in 2012. *J. Anhui Agri. Sci.* 17: 557–558. (in Chinese)
- Dalton DA, Boniface C, Turner Z, et al. 2009. Physiological roles of glutathione S-transferases in soybean root nodules. *Plant Physiol.* 150: 521–530.
- Desmond OJ, Manners JM, Schenk PM, et al. 2008a. Gene expression analysis of the wheat response to infection by *Fusarium pseudograminearum*. *Physiol. Mol. Plant Pathol.* 73: 40–47.
- Desmond OJ, Manners JM, Stephens AE, et al. 2008b. The Fusarium mycotoxin deoxynivalenol elicits hydrogen peroxide production, programmed cell death and defence responses in wheat. *Mol. Plant Pathol.* 9: 435–445.
- Dhokane D, Karre S, Kushalappa AC, et al. 2016. Integrated metabolo-transcriptomics reveals Fusarium head blight candidate resistance genes in wheat QTL-Fhb2. *PLoS ONE* 11: e0155851.

- Dill-Macky R and Jones RK. 2000. The effect of previous crop residues and tillage on Fusarium head blight of wheat. *Plant Dis.* 84: 71–76.
- Dodman RL, Wildermuth GB, Klein TA, et al. 1985. Field resistance of wheat cultivars to crown rot (*Fusarium graminearum* Group 1). In: Ecology and management of soilborne plant pathogens (Parker CA, Rovira AD, Moore KJ, et al., eds). 167–168. (*American Phytopathological Society*: St Paul, MI, USA).
- Dodman RL, Wildermuth GB. 1987. Inoculation methods for assessing resistance in wheat to crown rot caused by *Fusarium graminearum* Group 1. *Aus. J. Agr. Res.* 38: 473–486.
- Dvorak J, Akhunov E. 2005. Tempos of gene locus deletions and duplications and their relationship to recombination rate during diploid and polyploid evolution in the Aegilops-Triticum alliance. *Genetics* 17: 323–332.
- Dvorak J, Luo MC, Yang ZL, et al. 1998. The structure of the Aegilops tauchii genepool and the evolution of hexaploid wheat. *Theor. Appl. Genet.* 97: 657–670.
- Dyer AT, Johnston RH, Hogg AC, et al. 2009. Comparison of pathogenicity of the Fusarium crown rot (FCR) complex (*F. culmorum*, *F. pseudograminearum* and *F. graminearum*) on hard red spring and durum wheat. *Eur. J. Plant Pathol.* 125: 387–395.
- Early R. 2009. Pathogen control in primary production: crop foods. *Foodborne Pathogens* 205–279.
- Eckardt NA. 2000. Sequencing the rice genome. *Plant Cell* 12: 2011–2017.
- Erayman M, Turktas M, Akdogan G, et al. 2015. Transcriptome analysis of wheat inoculated with *Fusarium graminearum*. *Front Plant Sci.* 6: 867.
- Erginbasorakci G, Sehgal D, Sohail Q, et al. 2018. Identification of novel quantitative trait loci linked to crown rot resistance in spring 15 wheat. *Int. J. Mol. Sci.* 19: 2666.

- Eynck C, Koopmann B and von Tiedemann A. 2009. Identification of Brassica accessions with enhanced resistance to *Verticillium longisporum* under controlled and field conditions. *J. Plant Dis. Prot.* 116: 63–72.
- FAO. 2019. Food outlook-Biannual report on global food markets-November 2019. Rome.
- Fauteux F, Wang Y, Rocheleau H, et al. 2019. Characterization of QTL and eQTL controlling early *Fusarium graminearum* infection and deoxynivalenol levels in a Wuhan 1 x Nyubai doubled haploid wheat population. *BMC Plant Biol.* 19: 536.
- Fernandez MR, Holzgang G and Turkington TK. 2009. Common root rot of barley in Saskatchewan and north-central Alberta. *Can. J. Plant Pathol.* 31: 96–102.
- Fernandez MR. and Conner RL. 2011. Black point and smudge in Wheat. *Prairie Soils and Crops* 4: 158–164.
- Foroud NA, Ouellet T, Laroche A, et al. 2012. Differential transcriptome analyses of three wheat genotypes reveal different host response pathways associated with *Fusarium* head blight and trichothecene resistance. *Plant Pathol.* 61: 296–314.
- Gadaleta A, Colasuonno P, Giove SL, et al. 2019. Map-based cloning of *QFhb.mgb-2A* identifies a *WAK2* gene responsible for *Fusarium* Head Blight resistance in wheat. *Sci. Rep.* 9: 6929.
- Gatti M, Choulet F, Macadré C, et al. 2018. Identification, molecular cloning, and functional characterization of a wheat UDP-glucosyltransferase involved in resistance to *Fusarium* head blight and to mycotoxin accumulation. *Front. Plant Sci.* 9: 1853.
- Golkari S, Gilbert J, Prashar S, et al. 2007. Microarray analysis of *Fusarium graminearum*-induced wheat genes: identification of organ-specific and differentially expressed genes. *Plant Biotechnol. J.* 5: 38–49.

- Golkari S, Gilbert J, Procuiner JD. 2009. QTL-specific microarray gene expression analysis of wheat resistance to *Fusarium* head blight in sumai-3 and two susceptible NILs. *Genome*. 52: 409–418.
- Goswami RS, Kistler HC. 2004. Heading for disaster: *Fusarium graminearum* on cereal crops. *Mol. Plant Pathol*. 5: 515–525.
- Goswami RS. 2006. Genomic analysis of host–pathogen interaction between *Fusarium graminearum* and wheat during early stages of disease development. *Microbiology* 152: 1877–1890.
- Gottwald S, Samans B, Lück S, et al. 2012. Jasmonate and ethylene dependent defence gene expression and suppression of fungal virulence factors: two essential mechanisms of *Fusarium* head blight resistance in wheat? *BMC Genomics* 13: 369.
- Gou L, Hattori J, Fedak G, et al. 2016. Development and validation of *Thinopyrum elongatum*-expressed molecular markers specific for the long arm of chromosome 7E. *Crop Sci*. 56: 354–364.
- Graf RJ, Beres BL, Laroche A, et al. 2013. Emerson hard red winter wheat. *Can. J. Plant Sci*. 93: 741–748.
- Guenther JC, Trail F. 2005. The development and differentiation of *Gibberella zeae* anamorph: *Fusarium graminearum* during colonization of wheat. *Mycologia*. 97: 229–237.
- Gullner G, Komives T, Király L, et al. 2018. Glutathione S-transferase enzymes in plant-pathogen interactions. *Front. Plant Sci*. 9: 1836.
- Gunnaiah R, Kushalappa AC, Duggavathi R, et al. 2012. Integrated metabolo-proteomic approach to decipher the mechanisms by which wheat QTL (*Fhb1*) contributes to resistance against *Fusarium graminearum*. *PLoS ONE* 7: e40695.

- Gunnaiah R, Kushalappa AC. 2014. Metabolomics deciphers the host resistance mechanisms in wheat cultivar Sumai-3, against trichothecene producing and non-producing isolates of *Fusarium graminearum*. *Plant Physiol. Biochem.* 83: 40–50.
- Gunupuru LR, Arunachalam C, Malla KB, et al. 2018. A wheat cytochrome P450 enhances both resistance to deoxynivalenol and grain yield. *PLoS ONE* 13: e0204992.
- Gunupuru LR, Perochon A and Doohan FM. 2017. Deoxynivalenol resistance as a component of FHB resistance. *Trop. Plant Pathol.* 42: 175.
- Guo J, Zhang X, Hou Y, et al. 2015. High-density mapping of the major FHB resistance gene *Fhb7* derived from *Thinopyrum ponticum* and its pyramiding with *Fhb1* by marker-assisted selection. *Theor. Appl. Genet.* 128: 2301–2316.
- Guo P, Bai G, Li R, et al. 2006. Resistance gene analogs associated with Fusarium head blight resistance in wheat. *Euphytica* 151: 251–261.
- Gustafson P, Raskind O, Ma XF. 2009. Wheat evolution, domestication, and improvement. In: *Wheat Science and Trade* (Carver BF, eds). 5–30. (Wiley-Blackwell: Ames, IA, USA).
- Hackett C. 2002. Statistical methods for QTL mapping in cereals. *Plant Mol. Biol.* 48: 585–599.
- Handa H, Namiki N, Xu D, et al. 2008. Dissecting of the FHB resistance QTL on the short arm of wheat chromosome 2D using a comparative genomic approach: from QTL to candidate gene. *Mol. Breeding* 22: 71–84.
- Hao Y, Rasheed A, Zhu Z, et al. 2020. Harnessing Wheat *Fhb1* for Fusarium Resistance. *Trends Plant Sci.* 25:1–3.
- Happstadius I, Ljungberg A, Kristiansson B, et al. 2003. Identification of *Brassica oleracea* germplasm with improved resistance to Verticillium wilt. *Plant Breeding* 122: 30–34.

- He X, Singh PK, Dreisigacker S, et al. 2016. Dwarfing Genes Rht-B1b and Rht-D1b Are Associated with Both Type I FHB Susceptibility and Low Anther Extrusion in Two Bread Wheat Populations. *PLoS ONE* 11: e0162499.
- He Y, Ahmad D, Zhang X, et al. 2018. Genome-wide analysis of family-1 UDP glycosyltransferases (UGT) and identification of *UGT* genes for FHB resistance in wheat (*Triticum aestivum* L.). *BMC Plant Biol.* 18: 67.
- He Y, Zhang X, Zhang Y, et al. 2018. Molecular characterization and expression of PFT, an FHB resistance gene at the Fhb1 QTL in wheat. *Phytopathology* 108: 730–736.
- Hofstad AN, Nussbaumer T, Akhunov E, et al. 2016. Examining the transcriptional response in wheat Fhb1 near-isogenic lines to *Fusarium graminearum* infection and deoxynivalenol treatment. *Plant Genome* 9: 10.3835.
- Hu X, Rocheleau H, McCartney C, et al. 2019. Identification and mapping of expressed genes associated with the 2DL QTL for Fusarium head blight resistance in the wheat line Wuhan 1. *BMC Genet.* 20: 47.
- Huang S, Sirikhachornkit A, Su X, et al. 2002. Genes encoding plastid acetyl-CoA carboxylase and 3-phosphoglycerate kinase of the Triticum/Aegilops complex and the evolutionary history of polyploid wheat. *Proc. Nat. Acad. Sci. USA* 99: 8133–8138.
- Hussain B, Lucas SJ, Ozturk L, et al. 2017. Mapping QTLs conferring salt tolerance and micronutrient concentrations at seedling stage in wheat. *Sci. Rep.* 7: 15662.
- Jansen C, von Wettstein D, Schäfer W, et al. 2005. Infection patterns in barley and wheat spikes inoculated with wild-type and trichodiene synthase gene disrupted *Fusarium graminearum*. *PNAS* 10246: 892–897.
- Jevtić R, Stošić N, Župunski V, et al. 2019. Variability of stem-base infestation and coexistence of *Fusarium* spp. causing crown rot of winter wheat in Serbia. *The Plant Pathol. J.* 35: 553–563.

- Jia HY, Cho S, Muehlbauer GJ. 2009. Transcriptome analysis of a wheat near-isogenic line pair carrying Fusarium head blight resistant and-susceptible alleles. *Mol. Plant Microbe Interact.* 22: 1366–1378.
- Jia HY, Zhou JY, Xue SL, et al. 2018. A journey to understand wheat Fusarium head blight resistance in the Chinese wheat landrace Wangshuibai. *The Crop J.* 61: 48–59.
- Jiang G, Dong Y, Shi J, et al. 2007a. QTL analysis of resistance to Fusarium head blight in the novel wheat germplasm CJ 9306. II. Resistance to deoxynivalenol accumulation and grain yield loss. *Theor. Appl. Genet.* 115: 1043–1052.
- Jiang M, Liu QE, Liu ZN, et al. 2016. Over-expression of a WRKY transcription factor gene *BoWRKY6* enhances resistance to downy mildew in transgenic broccoli plants. *Aus. Plant Pathol.* 45: 327–334.
- Jin H, Wen W, Liu J, et al. 2016. Genome-wide QTL mapping for wheat processing quality parameters in a Gaocheng 8901/Zhoumai 16 recombinant inbred line population. *Front. Plant Sci.* 7: 1032.
- Jin J, Duan S, Qi Y, et al. 2020. Identification of a novel genomic region associated with resistance to Fusarium crown rot in wheat. *Theor. Appl. Genet.* 133: 2063–2073.
- Jordan KW, Wang S, Lun Y, et al. 2015. A haplotype map of allohexaploid wheat reveals distinct patterns of selection on homoeologous genomes. *Genome Biol.* 16: 48.
- Jorgensen JH. 1992. Discovery, characterization and exploitation of *Mlo* powdery mildew resistance in barley. *Euphytica.* 63:141–52.
- Kage U, Karre S, Kushalappa AC, et al. 2017a. Identification and characterization of a Fusarium head blight resistance gene *TaACT* in wheat QTL-2DL. *Plant Biotechnol. J.* 154: 447–457.

- Kage U, Yogendra K and Kushalappa A. 2017b. TaWRKY70 transcription factor in wheat QTL-2DL regulates downstream metabolite biosynthetic genes to resist *Fusarium graminearum* infection spread within spike. *Sci. Rep.* 7: 42596.
- Kaur J, Sagaram US, Shah D. 2011. Can plant defensins be used to engineer durable commercially useful fungal resistance in crop plants? *Fungal Biol. Rev.* 25: 128–135.
- Kazan K, Gardiner DM. 2018. *Fusarium* crown rot caused by *Fusarium pseudograminearum* in cereal crops: recent progress and future prospects. *Mol. Plant Pathol.* 19: 1547–1562.
- Kellogg EA. 2001. Evolutionary history of the grasses. *Plant Physiol.* 125: 1198–1205.
- Khan MR, Fischer S, Egan D, et al. 2006. Biological control of *Fusarium* seedling blight disease of wheat and barley. *Phytopathology* 96: 386–394.
- Klahr A, Zimmermann G, Wenzel G, et al. 2006. Effects of environment, disease progress, plant height and heading date on the detection of QTLs for resistance to *Fusarium* head blight in an European winter wheat cross. *Euphytica* 154: 17–28.
- Klein TA, Burgess LW, and Ellison FW. 1991. The incidence and spatial patterns of wheat plants infected by *Fusarium graminearum* group 1 and the effect of crown rot on yield. *Aus. J. Agr. Res.* 42: 399–407.
- Klein TA, Liddell CM, Burgess LW, et al. 1985. Glasshouse testing for tolerance of wheat to crown rot caused by *Fusarium graminearum* Group 1. In: Ecology and management of soilborne plant pathogens' (Parker CA, Rovira AD, Moore KJ, et al., Eds). 167–168. (American Phytopathological Society: St Paul, MI, USA).
- Kong L, Anderson J, Ohm H. 2005. Induction of wheat defense and stress-related genes in response to *Fusarium graminearum*. *Genome / National Research Council Canada* 48: 29–40.

- Kong L, Ohm H, Anderson J. 2007. Expression analysis of defense-related genes in wheat in response to infection by *Fusarium graminearum*. *Genome* 50: 1038–1048.
- Kosaka A, Ban T, Manickavelu A. 2015b. Genome-wide transcriptional profiling of wheat infected with *Fusarium graminearum*. *Genomics Data* 5: 260–262.
- Kosaka A, Manickavelu A, Kajihara D, et al. 2015a. Altered gene expression profiles of wheat genotypes against Fusarium head blight. *Toxins* 7: 604–620.
- Kosambi DD. 1944. The estimation of map distance from recombination values. *Ann. Eugen.* 12: 172–175.
- Kovalchuk N, Li M, Wittek F, et al. 2010. Defensin promoters as potential tools for engineering disease resistance in cereal grains. *Plant Biotech. J.* 8: 47–64.
- Kruger WM, Pritsch C, Chao S, et al. 2002. Functional and comparative bioinformatic analysis of expressed genes from wheat spikes infected with *Fusarium graminearum*. *Mol. Plant-Microbe Interact.* 15: 445–455.
- Kubo K, Kawada N, Fujita M, et al. 2010. Effect of cleistogamy on Fusarium head blight resistance in wheat. *Breeding Sci.* 604: 405.
- Kugler KG, Siegwart G, Nussbaumer T, et al. 2013. Quantitative trait loci-dependent analysis of a gene co-expression network associated with Fusarium head blight resistance in bread wheat (*Triticum aestivum* L.). *BMC genomics* 14: 728.
- Lander E, Botstein D. 1989. Mapping Mendelian factors underlying quantitative traits using RFLP linkage maps. *Genetics* 121: 185–199.
- Lee Y, Son H, Shin JY, et al. 2018. Genome-wide functional characterization of putative peroxidases in the head blight fungus *Fusarium graminearum*. *Mol. Plant Pathol.* 19: 715–730.
- Lemes da Silva C, Fritz A, Clinesmith M, et al. 2019. QTL mapping of Fusarium head blight resistance and deoxynivalenol accumulation in the Kansas wheat variety ‘Everest’. *Mol. Breeding* 39: 35.

- Leslie JF, Summerell AB. 2006. Media-Recipes and Preparation. *The Fusarium Laboratory Manual 2*: S6–7.
- Leszczuk A, Pieczywek PM, Gryta A, et al. 2019. Immunocytochemical studies on the distribution of arabinogalactan proteins (AGPs) as a response to fungal infection in *Malus x domestica* fruit. *Sci. Rep.* 17428.
- Li C, Bai G, Chao S, et al. 2015. A high-density SNP and SSR consensus map reveal segregation distortion regions in wheat. *Biomed Res. Int.* 1–10.
- Li HB, Xie GQ, Ma J, et al. 2010. Genetic relationships between resistances to Fusarium head blight and crown rot in bread wheat (*Triticum aestivum* L.). *Theor. Appl. Genet.* 121: 941–950.
- Li N, Pu Y, Gong Y, et al. 2016. Genomic location and expression analysis of expansin gene family reveals the evolutionary and functional significance in *Triticum aestivum*. *Genes. Genom.* 38: 1021–103.
- Li P, Li YJ, Zhang FJ, et al. 2017. The Arabidopsis UDP-glycosyltransferases UGT79B2 and UGT79B3, contribute to cold, salt and drought stress tolerance via modulating anthocyanin accumulation. *Plant J.* 89: 85–103.
- Li T, Bai G, Wu S, et al. 2011. Quantitative trait loci for resistance to Fusarium head blight in a Chinese wheat landrace Haiyanzhong. *Theor. Appl. Genet.* 122:1497–1502.
- Li X, Liu C, Chakraborty S, et al. 2008. A simple Method for the assessment of crown rot disease severity in wheat seedlings inoculated with *Fusarium pseudograminearum*. *J. Phytopathol.* 156: 751–754.
- Li X, Michlmayr H, Schweiger W, et al. 2017. A barley UDP-glucosyltransferase inactivates nivalenol and provides Fusarium Head Blight resistance in transgenic wheat. *J. Exp. Bot.* 68: 2187–2197.

- Li X, Shin S, Heinen S, et al. 2015. Transgenic wheat expressing a Barley UDP-glucosyltransferase detoxifies deoxynivalenol and provides high levels of resistance to *Fusarium graminearum*. *Mol. Plant-Microbe Interact.* 28: 1237–1246.
- Li X, Zhang JB, Song B, et al. 2010. Resistance to Fusarium head blight and seedling blight in wheat is associated with activation of a cytochrome p450 gene. *Phytopathology* 100: 183–191.
- Li Z, Zhou M, Zhang Z, et al. 2011. Expression of a radish defensin in transgenic wheat confers increased resistance to *Fusarium graminearum* and *Rhizoctonia cerealis*. *Funct. Integr. Genomics* 11: 63–70.
- Liddell CM, Burgess LW, Taylor PWJ. 1986. Reproduction of crown rot of wheat caused by *Fusarium graminearum* Group 1 in the greenhouse. *Plant Dis.* 70: 632–35.
- Lin F, Xue SL, Zhang ZZ, et al. 2006. Mapping QTL associated with resistance to Fusarium head blight in the ‘Nanda2419’ × ‘Wangshuibai’ population II: type I resistance. *Theor. Appl. Genet.* 112: 528–535.
- Liu CJ, Ogonnaya FC. 2015. Resistance to Fusarium crown rot in wheat and barley: a review. *Plant Breeding* 134: 365–372.
- Liu S, Anderson JA. 2003. Targeted molecular mapping of a major wheat QTL for Fusarium head blight resistance using wheat ESTs and synteny with rice. *Genome* 46: 817–823.
- Liu SY, Hall MD, Griffey CA, et al. 2009. Meta-analysis of QTL associated with Fusarium head blight resistance in wheat. *Crop Sci.* 49: 1955–1968.
- Liu YX, Yang XM, Ma J, et al. 2010. Plant height affects Fusarium crown rot severity in wheat. *Phytopathology* 100: 1276–1281.

- Liu ZZ, Wang ZY. 1990. Improved scab resistance in China: sources of resistance and problems. In: Wheat for the non-traditional warm areas (Saunders DA, eds). 178–187. (A Proceeding of the International Conference. Foz do Iguacu, Brazil).
- Lulin M, Yi S, Aizhong C, et al. 2009. Molecular cloning and characterization of an up-regulated UDP-glucosyltransferase gene induced by DON from *Triticum aestivum* L. cv. Wangshuibai. *Mol. Biol. Rep.* 37: 785–795.
- Ma J, Li H, Zhang C, et al. 2010. Identification and validation of a major QTL conferring crown rot resistance in hexaploid wheat. *Theor. Appl. Genet.* 6: 1119–1128.
- Ma X, Du X, Liu G, et al. 2015. Cloning and characterization of a novel UDP-glycosyltransferase gene induced by DON from wheat. *J. Integr. Agr.* 14: 830–838.
- Makandar R, Essig JS, Schapaugh MA, et al. 2006. Genetically engineered resistance to Fusarium head blight in wheat by expression of *Arabidopsis* NPR1. *Mol. Plant Microbe Interact.* 19: 123–129.
- Malla S. 2012. Association of *Fhb1* and *Qfhs.ifa-5A* in spring versus winter growth habits in bread wheat (*Triticum aestivum* L.). *J. Agr. Sci.* 4: 39–48.
- Martin A, Bovill WD, Percy CD, et al. 2015. Markers for seedling and adult plant crown rot resistance in four partially resistant bread wheat sources. *Theor. Appl. Genet.* 128: 377–385.
- Matny ON. 2015. Fusarium head blight and crown rot on wheat and barley: Losses and health risks. *Adv. Plants Agric. Res.* 2: 38–43.
- Matsuoka Y, Nasuda S. 2004. Durum wheat as a candidate for the unknown female progenitor of bread wheat: An empirical study with a highly fertile F1 hybrid with *Aegilops tauschii* Coss. *Theor. Appl. Genet.* 109: 1710–1717.
- McFadden ES, Sears ER. 1946. The origin of *Triticum spelta* and its free-threshing hexaploid relatives. *J. Hered.* 37: 81–89.

- McHale L, Tan X, Koehl P, et al. 2006. Plant NBS-LRR proteins: adaptable guards. *Genome biology* 7: 212.
- McMullen M, Bergstrom GC, De Wolf E, et al. 2012. A unified effort to fight an enemy of wheat and barley: Fusarium head blight. *Plant Dis.* 96: 1712–1728.
- Menezes S, Silva EM, Lima E, et al. 2014. The pathogenesis-related protein PR-4b from *Theobroma cacao* presents RNase activity, Ca(2+) and Mg(2+) dependent-DNase activity and antifungal action on *Moniliophthora perniciosa*. *BMC plant biology*, 14: 161.
- Mesterhazy A. 1996. Types and components of resistance against Fusarium head blight of wheat. *Plant Breeding* 114: 377–386.
- Miedaner T, Cumagun CJR, Chakraborty S. 2008. Population genetics of three important head blight pathogens *Fusarium graminearum*, *F. pseudograminearum* and *F. culmorum*. *J. Phytopathol.* 156: 129–139.
- Miedaner T, Sieber AN, Desaint H, et al. 2017. The potential of genomic-assisted breeding to improve Fusarium head blight resistance in winter durum wheat. *Plant Breeding* 136: 610–619.
- Miller JD, Young JC, Sampson RD. 1985. Deoxynivalenol and Fusarium head blight resistance in spring cereals. *Phytopath. Z.* 113: 359–367.
- Miller SS, Watson EM, Lazebnik J, et al. 2011. Characterization of an alien source of resistance to Fusarium head blight transferred to Chinese Spring wheat. *Botany* 89: 301–311.
- Mitter V, Zhang MC, Liu CJ, et al. 2006. A high-throughput glasshouse bioassay to detect crown rot resistance in wheat germplasm. *Plant Pathol.* 55: 433–441.
- Mohammadi M, Kazemi H. 2002. Changes in peroxidase and polyphenol oxidase activities in susceptible and resistant wheat heads inoculated with *Fusarium graminearum* and induced resistance. *Plant Sci.* 162: 491–498.

- Moretti A, Pascale M, Logrieco FA. 2019. Mycotoxin risks under a climate change scenario in Europe. *Trends Food Sci. Tech.* 84: 38–40.
- Moretti A. 2009. Taxonomy of *Fusarium* genus: A continuous fight between lumpers and splitters. *Zbornik Matice Srpske Za Prirodne Nauke*, 117: 7–13.
- Moya-Elizondo E, Rew RL, Jacobsen B, et al. 2011a. Distribution and prevalence of *Fusarium* crown rot and common root rot pathogens of wheat in Montana. *Plant Dis.* 95:1099–1108.
- Moya-Elizondo E. 2013. *Fusarium* crown rot disease: Biology, interactions, management and function as a possible sensor of global climate change. *Ciencia e investigación agraria* 40: 235–252.
- Mudge AM, Macky DR, Dong Y, et al. 2006. A role for the mycotoxin deoxynivalenol in stem colonisation during crown rot disease of wheat caused by *Fusarium graminearum* and *Fusarium pseudograminearum*. *Physiol. Mol. Plant Pathol.* 69: 73–85.
- Muhovski Y, Batoko H, Jacquemin J. 2012. Identification, characterization and mapping of differentially expressed genes in a winter wheat cultivar (Centenaire) resistant to *Fusarium graminearum* infection. *Mol. Biol. Rep.* 39: 9583–9600.
- Murray GM, Brennan JP. 2009. Estimating disease losses to the Australian wheat industry. *Aus. Plant Pathol.* 38: 558.
- Nguema-Ona E, Vické-Gibouin M, Cannesan MA, et al. 2013. Arabinogalactan proteins in root-microbe interactions. *Trends Plant Sci.* 18: 440–449.
- Nucci M, Elias J, Anaissie M. 2009. CHAPTER 13-Hyalohyphomycosis. In: *Clinical Mycology* (Second Edition; Anaissie EJ, McGinnis MR, Pfaller MA, eds). 309–327. (Churchill Livingstone)
- Pan Y, Liu Z, Rocheleau H, et al. 2018. Transcriptome dynamics associated with resistance and susceptibility against *Fusarium* head blight in four wheat genotypes. *BMC genomics* 19: 642.

- Paranidharan V, Abu-Nada Y, Hamzehzarghani H, et al. 2008. Resistance-related metabolites in wheat against *Fusarium graminearum* and the virulence factor deoxynivalenol (DON). *Botany* 8: 1168–1179.
- Parikka P, Hakala K, Tiilikkala K. 2012. Expected shifts in *Fusarium* species' composition on cereal grain in Northern Europe due to climatic change. *Food Addit. Contam.: Part A* 29: 1543–1555.
- Pariyar SR, Erginbas-Orakci G, Dadshani S, et al. 2020. Dissecting the genetic complexity of Fusarium crown rot resistance in wheat. *Sci. Rep.* 10: 3200.
- Parry DW, Jenkinson P, McLeod L. 1995. Fusarium ear blight (scab) in small grains—a review. *Plant Pathol.* 44: 207–238.
- Paudel B, Zhuang Y, Galla A, et al. 2020. WFhb1-1 plays an important role in resistance against Fusarium head blight in wheat. *Sci. Rep.* 10: 7794.
- Peng JH, Sun DF, Nevo E. 2011. Domestication evolution, genetics and genomics in wheat. *Mol. Breeding* 28: 281–301.
- Poole GJ, Smiley RW, Paulitz TC, et al. 2012. Identification of quantitative trait loci (QTL) for resistance to Fusarium crown rot (*Fusarium pseudograminearum*) in multiple assay environments in the Pacific Northwestern US. *Theor. Appl. Genet.* 125: 91–107.
- Poole GJ, Smiley RW, Walker C, et al. 2013. Effect of climate on the distribution of *Fusarium* spp. causing crown rot of wheat in the Pacific Northwest of the United States. *Phytopathology* 103: 1130–1140.
- Powell JJ, Carere J, Fitzgerald T, et al. 2017. The Fusarium crown rot pathogen *Fusarium pseudograminearum* triggers a suite of transcriptional and metabolic changes in bread wheat (*Triticum aestivum* L.). *Annals of Botany.* 119: 853–867.
- Prieto KR, Echaide-Aquino F, Huerta-Robles A, et al. 2017. Endophytic bacteria and rare earth elements; promising candidates for nutrient use efficiency in plants. *Plant Macronutrient Use Efficiency* 285–306.

- Pritsch C, Muehlbauer GJ, Bushnell WR, et al. 2000. Fungal development and induction of defense response genes during early infection of wheat spikes by *Fusarium graminearum*. *Mol. Plant–Microbe Interact.* 13: 159169.
- Pritsch C, Vance CP, Bushnell WR, et al. 2001. Systemic expression of defense response genes in wheat spikes as a response to *Fusarium graminearum* infection. *Physiol. Mol. Plant Pathol.* 58: 1–12.
- Qi H, Jiang Z, Zhang K, et al. 2018. PlaD: A Transcriptomics Database for Plant Defense Responses to Pathogens, Providing New Insights into Plant Immune System. *Genomics Proteomics Bioinf.* 16: 1672–0229.
- Qi L, Pumphrey M, Friebe B, et al. 2008. Molecular cytogenetic characterization of alien introgressions with gene *Fhb3* for resistance to Fusarium head blight disease of wheat. *Theor. Appl. Genet.* 117: 1155–1166.
- Rahman M, Davies P, Bansal U, et al. 2020. Marker-assisted recurrent selection improves the crown rot resistance of bread wheat. *Mol. Breeding* 40: 28.
- Ramamoorthy V, Zhao X, Snyder AK, et al. 2007, Two mitogen-activated protein kinase signalling cascades mediate basal resistance to antifungal plant defensins in *Fusarium graminearum*. *Cellular Microb.* 9: 1491–1506.
- Ravensdale M, Rocheleau H, Wang L, et al. 2014. Priming-induced resistance to FHB in wheat. *Mol. Plant Pathol.* 15: 948–956.
- Ruckenbauer P, Buerstmayr H, Lemmens M. 2001. Present strategies in resistance breeding against scab *Fusarium* spp.. *Euphytica* 119: 121–127.
- Ruckenbauer P, Buerstmayr H, Lemmens M. 2007. Strategies of the European initiative for resistance breeding against Fusarium head blight. In: Wheat Production in stressed environments developments in plant breeding (Buck HT, Nisi JE, Salomón N, eds). 12: 103–107. (Springer: Dordrecht).

- Rygulla W, Snowdon RJ, Eynck C, et al. 2007. Broadening the genetic basis of *Verticillium longisporum* resistance in *Brassica napus* by interspecific hybridisation. *Phytopathology* 97: 1391–1396.
- Salgado JD, Madden LV, Paul PA. 2015. Quantifying the effects of Fusarium head blight on grain yield and test weight in soft red winter wheat. *Phytopathology* 105: 295–306.
- Salgado JD, Wallhead M, Madden LV, et al. 2011. Grain harvesting strategies to minimize grain quality losses due to Fusarium head blight in wheat. *Plant Dis.* 95: 1448–1457.
- Samad-Zamini M, Schweiger W, Nussbaumer T, et al. 2017, Time-course expression QTL-atlas of the global transcriptional response of wheat to *Fusarium graminearum*. *Plant Biotechnol. J.* 15: 1453–1464.
- Schroeder HW, Christensen JJ. 1963. Factors affecting resistance of wheat to scab caused by *Gibberella zeae*. *Phytopathology* 53: 831–838.
- Schweiger W, Steiner B, Ametz C, et al. 2013. Transcriptomic characterization of two major Fusarium resistance quantitative trait loci QTLs, *Fhb1* and *qfhs.ifa-5A*, identifies novel candidate genes. *Mol. Plant Pathol.* 148: 772–785.
- Schweiger W, Steiner B, Vautrin S, et al. 2016. Suppressed recombination and unique candidate genes in the divergent haplotype encoding *Fhb1*, a major Fusarium head blight resistance locus in wheat. *Theor. Appl. Genet.* 129: 1607–1623.
- Semagn K, Skinnes H, Tarkegne Y, et al. 2007. Quantitative trait loci controlling Fusarium head blight resistance and low deoxynivalenol content in hexaploid wheat population from ‘Arina’ and ‘NK93604’. *Crop Sci.* 47: 294–303.
- Serfling A, Kopahnke D, Habekuss A, et al. 2017. Wheat diseases: an overview. In: Achieving sustainable cultivation of wheat, breeding, quality traits, pests and diseases (Langridge P, eds). 1: 3. (*Burleigh Dodds Sci. Publ.*, Cambridge).

- Shah L, Ali A, Yahya M, et al. 2018. Integrated control of Fusarium head blight and deoxynivalenol mycotoxin in wheat. *Plant Pathol.* 67: 532–548.
- Sharma P, Gangola MP, Huang C, et al. 2018. Single nucleotide polymorphisms in B-Genome specific UDP-glucosyl transferases associated with Fusarium head blight resistance and reduced deoxynivalenol accumulation in wheat grain. *Phytopathology* 108: 124–132.
- Shen J, Li C, Mi G, et al. 2013. Maximizing root/rhizosphere efficiency to improve crop productivity and nutrient use efficiency in intensive agriculture of China. *J. Exp. Bot.* 64: 1181–1192.
- Shen X, Francki MG, Ohm HW. 2006. A resistance-like gene identified by EST mapping and its association with a QTL controlling Fusarium head blight infection on wheat chromosome 3BS. *Genome* 4: 631–635.
- Shi J, Gao H, Wang H, et al. 2017. ARGOS8 variants generated by CRISPR-Cas9 improve maize grain yield under field drought stress conditions. *Plant Biotechnol. J.* 152: 207–216.
- Sitton JW, Cook RJ. 1981. Comparative morphology and survival of chlamydospores of *Fusarium roseum* 'Culmorum' and 'Graminearum'. *Phytopathology* 71: 85–90.
- Smiley RW, Gourlie JA, Easley SA, et al. 2005. Crop damage estimates for crown rot of wheat and barley in the Pacific Northwest. *Plant Dis.* 89: 595–604.
- Smiley RW, Patterson L. 1996. Pathogenic fungi associated with Fusarium foot rot of winter wheat on the semiarid Pacific northwest. *Plant Dis.* 80: 944–949.
- Sobrova P, Adam V, Vasatkova A, et al. 2010. Deoxynivalenol and its toxicity. *Interdisc. toxicol.* 3: 94–99.
- Soltis PS, Marchant DB, Van de Peer Y, et al. 2015. Polyploidy and genome evolution in plants. *Curr. Opin. Genet. Dev.* 35: 119–125.

- Son H, Seo YS, Min K, et al. 2011. A phenome-based functional analysis of transcription factors in the cereal head blight fungus, *Fusarium graminearum*. *PLoS Pathog.* 7: e1002310.
- Sorahinobar M, Niknam V, Jahedi A, et al. 2019. Application of sodium salicylate up-regulates defense response against *Fusarium graminearum* in wheat spikes. *Biologia plantarum* 63: 690–698.
- Sorahinobar M, Soltanloo H, Niknam V, et al. 2017. Physiological and molecular responses of resistant and susceptible wheat cultivars to *Fusarium graminearum* mycotoxin extract. *Can. J. Plant Pathol.* 39: 444–453.
- Spanic V, Viljevac Vuletic M, Abicic I, et al. 2017. Early response of wheat antioxidant system with special reference to Fusarium head blight stress. *Plant Physiol. Biochem.* 115: 34–43.
- Spolti P, Shah DA, Fernandes JMC, et al. 2015. Disease risk, spatial patterns, and incidence-severity relationships of Fusarium head blight in no-till spring wheat following maize or soybean. *Plant Dis.* 99: 1360–1366.
- Stack RW. 1999. Return of an old problem: Fusarium head blight of small grains. *Plant Health. Prog.*
- Steiner B, Kurz H, Lemmens M, et al. 2009. Differential gene expression of related wheat lines with contrasting levels of head blight resistance after *Fusarium graminearum* inoculation. *Theor. Appl. Genet.* 118: 753–764.
- Stephens AE, Gardiner DM, White RG, et al. 2008. Phases of infection and gene expression of *Fusarium graminearum* during crown rot disease of wheat. *Mol. Plant-Microbe Interact.* 21: 1571–1581.
- Su Z, Bernardo A, Tian B, et al. 2019. A deletion mutation in TaHRC confers Fhb1 resistance to Fusarium head blight in wheat. *Nat. Genet.* 517: 1099–1105.

- Sudisha J, Sharathchandra RG, Amruthesh KN, et al. 2012. Pathogenesis related proteins in plant defense response. In: *Plant Defence: Biological control* (Mérillon J, Ramawat K, eds). 12: 379–403. (*Springer*: Dordrecht).
- Sun Y, Xiao J, Jia X, et al. 2016. The role of wheat jasmonic acid and ethylene pathways in response to *Fusarium graminearum* infection. *Plant growth regul.* 80: 69–77.
- Thapa G, Gunupuru LR, Hehir JG, et al. 2018. A Pathogen-Responsive Leucine Rich Receptor Like Kinase Contributes to Fusarium Resistance in Cereals. *Front. plant sci.* 9: 867.
- Thomas J, Chen Q, Howes N. 1997. Chromosome doubling of haploids of common wheat with caffeine. *Genome* 40: 552–558.
- Trail F. 2009. For blighted waves of grain: *Fusarium graminearum* in the postgenomics era. *Plant Physiol.* 149: 103–110.
- Turkington TK, Petran A, Yonow T, et al. 2016. *Fusarium graminearum* (Fusarium Head Blight). *Harvest Choice Pest Geography*.
- Van der Weerden NL, Hancock REW, Anderson MA. 2010. Permeabilization of fungal hyphae by the plant defensin NaD1 occurs through a cell wall-dependent process. *J. Biol. Chem.* 285: 37513–37520.
- Van Ooijen JW 2006. JoinMap 4: Software for the calculation of genetic linkage maps in experimental populations. *Kyazma B.V.* Wageningen.
- Van Schie CCN, Takken FLW. 2014. Susceptibility Genes 101: How to Be a Good Host. *Annu. Rev. Phytopathol.* 52: 551–581.
- Venske E, Dos Santos RS, Busanello C, et al. 2019. Bread wheat: a role model for plant domestication and breeding. *Hereditas.* 156: 16.
- Visscher PM, Thompson R, Haley CS. 1996. Confidence intervals in QTL mapping by bootstrapping. *Genetics* 143: 1013–1020.

- Voorrips RE. 2002. MapChart: Software for the graphical presentation of linkage maps and QTLs. *J. Hered.* 93: 77–78.
- Voss-Fels KP, Qian L, Gabur I, et al. 2018. Genetic insights into underground responses to *Fusarium graminearum* infection in wheat. *Sci. Rep.* 8: 13153.
- Wagner GP, Kin K, Lynch VJ. 2013. A model based criterion for gene expression calls using RNA-seq data. *Theory Biosci.* 132: 159.
- Waldron BL, Moreno-Sevilla B, Anderson JA, et al. 1999. RFLP mapping of QTL for *Fusarium* head blight resistance in wheat. *Crop Sci.* 39: 805–811.
- Wallwork H, Butt M, Cheong JPE, et al. 2004. Resistance to crown rot in wheat identified through an improved method for screening adult plants. *Aus. Plant Pathol.* 33: 1–7.
- Walter S, Brennan JM, Arunachalam C, et al. 2008. Components of the gene network associated with genotype-dependent response of wheat to the *Fusarium* mycotoxin deoxynivalenol. *Funct. Integr. Genomics.* 8: 421–427.
- Walter S, Doohan F. 2011. Transcript profiling of the phytotoxic response of wheat to the *Fusarium* mycotoxin deoxynivalenol. *Mycotox. Res.* 27: 221–230.
- Walter S, Nicholson P, Doohan FM. 2009. Action and reaction of host and pathogen during *Fusarium* head blight disease. *New Phytol.* 185: 54–66.
- Wang G, Hou W, Zhang L, et al. 2016. Functional analysis of a wheat pleiotropic drug resistance gene involved in *Fusarium* head blight resistance. *J. Integr. Agr.* 15: 2215–2227.
- Wang H, Sun S, Ge W, et al. 2020. Horizontal gene transfer of *Fhb7* from fungus underlies *Fusarium* head blight resistance in wheat. *Science* 368: eaba5435.
- Wang N, Xia EH, Gao LZ. 2016. Genome-wide analysis of WRKY family of transcription factors in common bean, *Phaseolus vulgaris*: chromosomal localization, structure, evolution and expression divergence. *Plant Gene* 5: 22–30.

- Wang Q, Buxa SV, Furch A, et al. 2015. Insights into *Triticum aestivum* seedling root rot caused by *Fusarium graminearum*. *Mol. Plant-Microbe Interact.* 28: 1288–1303.
- Wang Q, Shao B, Shaikh FI, et al. 2018. Wheat resistances to Fusarium root rot and head blight are both associated with deoxynivalenol and jasmonate related gene expression. *Phytopathology* 108: 602–616.
- Wang Q. 2015. The pathosystem wheat *Triticum aestivum* root-Fusarium *graminearum*: complex plant responses and fungal strategies [Dissertation], Justus Liebig University.
- Wang S, Wong D, Forrest K, et al. 2014. Characterization of polyploid wheat genomic diversity using a high-density 90,000 single nucleotide polymorphism array. *Plant Biotechnol. J.* 12: 787–796.
- Wang Y, Cheng X, Shan Q, et al. 2014. Simultaneous editing of three homoeoalleles in hexaploid bread wheat confers heritable resistance to powdery mildew. *Nat. Biotechnol.* 32: 947–951.
- Wang Y, Yang L, Xu H, et al. 2005. Differential proteomic analysis of proteins in wheat spikes induced by *Fusarium graminearum*. *Proteomics* 5: 4496–4503.
- Wegulo SN, Baenziger PS, Hernandez-Nopsa J, et al. 2015. Management of Fusarium head blight of wheat and barley. *Crop Prot.* 73: 100–107.
- Wen W, He Z, Gao F, et al. 2017. A high-density consensus map of common wheat integrating four mapping populations scanned by the 90K SNP array. *Front. Plant Sci.* 8: 1389.
- Wheat@URGI portal. <https://wheat-urgi.versailles.inra.fr>. Accessed 10 April 2018.
- Wildermuth GB, McNamara RB. 1994. Testing wheat seedlings for resistance to crown rot caused by *Fusarium graminearum* Group 1. *Plant Dis.* 78: 949–953.

- Wu S, Wang H, Yang Z, et al. 2014. Expression Comparisons of Pathogenesis-Related (PR) Genes in Wheat in Response to Infection/Infestation by Fusarium, Yellow dwarf virus (YDV) Aphid-Transmitted and Hessian Fly. *J. Integr. Agr.* 13: 926–936.
- Xiao J, Jin XH, Jia XP, et al. 2013. Transcriptome-based discovery of pathways and genes related to resistance against Fusarium head blight in wheat landrace Wangshuibai. *BMC Genomics.* 14: 197.
- Xing L, Gao L, Chen Q, et al. 2018. Over-expressing a UDP-glucosyltransferase gene (Ta-UGT3) enhances Fusarium head blight resistance of wheat. *Plant Growth Regul.* 84: 561–571.
- Xing LP, Wang HZ, Jiang ZN, et al. 2008. Transformation of wheat thaumatin-Like protein gene and analysis of reactions to powdery mildew and Fusarium head blight in transgenic plants. *Acta Agronomica Sinica* 34: 349–354.
- Xu F, Yang G, Wang J, et al. 2018. Spatial distribution of root and crown rot fungi associated with winter wheat in the north China plain and its relationship with climate variables. *Front. Microbiol.* 9: 1054.
- Xue AG, Chen Y, Voldeng HD, et al. 2014. Concentration and cultivar effects on efficacy of CLO-1 biofungicide in controlling Fusarium head blight of wheat. *Biological Control* 73: 2–7.
- Xue S, Li G, Jia H, et al. 2010. Fine mapping *Fhb4*, a major QTL conditioning resistance to Fusarium infection in bread wheat *Triticum aestivum* L. *Theor. Appl. Genet.* 121: 147.
- Xue S, Xu F, Tang M, et al. 2011. Precise mapping *Fhb5*, a major QTL conditioning resistance to Fusarium infection in bread wheat *Triticum aestivum* L. *Theor. Appl. Genet.* 123: 1055.
- Yan J, Su P, Li W, et al. 2019. Genome-wide and evolutionary analysis of the class III peroxidase gene family in wheat and *Aegilops tauschii* reveals that some members are involved in stress responses. *BMC Genomics* 20: 666.

- Yan W, Li HB, Cai SB, et al. 2011. Effects of plant height on type I and type II resistance to fusarium head blight in wheat. *Plant Pathol.* 60: 506–512.
- Yang J, Bai GH, Shaner GE. 2005a. Novel quantitative trait loci (QTL) for Fusarium head blight resistance in wheat cultivar Chokwang. *Theor. Appl. Genet.* 111: 1571–1579.
- Yang M, Wang X, Dong J, et al. 2020. Proteomics reveals the changes that contribute to Fusarium head blight resistance in wheat. *Phytopathology* 2020: 10.1094.
- Yang X, Pan Y, Singh PK, et al. 2019. Investigation and genome-wide association study for Fusarium crown rot resistance in Chinese common wheat. *BMC Plant Biol.* 19: 153.
- Yang X, Zhong S, Zhang S, et al. 2021. A loss-of-function of the dirigent gene TaDIR-B1 improves resistance to Fusarium crown rot in wheat. *Plant Biotechnol J.*
- Yang Z, Gilbert J, Fedak G, et al. 2005b. Genetic characterization of QTL associated with resistance to Fusarium head blight in a doubled-haploid spring wheat population. *Genome.* 48: 187–196.
- Ye J, Zhang Y, Cui H, et al. 2018. WEGO 2.0: a web tool for analyzing and plotting GO annotations, 2018 update. *Nucleic Acids Res.* 46: W71–W75.
- Zadoks JC, Chang TT, Konzak CF. 1974. A decimal code for the growth stages of cereals. *Weed Res.* 14: 415–421.
- Zhang A, Yang W, Li X, et al. 2018. Current status and perspective on research against Fusarium head blight in wheat[J]. *Hereditas (Beijing)*, 40: 858–873. (in Chinese)
- Zhang P, Zhou MP, Zhang X, et al. 2013. Change of defensive-related enzyme in wheat crown rot seedlings infected by *Fusarium graminearum*. *Cereal res. Commun.* 41: 431–439.
- Zhang Q, Axtman JE, Faris JD, et al. 2014. Identification and molecular mapping of quantitative trait loci for Fusarium head blight resistance in emmer and durum

- wheat using a single nucleotide polymorphism-based linkage map. *Mol. Breeding* 34: 1677–1687.
- Zhang W, Francis T, Gao P. 2018. Genetic characterization of type II Fusarium head blight resistance derived from transgressive segregation in a cross between Eastern and Western Canadian spring wheat. *Mol. Breeding* 38: 13.
- Zhang X, Bai G, Bockus W, et al. 2012. Quantitative trait loci for Fusarium head blight resistance in U.S. hard winter wheat cultivar Heyne. *Crop Sci.* 52: 1187.
- Zhang X, Fu J, Hiromasa Y, et al. 2013. Differentially expressed proteins associated with Fusarium head blight resistance in wheat. *Plos ONE* 8: e82079.
- Zhang X, Rouse MN, Nava IC, et al. 2016. Development and verification of wheat germplasm containing both *Sr2* and *Fhb1*. *Mol. Breeding* 36: 85.
- Zhang Z, Yao W, Dong N, et al. 2007. A novel ERF transcription activator in wheat and its induction kinetics after pathogen and hormone treatments. *J. Exp. Bot.* 58: 2993–3003.
- Zhao L, Ma X, Su P, et al. 2018. Cloning and characterization of a specific UDP-glycosyltransferase gene induced by DON and *Fusarium graminearum*. *Plant Cell Rep.* 37 :641–652.
- Zheng Z, Gao S, Zhou M, et al. 2017. Enhancing Fusarium crown rot resistance by pyramiding large-effect QTL in common wheat *Triticum aestivum* L. *Mol. Breeding* 37: 107.
- Zheng Z, Ma J, Stiller J, et al. 2015. Fine mapping of a large-effect QTL conferring Fusarium crown rot resistance on the long arm of chromosome 3B in hexaploid wheat. *BMC genomics* 16: 850.
- Zheng Z, Kilian A, Yan G, et al. 2014. QTL conferring Fusarium crown rot resistance in the elite bread wheat variety EGA Wylie. *PLoS ONE* 94: e96011.

- Zhou W, Eudes F, Laroche A. 2006. Identification of differentially regulated proteins in response to a compatible interaction between the pathogen *Fusarium graminearum* and its host, *Triticum aestivum*. *Proteomics* 6: 4599–4609.
- Zhou W, Kolb FL, Riechers DE. 2005. Identification of proteins induced or upregulated by Fusarium head blight infection in the spikes of hexaploid wheat (*Triticum aestivum*). *Genome* 48: 770–780
- Zhu JK. 2016. Abiotic stress signaling and responses in plants. *Cell* 167: 313–324.
- Zhu Z, Chen L, Zhang W, et al. 2020. Genome-wide association analysis of Fusarium head blight resistance in Chinese elite wheat lines. *Front. Plant Sci.* 11: 206.

Appendix

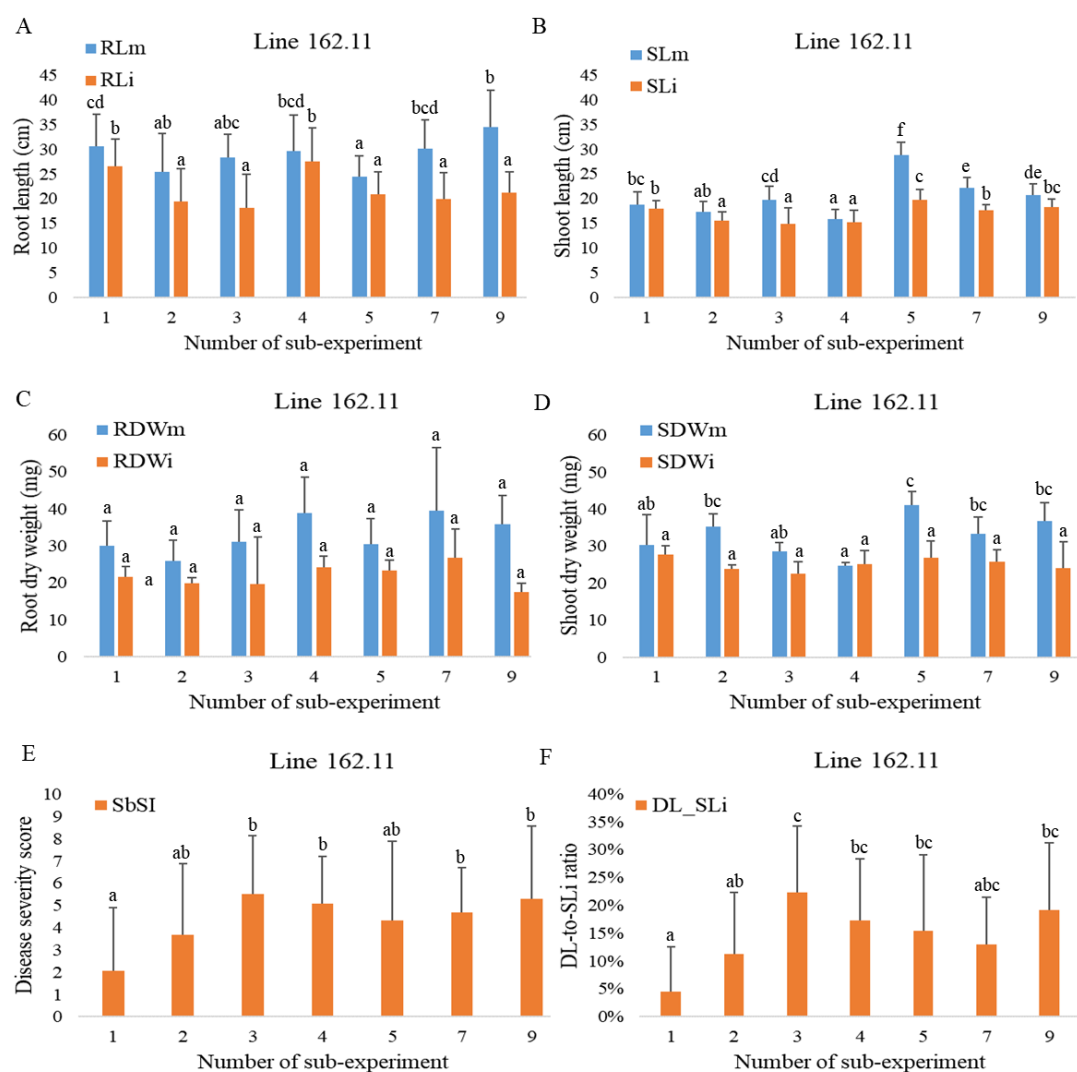


Figure A 1. Comparison of phenotypic data for different traits for line 162.11 in seven sub-experiments upon mock and *F. graminearum* root inoculations. (A) root length, (B) shoot length, (C) root dry weight, (D) shoot dry weight, (E) and (F) disease severity indices. Bars represent standard deviation. SL= Shoot length, RL= Root length, SDW= Shoot dry weight, RDW= Root dry weight, SbSI= Stem base symptom index, DL_SL= Ratio of discoloration section length on stem base to shoot length, i= infected, m= mock, a-f= Groups from a Duncan's multiple range test. Three biological replicates were assessed in each sub-experiment for dry weight, 15 biological replicates for all other traits.

Table A 1. Raw phenotypic data in mock and *F. graminearum* root inoculations experiment.

Treatment	Traits	Traits (Abbreviations)	Means for parents ^a			Population statistics ^b					
			Line 162.11	cv. Tobak	<i>P</i> -value ^c	Min.	Max.	Mean	Median	CoV (%)	
Control	Root length	RLm	29.01	25.97	0.00	***	18.64	45.67	28.37	28.01	2.28
	Shoot length	SLm	20.50	22.71	0.00	***	15.47	34.54	21.96	20.68	1.17
	Root dry weight	RDWm	33.07	30.57	0.45		16.03	58.86	33.17	33.45	2.00
	Shoot dry weight	SDWm	32.88	37.80	0.12		19.47	55.01	37.06	36.03	1.24
Infected	Root length	RLi	21.97	19.43	0.01	*	12.88	36.96	20.77	20.85	2.47
	Shoot length	SLi	17.05	17.50	0.23		13.72	28.93	18.90	18.45	1.49
	Root dry weight	RDWi	21.88	18.74	0.26		5.99	49.91	18.69	18.01	2.61
	Shoot dry weight	SDWi	25.14	24.27	0.92		10.29	44.33	26.14	26.65	1.86
	Discoloration scale	DS	2.17	2.43	0.09		0.73	4.00	2.71	2.82	5.09
	Discoloration extension scale	DES	2.21	2.62	0.03	*	0.93	3.89	2.73	2.73	5.44
	Stem base symptom index	SbSI	4.38	5.04	0.04	*	1.87	7.89	5.44	5.54	4.97
	Discoloration section length	DL	2.40	2.62	0.21		0.87	5.02	2.80	2.79	6.06
	DL to SL ratio	DL_SLi	0.15	0.16	0.26		0.04	0.24	0.15	0.15	6.34
Reduction	Root length	RLR	0.24	0.25	0.85		0	0.59	0.26	0.27	11.52
	Shoot length	SLR	0.15	0.2	0.4		0	0.43	0.13	0.12	12.65
	Root dry weight	RDWR	0.33	0.38	0.51		0	0.83	0.43	0.48	5.67
	Shoot dry weight	SDWR	0.22	0.35	0.17		0	0.67	0.29	0.25	6.16

^a Parents of the DH mapping population consisting of 104 individuals

^b Basic statistical parameters for the DH population derived from the cross of line 162.11 and cv. Tobak

^c *P*-values represent significant differences between the means for line 162.11 and cv. Tobak at *P* < 0.05

Table A 2. Raw phenotypic data in mock and *F. graminearum* seed inoculations experiment.

Treatment	Traits	Traits (Abbreviations)	Means for parent ^a			Population statistics ^b				
			Line 162.11	cv. Tobak	<i>P</i> -value ^c	Min.	Max.	Mean	Median	CoV (%)
Control	Root dry weight	RDWm	27.82	26.90	0.89	10.63	67.04	33.28	33.47	1.73
	Shoot dry weight	SDWm	26.63	27.38	0.31	16.75	54.82	33.61	33.73	0.99
	Survival rate	Srm	0.92	0.88	0.19	0.85	1.00	0.98	1.00	0.38
Infected	Shoot length	SLi	8.74	4.23	0.00 ***	0.00	30.88	16.90	17.26	6.05
	Root dry weight	RDWi	20.05	15.81	0.28	0.00	50.83	19.72	19.32	2.22
	Shoot dry weight	SDWi	22.80	20.13	0.37	0.00	47.49	24.86	24.30	1.21
	Survival rate	Sri	0.39	0.21	0.02 *	0.00	1.00	0.67	0.71	2.04
	Discoloration scale	DS	3.50	4.26	0.00 ***	0.18	5.00	2.33	2.33	7.39
	Discoloration extension scale	DES	3.39	4.26	0.00 ***	0.27	5.00	2.32	2.23	14.70
	Stem base symptom index	SbSI	6.88	8.52	0.00 ***	0.45	10.00	4.62	4.56	8.27
	Discoloration section length	DL	0.89	1.43	0.04 *	0.05	2.85	1.08	0.96	11.29
	DL to SL ratio	DL_SLi	0.05	0.09	0.01 *	0.00	0.16	0.05	0.04	12.46
Reduction	Root dry weight	RDWR	0.29	0.47	0.25	0	1	0.41	0.41	6.11
	Shoot dry weight	SDWR	0.20	0.30	0.47	0	1	0.27	0.28	5.08

^a Parents of the DH mapping population consisting of 103 individuals

^b Basic statistical parameters for the DH population derived from the cross of line 162.11 and cv. Tobak

^c *P*-values represent significant differences between the means for line 162.11 and cv. Tobak at *P* < 0.05

Declaration

I declare: this dissertation submitted is a work of my own, written without any illegitimate help by any third party and only with materials indicated in the dissertation. I have indicated in the text where I have used texts from already published sources, either word for word or in substance, and where I have made statements based on oral information given to me. At any time during the investigations carried out by me and described in the dissertation, I followed the principles of good scientific practice as defined in the “Statutes of the Justus Liebig University Giessen for the Safeguarding of Good Scientific Practice”.

Signature: 

Date: 11.03.2021

Acknowledgement

First of all, I would like to express my sincere gratitude to Prof. Dr. Rod Snowdon and Prof. Dr. Dr. h.c. Wolfgang Friedt who gave me the opportunity to work in the Institute of Plant Breeding and for the continuous support and encouragement to my PhD research. Thanks for their patience, motivation, enthusiasm, and immense knowledge of plant breeding. Their guidance helped me in all the time of research and writing of thesis.

I also thank to Prof. Dr. Karl-Heinz Kogel, Institute of Phytopathology and Applied Zoology, Justus Liebig University, Giessen, Germany for accepting to be the co-supervisor for my work and his valuable suggestions to improve the manuscript.

My sincere thanks go to Dr. Christian Obermeier, Dr. Sven Gottwald and Dr. Qing Wang under whose guidance I chose this topic. I thank them so much for their great help, guidance, constructive thought during the project and valuable advice and comments on my thesis. I am very grateful to work with them and learn a lot from them.

This work would not have been done without the help of many people in the laboratory, especially the valuable technical support from Stavros Tzigos and Liane Renno. I also thank to the help, advice and encouragement from all of my colleague and friends.

I express my gratitude to my parents and sister, without their support I would never able to finish my study. I would like to thank them for their encouragement and supporting in my life.

Last but not the least; I am very grateful to the China Scholarship Council (CSC) for financing my studies.